NTNU – Trondheim
Norwegian University of
Science and Technology

Climate Change Impacts of Co-firing Forest Biomass from Russia with Coal in the Russian Power Sector

Monica Kviljo

Master of Energy and Environmental Engineering
Submission date: June 2013
Supervisor: Anders Hammer Strømman, EPT

Norwegian University of Science and Technology
Department of Energy and Process Engineering

NTNU
Norwegian University
of Science and Technology

Department of Energy
and Process Engineering

EPT-M-2013-72

MASTER THESIS

for

Monica Kviljo

Spring 2013

Climate change impacts of co-firing forest biomass from Russia with coal in the EU power sector
Klimaeffekter av ko-forbrenning av biomasse fra russisk skog med kull i den europeiske kraftsektoren.

Background

About 30 percent of the current European electricity generation mix depends on coal. Co-firing of biomass with coal is one of the most mature and promising technological options to reduce the environmental cost of this dependence and to allow a smooth transition to sustainable renewable energy. Also, the environmental regulations have tightened the allowable emissions from power plants, mandating the sector to incorporate improved and efficient tail-pipe treatment techniques. However, the sustainable constant supply of biomass sources is necessary to achieve important reductions in coal usage. Such a provision should be preferably based on sustainable forest biomass, so as to minimize conflicts with land uses and other material production chains. Further, the net climate change mitigation of this replacement should be accurately estimated in order to predict the magnitude and timing of the benefits

Aim

The primary objective of this work is to assess the climate impacts for various shares of co-firing forest biomass with coal to produce electricity in Europe. Given the high volumes of feedstock required, biomass is imported from areas rich in renewable resources, like Russian forests. The climate impact analysis considers the two most important contributions to global climate change, namely the temporary change in atmospheric CO_2 concentration caused by biogenic CO_2 emissions and cooling effects from changes in surface albedo following harvest.

The analysis should include following elements:

1) Compilation, synthesis and benchmarking of existing literature on co-firing technology and forest harvest in Russia.
2) Development of life cycle inventories for forestry operation and co-firing.
3) Development of life cycle assessment of various scenarios based on different shares of co-firing (and hence biomass volumes).
4) Estimation of the impacts from temporary changes in surface albedo and biogenic CO_2 fluxes.
5) Life cycle assessment of the selected co-firing value chains.
6) Analysis and discussion.

Within 14 days of receiving the written text on the master thesis, the candidate shall submit a research plan for his project to the department.

When the thesis is evaluated, emphasis is put on processing of the results, and that they are presented in tabular and/or graphic form in a clear manner, and that they are analyzed carefully.

The thesis should be formulated as a research report with summary both in English and Norwegian, conclusion, literature references, table of contents etc. During the preparation of the text, the candidate should make an effort to produce a well-structured and easily readable report. In order to ease the evaluation of the thesis, it is important that the cross-references are correct. In the making of the report, strong emphasis should be placed on both a thorough discussion of the results and an orderly presentation.

The candidate is requested to initiate and keep close contact with his/her academic supervisor(s) throughout the working period. The candidate must follow the rules and regulations of NTNU as well as passive directions given by the Department of Energy and Process Engineering.

Risk assessment of the candidate's work shall be carried out according to the department's procedures. The risk assessment must be documented and included as part of the final report. Events related to the candidate's work adversely affecting the health, safety or security, must be documented and included as part of the final report. If the documentation on risk assessment represents a large number of pages, the full version is to be submitted electronically to the supervisor and an excerpt is included in the report.

Pursuant to "Regulations concerning the supplementary provisions to the technology study program/Master of Science" at NTNU §20, the Department reserves the permission to utilize all the results and data for teaching and research purposes as well as in future publications.

The final report is to be submitted digitally in DAIM. An executive summary of the thesis including title, student's name, supervisor's name, year, department name, and NTNU's logo and name, shall be submitted to the department as a separate pdf file. Based on an agreement with the supervisor, the final report and other material and documents may be given to the supervisor in digital format.

☐ Work to be done in lab (Water power lab, Fluids engineering lab, Thermal engineering lab)
☐ Field work

Department of Energy and Process Engineering, 1. February 2013

Olav Bolland
Department Head

Anders H. Strømman
Academic Supervisor

Co-supervisor: Bhawna Singh, PhD

Comment to Master Thesis description

The decision was made to limit the scope of the thesis to the power market of the Russian Federation and primarily European Russia, rather than the power market in the EU. This was done in agreement with supervisor Professor Anders Hammer Strømman and co-supervisor Francesco Cherubini in the course of the work done on the master thesis during the spring of 2013. The primary objective has therefore changed, along with the title. The new title is *"Climate change impacts of co-firing forest biomass from Russia with coal in the Russian power sector"*. In Norwegian the new title is *"Klimaeffekter av ko-forbrenning av biomasse fra russisk skog med kull i den russiske kraftsektoren"*.

Preface

This report is the result of my master thesis work conducted during the spring of 2013 at the Norwegian University of Science and Technology. The thesis completes my final year of the integrated Master of Science degree within Energy and Environmental engineering at the Institute for Energy and Process Engineering.

There are several people that deserve to be mentioned in connection with my work done on this thesis. First and foremost, I would like to thank my supervisor Professor Anders Hammer Strømman for all the knowledge, inspiration and support in the past year. In addition I would like to express my sincere gratitude to my co-supervisor Francesco Cherubini. Thank you for all your enthusiasm, encouragement and patience with me, I have learnt a tremendous amount from you this spring. Moreover I would like to thank Ryan M. Bright for his contributions to the calculations on the albedo effect. It has been a great joy for me to work on the thesis, much due to a stimulating working environment and the aforementioned expertise provided at the Programme for Industrial Ecology.

I would also like to use this opportunity to thank my parents, Joan and Karstein Kviljo, and my sister Madeleine, for always being there for me and encouraging and supporting me at all times.

I hope you find this thesis of interest and that it contributes to an increased awareness and understanding, especially concerning the temporary changes in the atmospheric CO_2 concentration in connection with bioenergy, where many are misinformed due to governmental policies and media.

Trondheim, June 2013

Monica Kviljo

Abstract

The primary objective of this thesis has been to assess the climate change impacts of co-firing with biomass from Russian forest areas with coal, with special emphasis on the temporary change in atmospheric CO_2 concentration caused by biogenic CO_2 and surface albedo. With a mixture of boreal and temperate climate, the European part of Russia was chosen as the focus area and divided into eight regions. The scenarios looked into were 10% co-firing of biomass, 20% co-firing and the ideal case of 100% bioenergy production, covering the coal demand in Russia for heat and electricity production.

Currently only around 2% of the heat and power in Russia is from bioenergy. With an annual allowable cut of 633 million cubic metres forest and only 173,6 million cubic metres being harvested, it is apparent that there is a large unused potential for bioenergy in Russia, both for domestic use and export to the European power sector. Estimates show that by increasing current harvest by 30%, 20% of the coal demand in Russia can be covered with bioenergy. Covering the coal demand completely will require an increase in harvesting by 150%, but this would still only equal around 50% of the annual increment available for exploitation. With well-designed governmental policies and improved infrastructure, especially in the forest rich areas, this could be a feasible scenario in the future for Russia.

Co-firing can contribute to a smooth transition to renewable energy sources. Bioenergy is often assumed CO_2 neutral, but this highly underestimates its true climate change impact. Through this assessment, both biogenic CO_2 and the effect of surface albedo has been quantified for chosen sites in each of the eight regions, with focus on the time horizons of 20, 100 and 500 years. The total climate change impact has further been found for each of the scenarios.

The impacts are especially significant for short time horizons combined with boreal areas with seasonal snow cover and forest with long rotation periods. In the Northern, Northwestern and Urals region there was a net cooling effect from the beginning of the assessment period for the 100% bioenergy scenario due to surface albedo. It is therefore important to consider these climate forcings in the national and global environmental policies, especially when designing frameworks for bioenergy and forest management strategies in boreal areas.

Sammendrag

Hovedformålet for denne masteroppgaven har vært å analysere klimaeffektene av ko-forbrenning av biomasse fra russisk skog med kull, med særlig fokus på de midlertidige endringene i den atmosfæriske CO_2-konsentrasjonen som følge av biogent CO_2 og overflatealbedo. Med en kombinasjon av borealt og temperert klima ble fokusområdet den europeiske delen av Russland, som videre ble delt inn i åtte regioner. Scenarioene som ble analysert var 10% ko-forbrenning, 20% ko-forbrenning og det ideelle scenarioet med 100% bioenergi, som ville kunne dekke hele etterspørselen for kull til kraftproduksjon i Russland.

I dagens Russland har kun rundt 2% av kraftforsyningen opphav fra bioenergi. 633 millioner kubikkmeter skoghogst er lovlig på årlig basis, men ettersom det kun blir hogget 173,6 millioner kubikkmeter årlig, har Russland tilsynelatende et stort ubrukt potentisale for bioenergi, både innenriks og gjennom eksport til den europeiske kraftsektoren. Beregnede estimater viser at ved å øke dagens skogsvirke med 30%, kan 20% av kulletterspørselen dekkes av bioenergi. Dersom hele etterspørselen for kull i kraftsektoren skal dekkes, må skoghogsten øke med 150%, men dette vil fortsatt kun tilsvare rundt 50% av den årlige utnyttbare tilveksten av skog. Med politiske tiltak og forbedret infrastruktur, særlig i de skogrike områdene, er scenarioet mulig i et framtidig Russland.

Ko-forbrenning can bidra til en smidig overgang til fornybare energiressurser. Bioenergi er ofte karakterisert som CO_2 nøytralt, men denne antakelsen gjør at den virkelige klimaeffekten blir sterkt undervurdert. Gjennom denne masteroppgaven har både biogent CO_2 og overflatealbedo blitt beregnet for utvalgte områder i hver av de åtte regionene, med fokus på tidshorisontene 20, 100 og 500 år. Videre har de totale klimaeffektene blitt funnet for hvert av scenarioene.

Klimaeffektene er særlig betydelige for korte tidshorisonter og for boreale skogområder med lange snøsesonger, samt for skog med lang rotasjonstid. I regionene Nord, Nordvest og Uralfjellene var resultatet en netto kjølingseffekt grunnet overflatealbedo for scenarioet 100% bioenergi. Det er derfor svært viktig å ta disse klimapådriverne i betraktning både i nasjonale og internasjonale politiske rammeverk, og særlig i rammeverk knyttet til bioenergi og skogforvaltning i boreale skogområder.

Table of Contents

List of Tables

List of Figures

Abbreviations

AAC – Annual Allowable Cut

AGWP – Absolute Global Warming Potential

AIAE – Annual Increment Available for Exploitation

CHP – Combined Heat and Power

CO_2 – Carbon dioxide

EJ - Exajoule

eq – equivalents

ERF – Effective Radiative Forcing

FAO – Food and Agriculture Organization of the United Nations

FAWS – Available Forest for Wood Supply

GWh – Gigawatt hour

GWP – Global Warming Potential

GWP_{albedo} – GWP for albedo

GWP_{bio} – GWP for biogenic CO_2

GHG – Greenhouse Gas Emissions

GJ – Gigajoule

IEA – International Energy Agency

IRF – Impulse Response Function

IPCC – Intergovernmental Panel on Climate Change

kWh – kilowatt hour

LCA – Life Cycle Assessment

LCE – Life Cycle Emission

LUC – Land Use Change

LVH – Lower Heating Value

MJ – Megajoule

MODIS – The MODerate Resolution Imaging Spectroradiometer

NAI – Net Annual Increment

NEP – Net Ecosystem Productivity

NPP – Net Primary Productivity

OECD – Organisation for Economic Co-operation and Development

PL - Poland

RER – Europe

RF – Radiative Forcing

RU – The Russian Federation

TH – Time Horizon

TOA – Top Of the Atmosphere

TOP – Torrefaction and pelletisation

TJ – Terrajoule

1. Introduction

In this part, first the motivation for the topic of this thesis is presented, based on the current situation both on a worldwide basis, as well as more specifically for the Russian Federation. The state of the field is also presented and the objectives of the thesis are introduced. As a final part, an outline of the content of the report is presented.

1.1. Motivation

As coal is a low-cost, highly available and reliable resource, it is widely used in power generation throughout the world. In 2010 it contributed to as much as around 30% of global primary energy consumption (IEA, 2012c; IEA, 2011). Accounting for over 40% of the electricity output in the same year, it can be defined as the backbone of global electricity generation (IEA, 2011).

The increase in usage of coal for electricity generation is currently the single most problematic trend is the relationship between energy requirement and climate change. Due to the dependency on coal in several regions, it is likely that coal-fired power generation will continue to be substantial. To reduce the climate change impact of coal power, increasing the efficiency of the power plants, as well as having carbon-capture storage are important solutions. A more low cost alternative however is to increase the usage of co-firing with biomass, which is currently one of the most mature and promising technological options to reduce the dependency on coal and the climate change impacts that follow it. Co-firing is therefore looked upon as a way to give a smooth transition to energy sources that are both renewable and sustainable.

Co-firing of biomass in a coal power plant only requires minor retrofitting of existing coal power plants, and is therefore seen as an easy and feasible way of integrating biomass into the power generation sector (Kabir and Kumar, 2012; Sebastián et al., 2011) Investment costs can therefore be reduced, and the biomass conversion can take advantage of the generally higher efficiency of large-scale power plants (Sebastián et al., 2011). Agricultural and forest biomass are the main resources used for power production, in the form of bale and chips (Kabir and Kumar, 2012).

Traditionally it is assumed that carbon dioxide (CO_2) emissions from biomass combustion are climate neutral if the bioenergy system is carbon (C) flux neutral, i.e. that the CO_2 released from biofuel combustion equals the CO_2 sequestered in biomass (Cherubini et al., 2011a). This is strengthened with the guideline the Organisation for Economic Cooperation and Development (OECD) introduced in 1991, which states that "CO_2 emissions resulting from bioenergy consumption should not be included in a country's official emissions inventory" (OECD, 1991). In the field of industrial ecology and more specifically life cycle assessment (LCA), carbon neutrality has been assumed by a great majority. This results however in underestimating the true climate change impact of bioenergy (Cherubini et al., 2011a).

The contributions from biogenic CO_2 are divided between emissions from direct combustion of the final form of the bioenergy or biofuel, and the emissions from upstream processes such as harvesting (Bright et al., 2012). Carbon neutrality may be a reasonable assumption when the bioenergy is derived from fast growing biomass feedstock such as willow or rapeseed, but becomes more questionable for slow growing feedstock, for instance forest biomass with long rotation periods. This especially applies to boreal forest, which also has slow carbon turnover rates. For near-term climate change mitigation, this type of biomass is therefore not the best feedstock to utilise (Bright et al., 2012). The biogenic CO_2 connected to direct biomass combustion as well as the albedo effect are therefore important metrics to take into consideration in LCA.

In areas such as high latitude boreal regions, which have a long winter season, the albedo effect plays an important role. This is due to the albedo of forests being the dominant biophysical factor in terms of regulating the surface energy fluxes and hydrologic cycle. As it is in direct opposition with the carbon cycle, when particularly strong, it can even outweigh the biogenic CO_2 and create a cooling effect at the site. Albedo is site-specific, so therefore it is important to quantify it for the forest management or site in question (Bright et al., 2011). The cumulative effects of albedo changes in forests over time and it is therefore of interest to investigate if an increased forest harvest for bioenergy purposes in Russia would give a net cooling effect due to enhanced surface albedo.

Several studies have been conducted with focus on bioenergy and co-firing. The amount of studies that consider the temporary change in atmospheric CO_2 concentration caused by

biogenic CO_2 emissions and cooling effects from changes in surface albedo following harvest, are however limited. Moreover, the amount of studies undertaken in Russia is scarce, despite the large biomass resources available in this region. This is emphasised in a review done by Cherubini and Strømman in 2011 on life cycle assessments of bioenergy systems (Cherubini and Strømman, 2011b). 94 studies were reviewed, with 74 being papers published in scientific journals, and none of them covered the Russian Federation. The lack of studies and documentation is also highlighted in an article by Kraxner et al from 2011 that explores forest-based energy in a Eurasian context (Kraxner et al., 2011).

The constant supply of sustainable biomass resources is vital to achieve reductions in coal usage. There are multiple sources of biomass, but forest wood is one of the most widespread raw materials, which can be used in many applications connected to bioenergy. In addition it can be used for gas-, solid and liquid biofuels and domestic heating and cooking purposes (Michelsen et al., 2012; Cherubini et al., 2011a). For bioenergy and co-firing opportunities, the forest areas of the Russian Federation are the basis for this study. The total area of forestland in Russia in 2010 amounted to 882 million hectares, with 611 million hectares being exploitable (FAO, 2012). Even with being a "biomass superpower", looking at an industrial scale, the energy sector, forest biomass and associated bioenergy production plays a rather minor role in the Russian society. In 2010 only around 2% of the total energy consumption was from bioenergy (IEA, 2012b). The annual harvest was 173,6 million m^3, but with an annual allowable cut of 633 million m^3 and an annual increment available for exploitation of 552 million m^3, it is apparent that there is a significant unused potential (FAO, 2012).

Certain studies claim a bioenergy potential for Russia of 50-205 EJ[1] annually by 2050 (Smeets et al., 2007) while studies on the global energy potential indicate a total of 10-76 EJ annually for non-European OECD countries (184 EJ/yr globally) (Offermann et al., 2011). The Intergovernmental Panel on Climate Change (IPCC) reports that the upper bound for the technical potential of biomass for energy may be as much as 500 EJ/yr by 2050 on a global scale (IPCC, 2012). These estimates consider all types of biomass. Based on numbers from the Forest Sector Outlook Study conducted by United Nations Food and Agriculture Organization (FAO), the current potential in Russia is 8-9 EJ based on the exploitable forest

[1] Exajoule – 10^{18} joule

resources. Even with significant differences in the estimated values, there is a consensus that there is unexploited potential currently in the Russian Federation, and that the forest sector in Russia does not contribute to a significant share of the output in value terms (Backman, 1997).

However, reaching a substantial fraction of these potentials would require measures such as a sophisticated land and water management and a large increase in worldwide plant productivity (IPCC, 2012). The assessment from International Energy Agency (IEA) concerning the world energy outlook (IEA, 2012e), concludes that the global energy resources are more than sufficient to meet the projected demand without competing with food production, although the land use implications will have to be managed in a sustainable manner. In some regions, the policy goals will exceed the production capacity, and international trade of solid biomass is estimated to increase about six-fold, with import focus especially on the European Union, India and Japan (IEA, 2012e).

In 2010, the Russian Federation produced 10% of global energy, 20% of global natural gas and 12% of global oil, and is increasing its production faster than its domestic supply. Worldwide, Russia currently holds the position as first exporter of natural gas, second exporter of crude oil and third exporter of coal (IEA, 2012b). Why focus on all the unexploited forest biomass in the country?

The share of bioenergy in the total energy consumption is generally increasing in the G8 countries[2], a lot due to the use of modern biomass forms (i.e. co-firing or co-combustion for electricity generation) (GBEP, 2008). This is especially happening in Germany, Italy and the UK, but with improved policies and subsidies, the remaining countries may also increase their usage. In addition, the global primary energy demand for bioenergy, excluding traditional biomass, is forecasted to more than double from 2010 to 2035 (from 526 Mtoe to 1200 Mtoe), growing at an average of 3% per year (IEA, 2012e).

Recently the United Nations launched its Sustainable Energy for All initiative, which has the target of doubling the share of renewable energy globally by 2030. There is also the ongoing schemes of the European Union since 2009 through the Renewable Energy Directive which has set legally binding targets that the share of renewable energy (covering electricity, heat

[2] G8 countries: Canada, France, Germany, Italy, Japan, Russia, the United Kingdom, and the United States

and biofuels) in gross final energy consumption has to equal 20% by 2020 (IEA, 2012e). Russia is not a part of the European Union, but with these policies there will be an increased pressure in the future for the country to further improve its environmental focus, especially due to currently being one of the lead exporters of oil and gas worldwide (IEA, 2012b).

A study by Pantskhava et al from 2006 concludes that Russia has the possibilities of becoming a large exporter of wood chips and pellets to the world, but there are certain factors that hold back the wide use of biomass in the power industry. Three of the most pressing are the lack of special laws and policies concerning renewable energy sources, the lack of leasing for development and selling equipment, and high interest rates on loans, which do not provide attractive conditions for development of equipment. Moreover the transportation infrastructure needs to be further developed (Pantskhava and Pozharnov, 2006).

The capacity of the logging companies allow to some extent an increased volume of forest harvesting, but the main challenges are the limited transportation capabilities. Unutilised energy wood can currently only be supplied if the quantity of all the machines, harvesters, forwarders and especially trucks and chippers are increased (Goltsev et al., 2010). This requires investments in more efficient equipment, but highly productive systems require fewer operators, which can cause negative effects on the labour market. On the contrary, increased harvest may also bring prosperity to areas that are more rural. Therefore one needs to find a balance between cost of equipment, production and the social effects connected to a further exploitation (Goltsev et al., 2010).

Concerning the climate change impact of the upstream processes for bioenergy, a study by Kabir et al (2012) which compared the energy and environmental performances of nine biomass/coal co-firing processes, had upstream processes for biomass resulting in 5,6 g CO_2-eq/$MJ_{fuel\text{-}mix}$ using wood chips from whole tree (Kabir and Kumar, 2012). In an article by Cherubini et al (2012), four cases were compared which also gave various results for upstream process emissions for biomass. For heat production using domestic wood, Canadian wood had upstream processes of 10g CO_2-eq/$MJ_{fuel\text{-}mix}$, wood from the Pacific Northwest in the United States had biomass upstream emissions of 17 g CO_2-eq/$MJ_{fuel\text{-}mix}$, whilst for Wisconsin (USA), the total emissions were 18 g CO_2-eq/$MJ_{fuel\text{-}mix}$. For the case of

Norway, the emissions were significantly lower with 4,4 g CO_2-eq/$MJ_{fuel-mix}$. The total emissions connected to the upstream processes of coal and the coal combustion was 105 g CO_2-eq/MJ_{fuel} (Cherubini et al., 2012).

Furthermore, a study by Mann and Spath (2001) showed that co-firing significantly reduced the environmental footprint of the average coal-fired power plant. By co-firing with 5% and 15%, the greenhouse gas emissions were reduced with 5% and 18% respectively (Mann and Spath, 2001). However, this study, along with most other literature on the subject, does not take biogenic CO_2 and the albedo effect into consideration, so they are not suitable for benchmarking.

For the research connected to biogenic CO_2 and the albedo effect, apart from the aforementioned article by Cherubini et al. (2012), which focuses on the site-specific global warming potentials of biogenic CO_2 for bioenergy, GWP characterisation factors for biogenic CO_2 were developed based on rotation periods of the biomass in an article by Cherubini et al (2011a). These GWP_{bio} factors are used as a basis for the calculations in this thesis. Furthermore, for surface albedo, in addition to Cherubini et al (2012), one of the most important contributions to this field is Bright et al (2012), which focus on how to include the carbon cycle and albedo dynamics in life cycle assessment. These two articles have been the main sources for assessing the surface albedo in this thesis assessment.

For environmental assessments, a framework called Life Cycle Assessment (LCA) is often used. By using this method one takes on a holistic approach, looking at all parts of the life cycle of the system in question, and thereby being able to assess the overall environmental impacts. In addition, the method gives the possibility to compare the results with other examples of energy production, both fossil and renewable. However, the site- and time-generic framework of LCA limits its ability to assess the temporary stock changes and issues of carbon cycling, as this requires a full linkage of atmosphere-biosphere flows of carbon in time and space (Bright et al., 2011). Biogenic CO_2 and surface albedo have for instance proved to far outweigh the GHG emission impacts throughout the life cycle in the cases where biomass is derived from slow growing biomass feedstock, and especially with short time horizons (Bright et al., 2012).

An LCA has therefore been conducted for the upstream emissions connected to biomass and coal, as well as the coal combustion together with additional biogenic CO_2- and albedo calculations, to find the total climate change impact of co-firing of biomass with coal. The LCA framework is described in Chapter 2.1 and the methodology behind biogenic CO_2 and the albedo effect is found in 2.2 and 2.3 respectively.

1.2. Objective

The primary objective for this thesis is to assess the climate change impacts for various shares of co-firing forest biomass with coal to produce electricity and heat in the Russian Federation. The analysis of the climate change impact considers the two most important contributions to global climate change in connection with bioenergy, namely the temporary change in the atmospheric CO_2 concentration caused by biogenic CO_2 emissions and cooling effects following harvest due to changes in the surface albedo.

Three scenarios were chosen to be investigated - 10% co-firing of biomass in a coal power plant, 20% co-firing, and the ideal scenario of the coal demand being covered completely with 100% bioenergy. All the cases were narrowed down to having European Russia as the focus area, and were divided into eight regions, based on the economic regions of the Russian Federation. The case of 100% coal-fired power generation was used as a reference and the functional unit of 1 MJ fuel mix was chosen for all scenarios.

The functional unit may also vary from study to study, with climate change impact often being measured per unit output of electricity or heat. In this study however, the functional unit is input of biomass and coal, measured in energy content of 1 MJ. By having this approach, the results are independent from conversion processes and type of end products. This functional unit is also often chosen when the study aims at comparing the best uses for a given biomass feedstock (Cherubini and Strømman, 2011b; Sebastián et al., 2011).

The assessment is limited to the impact on climate change and focusing on the characterisation factor of Global Warming Potential (GWP) without considering other impact categories where bioenergy could contribute. This is supported by the fact that the main driving factors behind worldwide bioenergy development is climate change mitigation and reduction of fossil fuel consumption (Cherubini and Strømman, 2011b).

As a part of developing the life cycle inventory, for each of the regions a distribution was made of the amount of boreal and temperate climate that covered the region, as well as the amount of coniferous and deciduous forest that could be found there. Furthermore, transportation routes were developed for each region. A life cycle assessment was conducted for each region for each of the scenarios, with focus on the upstream processes connected to coal and biomass input needed for 1 MJ. The emissions from coal combustion were then added, as well as the climate change impact from direct biomass combustion, which was calculated based on the GWP characterisation factors developed for each region. As a final part, by choosing both a forested and open site centrally in each region, one was able to gather data on albedo, develop GWP_{albedo} and calculate the climate change impact. By combining these various results, one was able to get the total climate change impact for the three scenarios for each region. Moreover, information was extracted for the three most common time horizons of 20, 100 and 500 years so one could conduct a more in depth comparison of the various impacts.

It is important to emphasise that the increased harvesting in the scenarios would not stem from bringing new forest area into production, but rather exploiting more of the currently productive forest. Therefore there would be no direct land use change and issues concerning if the land should be for food or energy production (Bright et al., 2011).

1.3. Content outline

The first part of this thesis, Chapter 2, gives an overview of the life cycle framework used for the assessment, as well as the methodology behind calculations connected to biogenic CO_2 and the surface albedo. Chapter 3 provides background information on the current state of the coal power sector in Europe, along with information on the general power sector of the Russian Federation. Furthermore an overview of the forest sector in Russia is given, with special emphasis on the European part. This data has been collected to develop the scenarios, which will also be presented in detail in this chapter. In Chapter 4 the development of characterisation factors for biogenic CO_2 and albedo are shown, as well as results of the life cycle assessments conducted for the three scenarios in the eight regions. This further leads to Chapter 5 where the environmental impacts are discussed in a broad context and benchmarking is conducted, in addition to discussing the further implications

and future scenarios. As a final part, the conclusion is presented in Chapter 6, followed by relevant appendices in Chapter 8.

2. Methodology

This chapter contains three equally important parts. First the environmental assessment tool Life Cycle Assessment (LCA) is presented, which has been used as a basis for the analysis conducted in this project. The different parts of the framework will be explained, including the calculations that are used for reaching the results. In addition the applied life cycle impact assessment method ReCiPe is introduced. Secondly, the theory and calculations connected to biogenic CO_2 will be presented, and as a final part, the methodology behind climate forcing from changes in surface albedo will be explained.

2.1. Life Cycle Assessment (LCA)

Life cycle assessment as a tool has several purposes, but one of the main ones is considered compiling and evaluating the environmental impacts of a project from cradle to grave. In addition, LCA is often used to compare different options for fulfilling the same or a similar function and to identify the areas of the product life cycle where environmental impacts and energy efficiencies can be improved (Brattebø et al., 2007).

The framework of LCA is generally structured in four phases, which can be found below. It has been standardised through the ISO 14 040 international standard, but research, including this thesis, does not necessarily embrace all facets of the standard, but rather practice variations of it.

According to the standard, the phases are:

1. Goal and scope definition
2. Inventory analysis
3. Impact assessment
4. Interpretation

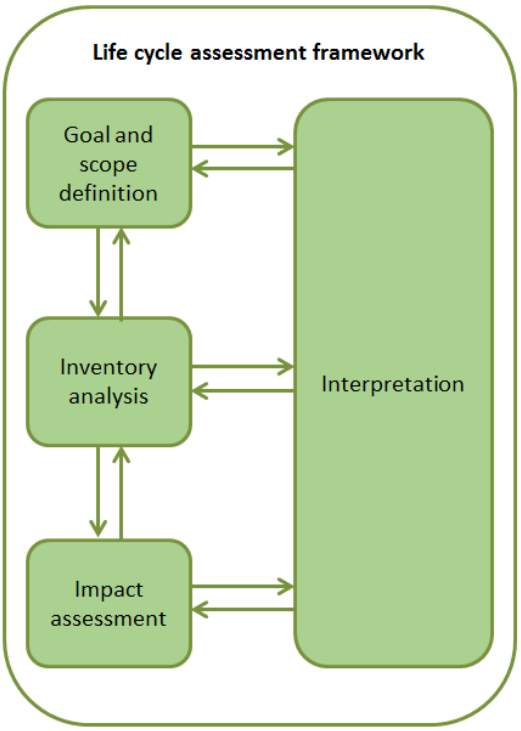

Figure 1: Framework for Life Cycle Assessment (LCA) (Brattebø et al. 2007)

Each of the phases are defined in the ISO 14 040 standard and structured in a number of possible or mandatory steps (Brattebø et al., 2007). As shown in Figure 1, the phases are interrelated and one is therefore able to have a holistic approach to the problem. This is a key part of the concept of industrial ecology.

In the first phase, the goal and scope definition, the aim of the intended study is defined as well as the limits (width) of the system (Brattebø et al., 2007). One of the core elements of the goal definition is defining the functional unit, which is a measure of the function of the system and defines what can be compared of input and output values. For this study, the functional unit is 1 MJ input of fuel mix from coal and biomass for energy production.

When defining the scope one is able to narrow down the width of the study and omit certain elements of the life cycle if they do not differ across product alternatives. Moreover, the environmental impact categories that are relevant to focus on can be defined (Brattebø et al., 2007).

The inventory analysis is the core of the modelling of the system and the most technical part of an LCA (Brattebø et al., 2007). It contains the environmental inputs and outputs for each of the different processes of the defined system and their interrelations. They are presented

as environmental flows (not in monetary values) and it is important that they each have a defined unit to be able to be used further in the analysis.

The aim of the third phase, the impact assessment, is to give an increased understanding of the results from the inventory analysis, so that the overall environmental impacts can be interpreted. It consists of an overview of all the emissions of pollutants and extractions from resources for the functional unit chosen for the assessment (Brattebø et al., 2007). The main focus of the impact assessment is how the various processes contribute to the impact categories. In total there are 18 categories defined, for example Ozone layer depletion and Acidification. For this thesis however, the category of Climate Change has been found the most important focus area. The corresponding indicator to climate change is Global Warming Potential (GWP) and is measured in CO_2-equivalents.

In the final phase, the interpretation part is in focus. The definitions and findings in phase one and two can also be interpreted, but the focus for this analysis is interpreting the results from part three, which is the impact assessment.

2.1.1. Basic contribution analysis

The calculations connected to the impact assessment are based on linear systems and consist of matrices and linear algebra (Brattebø et al., 2007). The calculations can be quite comprehensive if there are several processes involved and large sets of data. The matrices and variables that make up the contribution analysis will now be explained in further detail, with enclature for the LCA framework.

Table 1 presenting the nomenclature for the LCA framework.

Table 1: Nomenclature for the different matrices used in the mathematical framework of LCA (Strømman, 2009)

Sets	**pro**		**Processes**
	str		**Stressors**
	imp		**Impact categories**
Matrices and variables	A	*(pro x pro)*	Matrix of inter process requirements
	y	*(pro x 1)*	Vector of external demand of process
	x	*(pro x 1)*	Vector of outputs for a given external demand
	L	*(pro x pro)*	The Leontief inverse. Matrix of outputs per unit of external demand
	F	*(str x pro)*	Matrix of stressor intensities per unit output
	e	*(str x 1)*	Vector of total emissions generated for a given external demand
	E	*(str x pro)*	Matrix of emissions generated from each process for a given external demand
	C	*(imp x str)*	Characterization matrix
	d	*(imp x 1)*	Vector of impacts generated for a given external demand
	D_{pro}	*(imp x pro)*	Matrix of impacts generated from each process for a given external demand
	D_{str}	*(imp x str)*	Matrix of impacts generated from each stressor for a given external demand

The A-matrix is the main matrix and is called the process requirements matrix. It is built up like a cooking recipe and each element, a_{ij}, denotes how much input of process i is needed per output of process j (Strømman, 2009). The total A-matrix consists of a foreground processes matrix, A_{ff}, background processes matrix, A_{bb} and an A_{bf}-matrix, which represents the upstream inputs of background processes to the foreground system, see Equation (2.1.1) (Strømman, 2009). A foreground process refers to data that is collected for a specific study, whilst a background process consists of data gathered from a database, ecoinvent in the case of this thesis, together with own calculations. The A_{bf}-matrix links the foreground and the background processes together and represents the upstream activities.

$$A = \begin{pmatrix} A_{ff} & 0 \\ A_{bf} & A_{bb} \end{pmatrix} \tag{2.1.1}$$

The A-matrix is further used to set up a production balance and find the output vector x, see Equation (2.1.2).

$$x = Ax + y \tag{2.1.2}$$

The right hand side of the Equation represents the total demand for x. It consists of two parts, where Ax represents the intermediate (internal) demand of products between the various processes in the production network, and y is the external demand, which

represents the requirement of products that the network has to deliver (Strømman, 2009). y is typically the functional unit of the system.

The Equation is solved for the unknown output of the processes, the x vector, and can be expressed as Equation (2.1.3) (Strømman, 2009). The coefficients l_{ij}, shows how much output from process *i* that is required per unit of external demand *j*, see Equation (2.1.4).

$$x = (I - A)^{-1} y \tag{2.1.3}$$

$$L = (I - A)^{-1} \Rightarrow x = Ly \tag{2.1.4}$$

A contribution analysis needs to be conducted to be able to calculate the total amount of emissions and environmental load for a given external demand. The first part consists of establishing a stressor intensity matrix, S, which is a vector comprised of stressors per unit from each of the specific processes (Strømman, 2009). Stressors are a more general term for emissions, and are used to categorise other environmental impacts as well such as land use, and not only direct pollution.

When the S matrix is established, it can be applied to find the stressors associated with a given final demand, see Equation (2.1.5) (Strømman, 2009).

$$e = Sx \tag{2.1.5}$$

To more easily assess the environmental impacts, a characterisation matrix, C, is introduced. This matrix is used to "convert emissions of different substances with the same type of environmental impact into equivalents" (Strømman, 2009). An example is global warming potential (GWP), which is measured in CO_2-equivalents. There are several greenhouse gases that contribute to global warming, but the objective is to gather all of them into a common impact category, and therefore global warming as a whole is expressed in the form of CO_2- equivalents. If one is interested in finding the amount of CO_2-equivalents for methane (CH_4), one needs to multiply the value with a factor of 25, which is the most recent number from the Intergovernmental Panel on Climate Change (IPCC), and indicates that 1 kg of methane emitted equals the same as 25 kg of CO_2 (IPCC, 2006). Acidification is an example of another impact category and is expressed as SO_2-equivalents (Strømman, 2009). With the

characterisation matrix identified, one can further calculate the d vector, which represents the total impacts of a given external demand. See Equation (2.1.6).

$$d = Ce = CSx \tag{2.1.6}$$

It is important to understand how the various processes, as well as the stressors, contribute to the different impact categories. This can be expressed by D_{pro} and D_{str}, see Equation (2.1.7) and (2.1.8). Equation (2.1.9) illustrates that the sum of the rows in D_{pro} and D_{str} is the vector with total impacts, d (Strømman, 2009).

$$D_{pro} = CS\hat{x} \tag{2.1.7}$$

$$D_{str} = CSx \tag{2.1.8}$$

$$d = \sum_{pro} D_{pro} = \sum_{str} D_{str} \tag{2.1.9}$$

2.1.2. Life Cycle Impact Assessment (LCIA) – ReCiPe method

For the assessment of environmental impacts, several frameworks can be used. For this thesis, the ReCiPe method has been chosen. Characterisation models are a source of uncertainty, as one cannot completely comprehend the environmental mechanisms. The various sources of uncertainty and different choices are therefore modelled into three scenarios or perspectives. They are the individualistic (I), hierarchical (H) and egalitarian (E) perspective and are merely used to group similar types of assumptions and choices (Goedkoop et al., 2009). The individualistic perspective is based on short-term interest, undisputed impact types and technological optimism concerning human's way of adapting. The hierarchical perspective is based on the most common policy principles with regards to time frame in today's society. The egalitarian perspective, which is the most precautionary perspective, has the longest time-frame and takes into account both the impact categories that are already well established, and the ones that are still under development (Bare et al., 2000).

For the impact category of climate change, the individualist perspective uses a time frame of 20 years, the hierarchic perspective, 100 years, and the egalitarian world view assumes a 500 year time frame (Goedkoop et al., 2009). For this thesis, the hierarchic view has been chosen as the main time horizon as it represents an "average view", but most results have

been displayed in all three time horizons (TH) for comparison and illustrating the significant effect the time horizon can have on the results.

In the environmental impact assessment one also distinguishes between using midpoint- or endpoint indicators for the impact categories. In this thesis midpoint indicators have been chosen, which for climate change is CO_2-equivalents. If endpoint indicators had been chosen instead, the focus would have been Human health damage [DALY] or Ecosystem damage [Species, yr]. More information about the midpoint and endpoint indicators can be found in the article by Bare et al (2000) and is displayed in Figure 2 below.

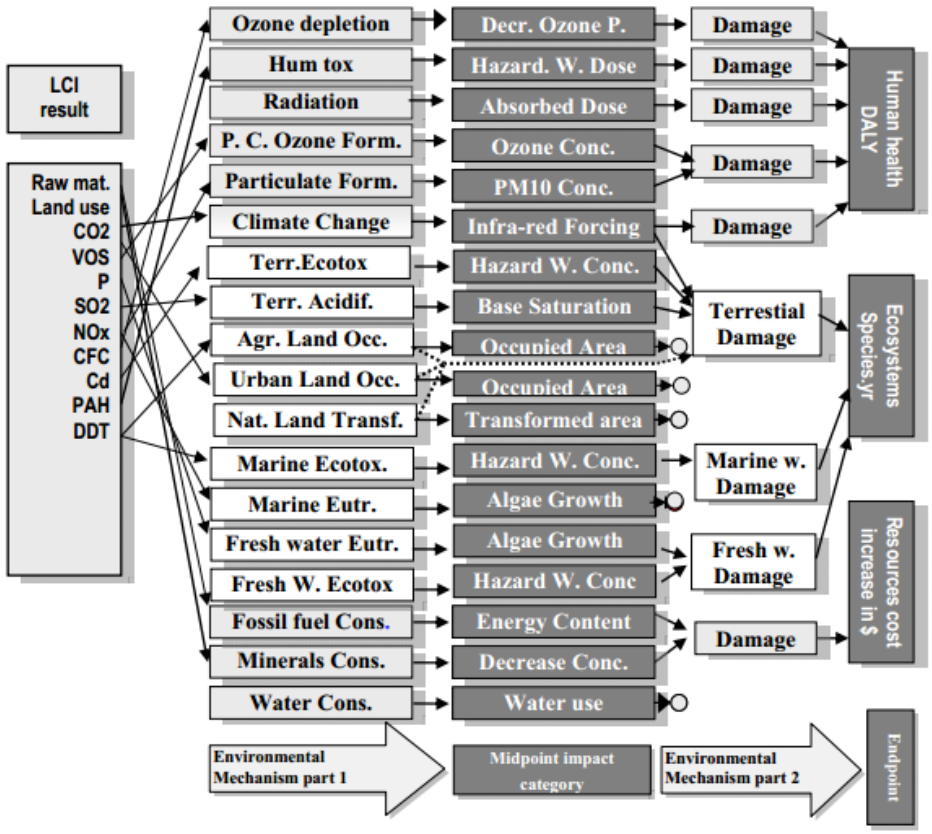

Figure 2: Relationship between life cycle inventory parameters (left), midpoint indicator (middle) and endpoint indicator (right) in ReCiPe 2008 (Goedkoop et al., 2009)

Whether it is best to use the midpoint indicators or endpoint indicators is a widely discussed topic in the research community of life cycle assessment. For further reading see the article by (Hertwich and Hammitt, 2001).

2.2. Biogenic CO_2 methodology

Biogenic CO_2 is defined as the CO_2 fluxes circulating between the vegetation and the atmosphere. An example is i.e. CO_2 from oxidation of carbon in bio-materials harvested for

energy (both at the conversion plant and through the various life-cycle stages), dead organic matter decomposition and CO_2 sequestered by growing biomass (Cherubini et al., 2012). CO_2 emissions from C flux neutral systems (which is from temporary C losses) contribute to climate change, alongside the CO_2 emissions from the permanent C losses. The reason for this is that before being captured by regrowth of the biomass, the CO_2 molecules spend time in the atmosphere and contribute to global warming. A forest may take up to 100 years to regrow, and it is only at the end of the proper time boundaries that the system can be defined as C neutral (Cherubini et al., 2012).

Cherubini et al (2011a) have developed a method to estimate the climate change impacts from biomass combustion and is the basis for the calculations in this thesis. The methodology will be explained in detail in the following paragraphs. In short, the method uses CO_2 impulse response functions (IRF) from C cycle models in the elaboration of atmospheric decay functions for biomass derived CO_2 emissions. The contributions to global warming are then estimated with a unit-based index, the characterisation factor GWP_{bio}, which is a function of the rotation period of biomass. Due to this, it can be applied to all cases of biomass species (Cherubini et al., 2011a).

Figure 3 below is a simplified graph explaining the carbon flux neutral system. In a) one sees the biomass stand in steady state. b) Represents all aboveground carbon being harvested and emitted to the atmosphere as CO_2. Simultaneously, the same biomass is replanted and starts growing by sequestering the CO_2 released from combustion. Finally in c) one sees that at the end of the rotation period, the same quantity of carbon originally released is sequestered once again in the vegetation (Cherubini et al., 2011a).

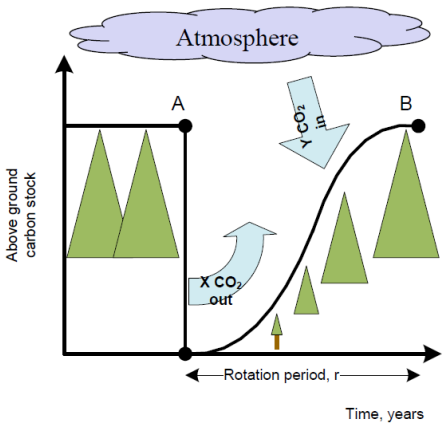

Figure 3: Simplified scheme of the carbon flux neutral system (Cherubini et al., 2011a)

In general, the concentration in the atmosphere of biogenic CO_2 over time can be described by the means of an IRF. The IRF refers to the reaction (as a function of time) of any dynamic system in response to some external change. The atmospheric decay of biogenic CO_2 is in this thesis therefore derived through a combination of the biomass regrowth sink together with the IRF modelling the removal of CO_2 by the ocean and/or terrestrial biosphere sinks. Furthermore, the atmospheric CO_2 concentration *f(t)* after a pulse emission can be represented as the sum of earlier emissions *g* at time *t',* multiplied by the fraction that has remained in the atmosphere after time *t-t'* (Cherubini et al., 2011a).

Once in the atmosphere, CO_2 molecules of biogenic origin are identical to fossil derived CO_2-molecules, but the time profile of the atmospheric decay should be understood as principally different. A more complex decay profile based on IRF's with several decay times is used for anthropogenic CO_2. The absolute global warming potential (AGWP) due to a pulse GHG emission, relative to that of a CO_2 over the same integration horizon, is known as GWP. This is expressed in terms of CO_2-equivalents (Bright et al., 2011).

The final Equation to be used is therefore as follows:

$$f(t) = y(t) - \int_0^t g(t')y(t-t')dt' \ (C_0=1) \tag{2.2.1}$$

This describes the atmospheric decay of a pulse of biogenic CO_2 over time, with *g(t')* representing the regrowth of biomass and being defined by the following Equation:

$$g(t) = \frac{1}{\sqrt{2\pi\sigma^2}} e^{-(t-\mu)^2/2\sigma^2} \tag{2.2.2}$$

For the specific case of CO_2-emissions:

$$f_{bio-CO_2}(t) = y_{CO_2}(t) - \int_0^t g(t')y_{CO_2}(t-t')dt' \tag{2.2.3}$$

Furthermore, *y(t)* represents the IRF and has three possible scenarios. The first scenario represents biogenic CO_2 emissions being removed from the atmosphere by the onsite biomass growth and thereby following the convention of OECD[3]. This is a closed perspective and referred to as the vegetation IRF (VIRF). The second option focuses on that the key role

[3] OECD: Organisation for Economic Co-operation and Development

of the oceans in the removal of CO_2 from the atmosphere. The ocean sink is therefore added to the vegetation regrowth sink by considering a proper climate model and thereby giving a specific profile for the atmospheric decay of biogenic CO_2. This scenario is called the ocean and vegetation IRF, OVIRF. The final case is the full IRF, FIRF, which is when a complete IRF is used and thereby represents the CO_2 being able to be removed by both the ocean and terrestrial biosphere (Cherubini et al., 2011a). The full IRF is used as the basis for this thesis assessment.

In all the cases, the resulting function *f(t)* is used to get an index of the relative climate change impact of CO_2 emissions from biomass combustion.

$$GWP_{bio} = \frac{AGWP_{bioCO_2}}{AGWP_{CO_2}} = \frac{C_0 \int_0^{TH} \alpha_{CO_2} f(t)dt}{C_0 \int_0^{TH} \alpha_{CO_2} y(t)dt} \quad (2.2.4)$$

where *f(t)* represents the IRF for biogenic CO_2 and *y(t)* the IRF for CO_2, and α_{CO_2} is the radiative efficiency, which for CO_2 is:

$$\alpha_{CO_2} = 5,35 \ln\left(\frac{[CO_2^*]}{[CO_2]}\right) \quad (2.2.5)$$

where $[CO_2^*]$ is the concentration in the atmosphere after small perturbation and $[CO_2]$ is the initial concentration of CO2 in the atmosphere.

In the FIRF alternative, the CO_2 emissions from biomass combustion are considered to be removed from all the possible sinks, both the oceans, terrestrial biosphere and on-site biomass regrowth. As the biogenic CO_2 emissions therefore become integrated fully into the global C cycle, one can refer to it as a full IRF.

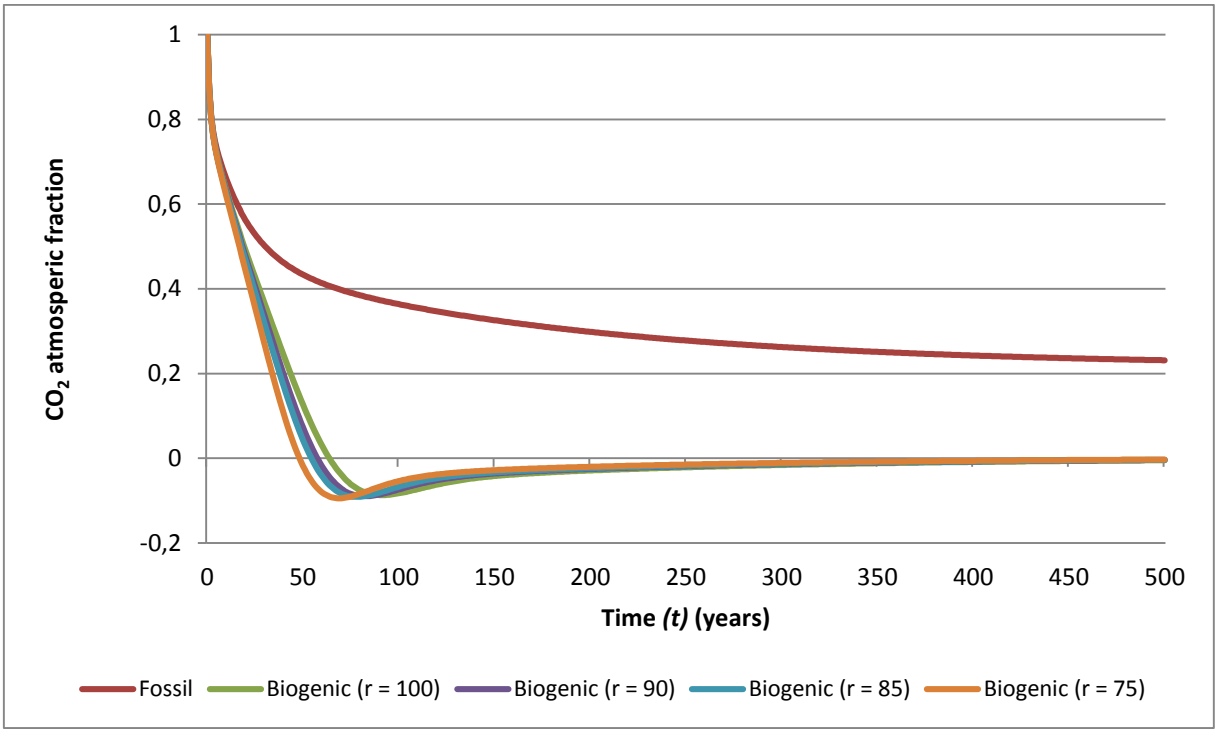

Figure 4: CO_2 atmospheric decay following the FIRF method for the selected rotation periods (*t*, years) of the cases presented in this thesis

Concerning the biomass rotation period, the longer it is, the longer is the average stay of CO_2 in the atmosphere. In the long term however, all the decays asymptotically tend to zero, as long as a C flux neutral system is modelled. At around t = 50-65 years in Figure 4 above, there are certain negative values, meaning that there is less CO_2 in the atmosphere than before the emissions occurred. This is due to the atmospheric CO_2 being taken up in different biogeochemical sinks at different time constants, which are also applied to the uptake of CO_2 in biomass regrowth.

Shortly after the emissions, when the biomass growth rate is still low, a significant fraction of the CO_2 originally released is quickly stored in the upper layer of the ocean. Next, the C is transported to the deeper ocean layers and is slower than the previous processes. Therefore, when the uptake by the onsite biomass regrowth increases, the C initially stored in the upper layer of the ocean will be released at a lower rate back to the atmosphere to compensate for the initial over absorption (out-gassing). The climate change impact derived from biomass combustion and further reabsorbed in terrestrial sinks and ocean can never become higher than the same quantity released by fossil fuel combustion or deforestation. In the long term, the airborne fraction of biogenic CO_2 reduces itself towards zero (Cherubini et al., 2011a).

See Figure 5 below for an illustration.

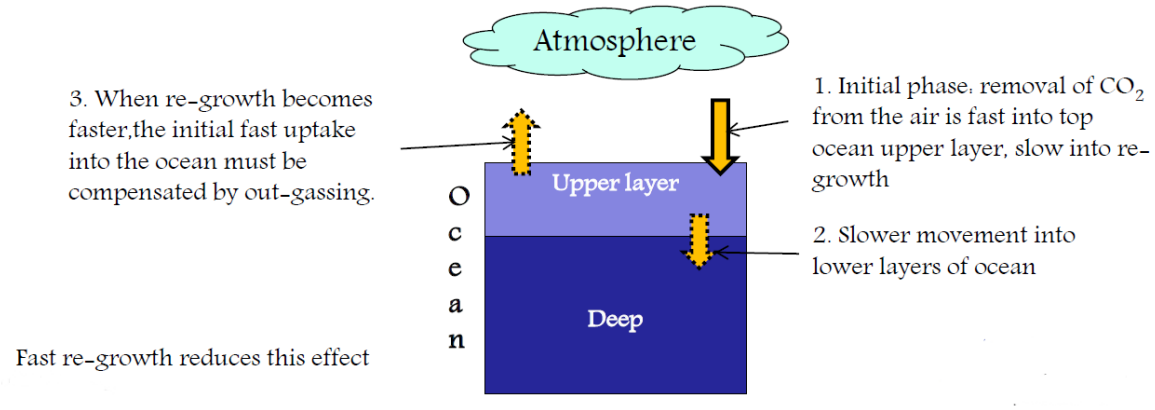

Figure 5: Illustration of the ocean uptake of CO_2 (Cherubini, 2012)

GWP_{bio} is used the same way as other GWP equivalency factors and is therefore to be multiplied by the direct CO_2 emissions from combustion of biomass to get their relative contribution to global warming in terms of kg CO_2-eq. This way one can incorporate the climate change impact of CO_2 flux neutral systems in LCA and other assessment tools. The GWP factor can be used for all types of biomass, but in the cases of biomass with short rotation periods such as annual crops, the GWP_{bio} is very small (Cherubini et al., 2011a). As this thesis is looking at temperate and boreal forest with rotation periods between 75 and 100 years, the GWP_{bio} has shown to have quite a significant contribution to the total climate change impact. In the results section in Chapter 4.2, one can also see a comparison between the three most common time horizons, 20, 100 and 500 years and illustrates that bioenergy is particularly an effective long-term strategy for climate change mitigation.

CO_2 fluxes on the forest site or plantation after harvest are site specific and based on Net Ecosystem Productivity (NEP). If it is not feasible to measure it directly at the site, it can be modelled indirectly. Due to lack of data, neither was possible for this thesis, but the methodology for modelling is still explained below.

$$NEP = NPP - R_h \tag{2.2.6}$$

where NPP is the Net Primary Productivity and R_h is the heterotrophic respiration, which is CO_2 emissions from oxidation of dead organic materials. If $NEP > 0$ (larger than zero), the forest (or ecosystem in question) is a CO_2 sink and NPP (photosynthetic production)

dominates. If $NEP < 0$, the forest is a CO_2 source and the respiration process, R_h, dominates. NEP profiles are usually shown in mass C per year (Cherubini et al., 2012).

To be able to compute the IRFs for biogenic CO_2 emissions, one can use the following Equation:

$$f(t) = \int_0^t \left[\delta(t') - NEP(t')\right] \cdot y(t - t')dt' \qquad (2.2.7)$$

where *f(t)* represents the change caused in the atmospheric CO_2 concentration (decay/IRF), $\delta(t')$ represents the emissions from combustion, $NEP(t')$ equals the fluxes on site after harvest and $y(t-t')$ represents the CO_2 decay (Cherubini et al., 2012).

2.3. Climate forcing from changes in surface albedo

2.3.1. Global energy flows

Before explaining the concept of albedo, an introduction to what factors determine the Earth's climate will be given. The amount of energy reaching the top of Earth's atmosphere each second on a surface area of one square meter facing the Sun during daytime is around 1 370 Watts. Approximately one quarter of this is the average amount of energy per square meter per second over the entire planet. Of the sunlight that reaches the top of the atmosphere, around 30% is reflected back to space. Clouds and small particles in the atmosphere known as "aerosols" are responsible for around two-thirds of the reflection back to space, and the remaining part is due to light-coloured areas of the Earth's surface, mainly snow, ice and deserts (IPCC 2007, 2007). An example here is the boreal areas in the Northern parts of Russia with seasonal snow cover.

The energy that is not reflected back to space is absorbed by the Earth's surface and atmosphere, with the total amount being around 240 W/m^2. To balance this incoming energy, the Earth itself radiates on average the same amount back to space by continuously emitting outgoing longwave radiation (IPCC 2007, 2007).

The global energy flows are illustrated in Figure 6.

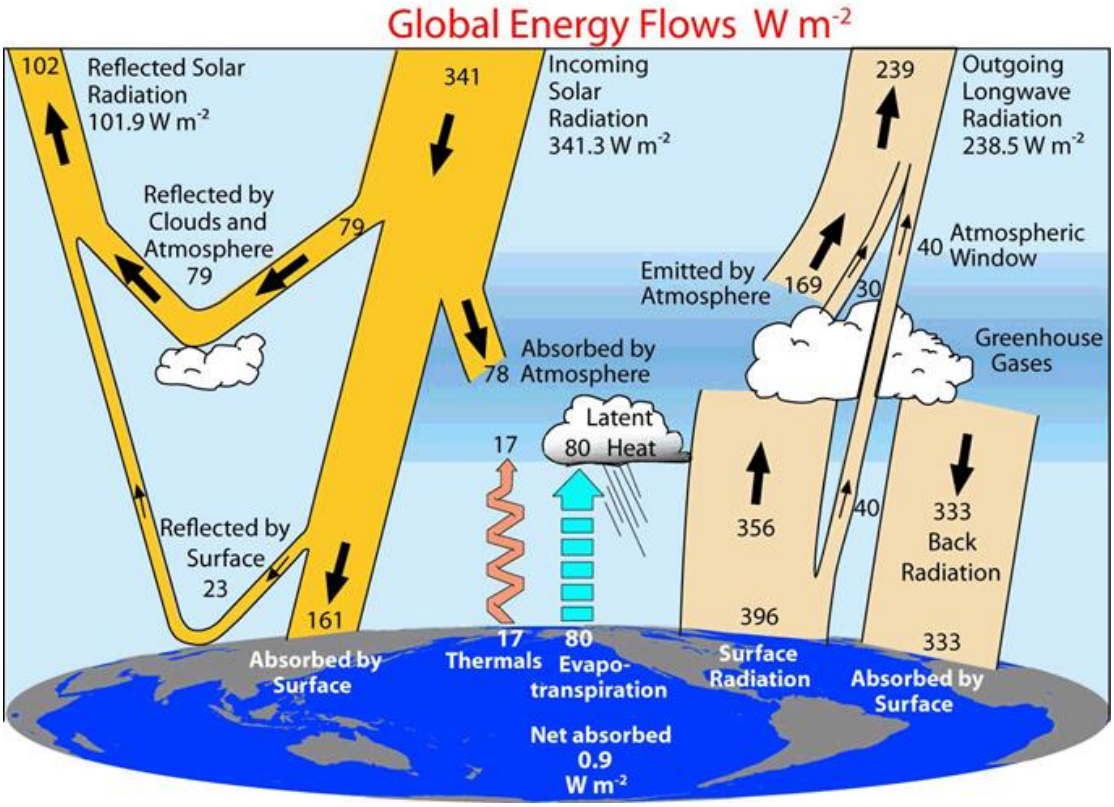

Figure 6: The global annual mean Earth's energy budget for the period of March 2000 to May 2004 [W/m²]. The broad arrows indicate the schematic flow of energy in proportion to their importance (Trenberth et al., 2008).

The presence of greenhouse gases is the reason the surface of the Earth is warm. They act as a partial "blanket" for the continuous longwave radiation being emitted from the surface, and this effect is known as the natural greenhouse effect. There are several feedback mechanisms in the climate system, both positive and negative, which influence the effects of a change in climate forcing. An example is the so-called "ice-albedo feedback loop". As rising concentrations of greenhouse gases warm the Earth's climate, snow and ice begin to melt, which result in darker areas and water surfaces appearing that initially were hidden under the ice and snow. These darker surfaces absorb more of the heat from the Sun, which causes an increased warming, which further results in more melting, and so on (IPCC 2007, 2007). This is why surface albedo and the cooling effect it gives in areas with seasonal snow cover is important to keep in mind when designing bioenergy strategies. Open landscape has more snow coverage, causing more cooling than a forested area, which has a darker surface.

2.3.2. Theory behind the albedo effect

Surface albedo, α_s, can be defined as the ratio of reflected radiation from the surface to incident radiation upon it, and is measured on a scale of zero for a black body and one for a white body (Bright et al., 2012). As a part of the calculations in this thesis, 16 sites were

chosen, two per region and the MODerate Resolution Imaging Spectroradiometer (MODIS) from NASA was used, which provides high quality, cloud-cleared albedo data for various land surface types. In general, global MODIS albedo product (BRDF/MCD43) subsets for all sites (by providing the coordinates), area and time period can easily be accessed online free of charge via the MODIS Data Subsetting and Visualization Tool (ORNL DAAC, 2010).

Concerning the calculations connected to radiative forcing from change in albedo, for the case of biomass grown for bioenergy, an instantaneous radiative forcing from albedo is given by this formula:

$$RF_{\alpha} = -R_{TOA}\Delta\alpha_{p} \quad (2.3.1)$$

where R_{TOA} represents the incoming solar radiation flux at the top of the Earth's atmosphere (TOA) and $\Delta\alpha_{p}$ shows the variation in planetary albedo (Bright et al., 2012). The latter part is linearly related to changes in surface albedo, $\Delta\alpha_{s}$, by a two-way atmospheric transmittance parameter called f_a, which accounts for the reflection and absorption of solar radiation throughout the atmosphere (Bright et al., 2012):

$$RF_{\alpha} = -R_{TOA}\, f_a(\alpha_{s,new} - \alpha_{s,old}) \quad (2.3.2)$$

where f_a is the product of the clearness index K_T, which is the fraction of R_{TOA} that reaches the surface of the Earth after reflection from clouds and absorption by the atmosphere, and T_a, which represents an atmospheric transmittance factor, or the fraction of the radiation reflected at the surface that arrives back at the TOA (Bright et al., 2012):

$$f_a = K_T T_a \quad (2.3.3)$$

To find the values for K_T, NASA has a database that freely offers information about minimum, maximum and average values for K_T for a given location and time, from one single month to a 22-year period (NASA, 2013). For the case of this thesis, the average monthly values for a period of 22 years was chosen. For T_a, a value of 0,854 (Lenton and Vaughan, 2009) was used and represents the global annual average, as literature with values for specific sites is limited.

Further, to find the R_{TOA} on any given Julian day of the year from 1 to 365, d_i, one needs to know the latitude *L* in degrees of the site, the declination angle δ in degrees, as well as the sunset hour angle in degrees, ω (Bright et al., 2012). With this information, one can then use the following formula:

$$R_{TOA,i} = \frac{R_{sc}}{\pi}(1+0.033\cos\frac{360d_i}{365})\cdot(\cos L\cos\delta\sin\omega+\frac{\pi\omega}{180}\sin L\sin\delta) \quad (2.3.4)$$

where R_{sc} is the solar constant (in W/m^2) and the further parameters are found using the following Equations (Bright et al., 2012):

$$\delta = 23.45\sin(360\frac{284+d_i}{365}) \quad (2.3.5)$$

and

$$\omega = \cos^{-1}(-\tan L\tan\delta) \quad (2.3.6)$$

Regarding the mean annual extraterrestrial radiation at the top of the atmosphere, $R_{TOA,ann}$ is then found by the formula below (Bright et al., 2012):

$$R_{TOA,ann} = \frac{\int_{i=1}^{i=365} R_{TOA,i}}{365} \quad (2.3.7)$$

By inserting $R_{TOA,ann}$ into Equation (2.3.2) together with the calculated mean values for $\Delta\alpha_s$ and f_a, one then gets the value for mean annual instantaneous forcing from a surface albedo change, RF_α (Bright et al., 2012).

When initial albedo change is only temporary, for instance when forest being harvested is immediately replanted again, the original surface albedo value, $\alpha_{s,old}$, will at a certain point return, e.g. when $\Delta\alpha_s$ = 0. However, until this point, an instantaneous forcing τ will occur, which needs to be accounted for. For this to be possible, an expression that describes the "decay" of the initial surface albedo change as a function of time, *t* is introduced:

$$\Delta\alpha_s(t) = y_\alpha(t)\Delta\alpha_s \tag{2.3.8}$$

where $y_\alpha(t)$ describes the time evolution of the initial albedo change and is dependent on the vegetation dynamics of the type of vegetation that is newly planted on the same site. $y_\alpha(t)$ is therefore always both case specific and a factor between 0 and 1, alongside y_{CO_2} (Bright et al., 2012).

With this accounted for, the local mean annual instantaneous radiative forcing from mean annual albedo change (in W/m^2) as a function of time can be expressed, as displayed below (Bright et al., 2012):

$$\Delta RF_\alpha(t) = -R_{TOA,ann}\, f_{a,ann} y_\alpha(t)\Delta\alpha_{s,ann} \tag{2.3.9}$$

Harvesting of biomass induces a radiative forcing due to a change in surface albedo in local W/m^2, and to be able to compare the forcing with emissions from CO_2, Equation (2.3.9) needs to be converted to a global forcing. This is simply done by dividing the local area with the Earth's surface area:

$$\Delta RF_\alpha^{Global}(t) = -R_{TOA,ann}\, f_{a,ann} y_\alpha(t)\Delta\alpha_{s,ann} A_A A_E^{-1} \tag{2.3.10}$$

where A_A is the local area affected (in m^2) and A_E is the area of the Earth's surface (Bright et al., 2012).

The final formula that describes the radiative forcing from changes in surface albedo on a monthly basis can be found below (updated from the work by Bright et al., 2012).

$$RF_\alpha(t) = \frac{\sum_{m=1}^{m=12} -\bar{R}(m)\,\bar{f}(m)\Delta\bar{\alpha}(m)A_{aff}}{12} y_\alpha(t) A_{Earth}^{-1} \tag{2.3.11}$$

where $\bar{R}(m)$ represents the mean incoming solar radiation at top of the atmosphere (TOA) over months (m), $\bar{f}(m)$ describes the atmospheric transmittance parameter accounting for the monthly mean reflection and absorption of solar radiation, $\Delta\bar{\alpha}(m)$ is the difference in monthly mean surface albedo between standing biomass and clear-cut sites and A_{aff}

represents the affected area. $y_\alpha(t)$ is the function describing the albedo return to pre-harvest levels and A_{Earth}^{-1} is the area of the Earth of $5{,}1 \cdot 10^{14}$ m² (Cherubini et al., 2012).

The next and final step is to find the characterisation factor GWP_{albedo}. For the derivation for this factor, one always assigns A_A with a factor of 1 m². GWP is defined as the time-integrated global radiative forcing (in W/m²) from a 1 kg pulse emission of a GHG type x, relative to that of CO_2 across any time horizon in kg CO-eq/m². Integrating $\Delta RF_\alpha^{Global}(t)$ over the same time horizon will therefore allow one to determine a characterisation factor for an albedo change in kg CO_2-eq/m² of the surface area of the local land, which is affected in the case-specific region (Cherubini et al., 2012). However, before this one needs to include the climate efficacy.

The climate efficacy corrects for the fact that certain forcing agents are more effective than others, and the albedo efficacy in terms of affecting the global surface temperature is 1,5-5 times higher than CO_2. The climate efficacy is defined as the global mean temperature change per unit forcing produced by the specific forcing agent, relative to the response produced by a standard CO_2 forcing (Cherubini et al., 2012).

$$E_i = \frac{\Delta T_i / RF_i}{\Delta T_{CO_2} / RF_{CO_2}} \tag{2.3.13}$$

An example of values can be found below.

Table 2: Climate efficacies for the most common forcing agents (Hansen et al., 2005)

Forcing agent	Climate efficacy
CO_2	1
CH_4	1,33
N_2O	1,17
Δ Albedo	1,94

Based on this, an efficacy of 1,94 for albedo was used for the calculations. The final characterisation factor for surface albedo when biomass is harvested for bioenergy is displayed below.

$$GWP_{Albedo} = \gamma^{-1} \frac{\int_0^{TH} E_{albedo} \Delta RF_\alpha(t) dt}{\int_0^{TH} E_{CO_2} \Delta RF_{CO_2}(t) dt} \tag{2.3.14}$$

where γ represents the carbon yield in kg-bioCO_2 per affected area.

The results can be found in Chapter 4.1.

Surface albedo is site-specific and the reason for this is that forested areas reflect less incoming radiation than open land areas, especially in regions that are affected by seasonal snow cover. An example could be that open land before afforestation has an albedo effect of $\alpha \approx 0{,}86$ and for forest land it would be $\alpha \approx 0{,}23$. Bioenergy from managed forests causes *temporary* changes in albedo, which is very significant when snow is present. If one goes from "open land" to "forest land" (harvesting), one causes a global warming. If one goes from "forest land" to "open land" one will experience a global cooling (Cherubini, 2012). This is why for instance a forest fire in Alaska caused a net cooling effect, as the warming from biogenic CO_2-emissions and cooling from albedo gave a "negative" net effect (Randerson et al., 2006). Another example is that deforestation in northern latitudes (and thereby snow-covered during parts of the year) cools the climate on a global scale (Bala et al., 2007).

The climate change impact can be quantified anywhere along the cause-effect chain, but the uncertainty greatly increases along the chain for the case of forcing. An example is radiative forcing, where if caused by a change in the albedo, it can be calculated with good certainty. What one lacks to understand though, is how the change in the surface energy and in the atmosphere leads to a change in latent and sensible heat fluxes, changes to cloudiness, air circulation or for instance local or regional pressure gradients, due to i.e. geographic location (Bright et al., 2011).

3. Case description

This part will give background information about the coal power sector in Europe, the general power sector in the Russian Federation and more importantly the forest sector in the Russian Federation, with special emphasis on the European part. An overview of the co-firing technology and opportunities connected to this will also be presented. This information has all been needed to develop the scenarios. As a final part, the models developed for the various co-firing scenarios chosen will be presented and explained with regards to the technical analysis.

3.1. Coal power and bioenergy sector in Europe

The increase in usage of coal for electricity generation is currently the single most problematic trend in the relationship between energy requirement and climate change. In 2010 it contributed to as much as around 30% of global primary energy consumption (IEA, 2012c; IEA, 2011) and with accounting for over 40% of the electricity output in the same year, it can be defined as the backbone of global electricity generation (IEA, 2011).

Table 3 shows that there are several countries in Europe heavily dependent on coal, in spite of countries such as the United States and China being even more dependent on it as an energy source.

Table 3: Overview of countries in Europe with coal power plants, their electricity production and average degree of efficiency for hard coal and lignite, in addition to the percentage amount of coal-fired power in each country (data from 2010) (IEA, 2012d)

Country	Hard coal		Lignite		% of total el.prod
	Production [GWh/y]	Efficiency	Production [GWh/yr]	Efficiency	
Austria	4 598	44,0 %	-	-	6,8 %
Belgium	4 095	38,3 %	-	-	4,4 %
Czech Republic	2 358	32,5 %	31 074	35,6 %	39,2 %
Estonia	-	-	10 729	32,5 %	82,8 %
Finland	10 075	42,5 %	14	33,2 %	12,5 %
France	22 867	40,9 %	-	-	4,1 %
Germany	102 429	41,3 %	140 428	38,3 %	39,0 %
Greece	421	35,9 %	22 058	35,2 %	39,2 %
Hungary	257	25,5 %	5 859	34,0 %	16,4 %
Ireland	4 135	41,0 %	-	-	14,5 %
Italy	38 835	37,9 %	769	37,3 %	13,3 %
Netherlands	13 266	41,6 %	-	-	11,2 %
Portugal	7 100	38,2 %	-	-	13,2 %
Slovakia	-	-	573	35,0 %	2,1 %
Spain	23 799	37,0 %	1 282	39,1 %	8,4 %
Turkey	16 393	38,4 %	36 491	33,3 %	25,0 %
United Kingdom	107 090	37,6 %	-	-	28,3 %
Total/Average:	357 718	39,2 %	249 277	36,5 %	19,9 %

The studies conducted by the International Energy Agency (IEA) are focusing primarily on the OECD-countries and if one shall rank them based on percentage of coal used for total electricity generation, the top four countries are Estonia with 83% and Czech Republic, Greece and Germany with 39% of their total generation. Bear in mind that the efficiency of the power plant varies between the countries, as well as the coal type used, as lignite has a lot lower quality and therefore contributes to an even higher degree of pollution. By looking at the total amount of coal fired electricity generation, Germany, United Kingdom and Turkey have the highest production.

Apart from electricity production, in certain countries coal is a major resource used for combined heat and power plants (CHP). In Poland, Denmark and the Czech Republic, coal contributes as fuel input in over 50% of their CHP electricity production (IEA, 2012d).

Certain countries are self-sustained regarding coal, but what is interesting is the amount of imported coal for the various European countries. If one were to export biomass from the Russian Federation to the rest of Europe in the future, it is more likely that the countries

interested in this would already be heavily importing coal. Based on data from "Coal Information 2012" published by the IEA, the largest coal importers in Europe/Eurasia in 2011 were Germany with 41,3 Mt, United Kingdom with 32,6 Mt and the Russian Federation and the Netherlands with 24,5 Mt. The Russian Federation, Poland and Ukraine were the largest European suppliers of coal to the rest of the world (IEA, 2012a).

The electricity information from 2012 reports that in 2011, biofuels and waste was used in electricity and CHP plants to produce 263 TWh of electricity in the OECD countries. This is the equivalent of 3,8% of OECD production using only combustible fuels, and 2,4% of the total electricity production of OECD from all sources. For non-OECD countries (Russia amongst others) in 2010, biofuels and waste produced 67,5 TWh of electricity in electricity and CHP plants, which is a total of 0,9% of combustible fuel-fired power generation. In addition, 1,8% of the total heat generation was provided from biofuels and waste combustion in 2010 (IEA, 2012d).

3.2. Power sector in the Russian Federation

To give an overview of the power sector in the Russian Federation, in 2010, the total electricity generation was 1 036 116 GWh and the heat generation was 6 015 631 TJ. As shown in Table 4, natural gas is the main provider of electricity and heat in the Russian Federation, but coal contributes a considerable amount with 16% of the electricity generated and 21% of the heat generation. In comparison, despite the large amount of forest resources, biofuels and waste is only responsible for 0,3% of the electricity generated and 2% of the heat generated. A great potential therefore exists for substituting coal as fuel with biomass by having a co-firing process in the power plant (IEA, 2012b).

Table 4: Percentage distribution of the energy sources in Russia for electricity and heat production (IEA, 2012b) [%]

Electricity and Heat Output [%]								
Supply and consumption	Coal and peat	Crude oil	Oil products	Natural gas	Nuclear	Hydro	Geothermal & solar	Biofuels & waste
Electricity generated [GWh]	16,0%	-	0,9%	50,2%	16,4%	16,1%	0,05%	0,3%
Electricity plants	-	-	*18,7%*	*1,0%*	*100%*	*100%*	*100%*	-
CHP plants	*100%*	*100%*	*81,3%*	*99,0%*	-	-	-	*100%*
Heat generated [TJ]	20,5%	0,4%	4,8%	66,7%	0,2%	-	5,4%	2,0%
CHP plants	*61,3%*	*0,8%*	*16,4%*	*46,5%*	*100%*	-	-	*29,7%*
Heat plants	*38,7%*	*99,2%*	*83,6%*	*53,5%*	-	-	*100%*	*70,3%*

The total primary energy production in Russia is around 1 293 049 ktoe, of which 46% (601 986 ktoe) is exported, mainly oil and gas (and some coal). 40% (177 109 ktoe) of the country's remaining total final energy consumption of 445 764 ktoe is used in the form of electricity and heat.

Table 4 further indicates that the primary energy for electricity generation in Russia is dominated by fossil sources such as gas (50%) and coal/peat (16%). Additionally, around 16% of the electricity is produced from nuclear power, the same amount for hydropower. Heat production is also dominated by the fossil sources natural gas (67%) and coal/peat (21%). Smaller contributions come from oil (5%) and other renewable sources than biomass (5% from geothermal and solar). The largest share of the produced electricity and heat comes from Combined Heat and Power (CHP) plants, with 33% of the electricity being produced at pure electricity plants and 54,9% being produced by pure heat plants (IEA, 2012b).

3.3. Forest sector in the Russian Federation

In September 2012, the Food and Agriculture Organization of the United Nations (FAO) published the report “The Russian Federation Forest Sector – Outlook study to 2030” and it shows that the Russian forest sector has considerable potential for development. The Russian forest sector has a crucial role concerning both the environment and from an economic perspective in local, national and global levels, with accounting for more than 20 percent of the planet’s forest estate (FAO, 2012).

In 2010, the total amount of forestland in the Russian Federation was 882 million hectares. Of this, available forest for wood supply (FAWS) was 677 million hectares and had an allowable cut of 633 million m^3, which included 61 million m^3 in protective forests and 573 million m^3 in exploitable forests. Depending on three future scenarios that have been developed, the forest areas are expected to increase with 0,8-1,5% by the year 2030. The study advises national policy-makers to start objective systematic calculations of the *economically* allowable cut, which excludes all physically and economically inaccessible forest resources (FAO, 2012). Regardless of this, it is clear that the Russian forest sector currently has a lot of unused potential.

For the forest industry, the study predicts that the wood biomass for energy usage will double, increasing from the current 32 million m^3 to 75 million m^3. The national market is the prime consumer of this biofuel and export is limited to pellets to those regions in Europe that have the necessary transportation and economic conditions intact (FAO, 2012). The national possibilities regarding bioenergy is the main scope of this thesis, with emphasis on the market in the European part of the Russian Federation.

Conventionally one can classify the Russian forest areas into two groups. The first one being the sparsely wooded and moderately wooded regions, which concerns Central, Volga, Ural, Southern and North Caucasus Federal districts, all in the European part of Russia. The richly wooded regions are looked upon as Northwestern (European Russia), Siberia and the Far Eastern Federal District. The Russian Federation is a vast country and more than half of the forest areas are grown on permafrost soils (Siberia and Far East), in climatic conditions that are very severe, and only around 45% of this forest area is available for exploitation. Therefore, the predominant part of the forest areas that have been exploited intensively are the Northern part of European Russia, the Urals and along the Trans-Siberian Railway (FAO, 2012).

In this thesis the resources in the European part of Russia has been focused on and a study done by Charles A. Backman in 1997 looked into the 9 economic regions of European Russia with a percentage distribution of the forest resources available (Backman, 1997). This distribution has been used as a basis for developing the current scenario with the numbers presented in the report by FAO (2012). A map of the economical regions of Russia can be

found below in Figure 7. As the thesis has its focus on European Russia, the regions of West Siberia, East Siberia and Far Eastern Siberia have been disregarded. In addition, Kaliningrad is not taken into consideration for the further model purposes, as the power production there has a very limited impact.

Figure 7: Map of the economic regions of the Russian Federation

Based on the upscaling, the forest resources that are exploitable in the economic regions in European Russia are as follows:

Table 5: Amount of exploitable forest land in each region of European Russia in [%] and [1000 ha]

Region	Share of forest land exploitable	Updated estimate for exploitable land [1000 ha]
North	88 %	92 466
Northwest	95 %	13 635
Central	91 %	25 561
Volga-Vyatka	94 %	17 286
Central Chernozem	81 %	1 644
Volga	75 %	4 946
North Caucasus	57 %	2 886
Urals	87 %	42 978
Kaliningrad Oblast	81 %	299
Russia	58 %	617 954
European Russia	88 %	201 700

The Russian forest consists of several different biomes, the most important ones for this study being the boreal forest and temperate forest. Based on maps from (McShaffrey; FAO, 2012; Peterson), a distribution was made that can be found below in Figure 8.

Figure 8: Map of the distribution of boreal and temperate climate in the Russian Federation

A biome is a large, naturally occurring, regional ecosystem that contains communities of plants and animals that are adapted to the conditions in which they occur. Biomes are strongly influenced by climate, and their distributions often coincide with climate regions, although many other factors also influence the distribution of plants and animals (Park, 2008). In European Russia, the boreal and temperate forest is the most dominant.

Boreal forests, or taiga, represents the largest terrestrial biome in the world and occurs at latitudes between 50 and 60 degrees north. Aside from parts of Eurasia (two-thirds can be found in Siberia), the rest can be found in Scandinavia, Alaska and Canada. The seasons are characterised by having long, cold and dry winters, with moist and moderately warm summers. The length of the growing season is around 130 days (UC Berkeley, 2004).

The temperate forests occur more in the eastern parts of North America, north-eastern Asia and western and central Europe. This forest biome has more well-defined seasons and a distinct winter, resulting in a moderate climate during the 4-6 frost free months and a growing season of around 140-200 days (UC Berkeley, 2004).

Moreover, due to calculations connected to biogenic CO_2-fluxes and albedo (further elaborated in Chapter 3.5) and system modelling, a distribution was needed for coniferous wood (softwood) and deciduous wood (hardwood). Based on data from the article by Backman (1997) and converting the values from hectares to cubic metres, an estimation was made which can be found in Table 6 below.

Table 6: Distribution of coniferous and deciduous wood in the boreal and temperate forest areas in European Russia [%]

Region	Boreal forest [%]		Temperate forest [%]	
	Con	Dec	Con	Dec
North	76,8 %	23,2 %	-	-
Northwest	24,5 %	25,5 %	24,5 %	25,5 %
Central	-	-	40,1 %	59,9 %
Volga-Vyatka	-	-	45,6 %	54,4 %
Central Chernozem	-	-	34,9 %	65,1 %
Volga	-	-	25,3 %	74,7 %
North Caucasus	-	-	20,5 %	79,5 %
Urals	34,0 %	36,0 %	14,6 %	15,4 %
Kaliningrad Oblast	76,8 %	23,2 %	-	-
Russia	62,3 %	22,7 %	14,6 %	15,4 %

3.4. Co-firing technologies

There exists several co-firing technologies, where the two main ones will be summarised. Direct co-firing consists of biomass and coal being fed simultaneously into the same boiler. First the coal and biomass is blended together and then the mixture is processed through a coal mill, crusher and pulveriser before going into the final burning stage. This process can be used for wood chips, and with slight modifications, this technique can be used for pellets and pellets from combined torrefaction and pelletisation (TOP). TOP pellets have some added advantages over conventional biomass-based pellets, including an improved durability, grindability and a coal-like combustion nature (Kabir and Kumar, 2012). For a continuous co-firing over 24 hour periods, an automated feeding system is needed to be able to supply biomass to the boiler continuously (Mann and Spath, 2001), with wood chips preferably pulverised down to 3 mm in size (Sebastián et al., 2011) and this can be done in a single-stage size reduction process.

Parallel co-firing involves having a separate biomass pre-treatment, feeding mechanism and combustion system in the power plant. Due to higher moisture content, particle size and non-uniform combustion behaviour, feedstock such as bale and wood chips can be more complicated for direct co-firing, and therefore parallel co-firing can be considered as an alternative option. Bale and wood chips are still suitable as feedstock for direct co-firing, but need to be dried beforehand, as the maximum allowable moisture content is usually 20% for co-firing (Kabir and Kumar, 2012).

Co-firing usually takes place in already existing coal-fired power plants and does not need to increase the capacity. Most boiler types have been tested for co-firing in the past, including pulverised coal boilers, cyclone boilers, stoker boilers and bubbling and circulating fluidised bed boilers. The type that can handle the highest amount of biomass is the pulverised coal boiler (Mann and Spath, 2001).

There are both advantages and disadvantages with co-firing. The plant capacity slightly decreases due to efficiency losses, which is reasoned with the biomass having lower heating value and also a higher moisture content than coal (Mann and Spath, 2001). The efficiency therefore decreases with increased level of co-firing. However, the total system also increases its energy efficiency. This is due to less coal being burned, which implies less

energy consumed by the system over all. In addition, the upstream processes connected to biomass are in less need of energy than for coal, so this would also result in energy savings, relative to the level of co-firing (Mann and Spath, 2001). The life cycle assessment also highlights this.

3.5. System models used for the LCA scenarios

In this part of the report, the models that have been used for the four scenarios will be described, both how they were developed and used. Furthermore, the considerations needed to be taken for the model and templates will be highlighted.

Four scenarios for the thesis were developed; a reference system of 100% coal-firing, one scenario with 10% biomass used as fuel input to the co-firing, one with 20% biomass co-firing and an ideal case of a 100% bioenergy as fuel input. Below in Figure 9 one can find a generic model used for all four cases, where one disregards the processes connected to coal and bioenergy for the two 100% scenarios.

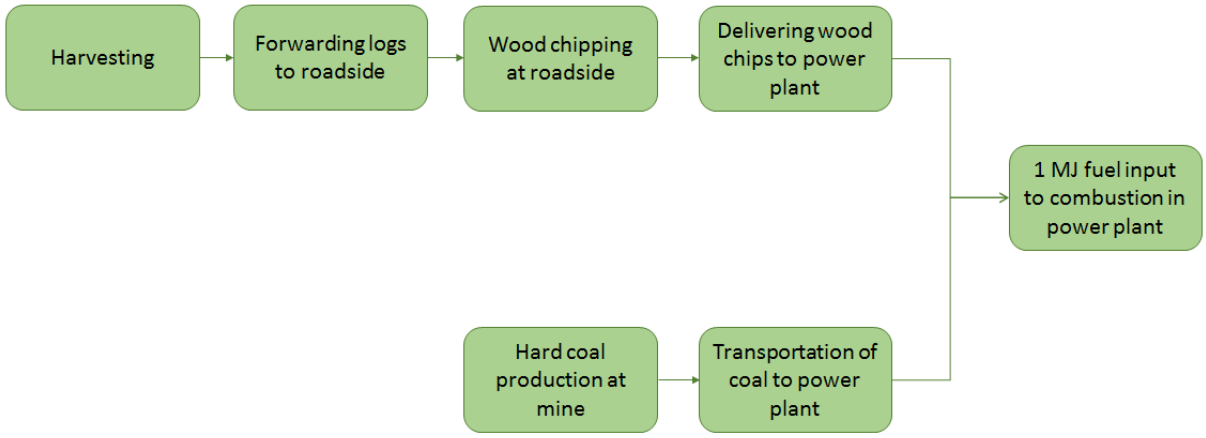

Figure 9: Flowchart for co-firing of biomass with coal power with functional unit as 1 MJ fuel mix

The functional unit of the analysis is 1 MJ fuel mix (input), which implies that it is converted by an energy system to an energy carrier. The input of coal and biomass has been calculated accordingly for each of the scenarios and each region.

3.5.1. Scenario 1: 100% coal-fired

As the base case for comparison of the three other scenarios and the variations in climate change impact, a scenario of 100% coal-firing was chosen. The model is built on the system developed for the thesis project in the autumn, “Life cycle assessment of coal based electricity generation with focus on coal bed methane” (Kviljo, 2012), and contains the

processes connected to extraction of coal until combustion in the power plant. The system consists of three main processes: coal production, transport and coal combustion at the power plant.

One of the main processes in the foreground system is “hard coal at mine” which is specified for the Russian Federation. Included in this process is everything connected to the coal extraction from the mine, both from underground and open cast mining, and materials such as concrete, steel, copper, explosives and wood, as well as energy requirements. Most of input represents European or Global conditions. Transport to the coal power plant is also included in this foreground process, and the final output is 1 kg of coal produced.

The efficiency of the power plant together with the lower heating value of the coal, which depends on the coal type, are the factors that influence the amount of coal needed for coal combustion. As the functional unit is 1 MJ fuel mix, the coal power plant and efficiency is not necessary, only the lower heating value for coal. For this, the value from ecoinvent for Russia was used, which is 23,4 MJ/kg (ecoinvent, 2010). The input of coal for the 100% coal-fired scenario is therefore 0,0427 kg/MJ.

3.5.2. Scenario 2: 10% co-firing with biomass

In this scenario, the processes and technology connected to the coal production and combustion are the same as in scenario 1, but the input of coal is now 90% (0,9 MJ) and there is a 10% input of biomass (0,1 MJ). The biomass is a combination of hardwood and softwood. These are the two broad classes trees are divided into, with hardwoods usually being broadleaved and softwoods being coniferous. The processes chosen for biomass are “wood chips, hardwood, u=80%, at forest/RER/m^3” and “wood chips, softwood, u=140%, at forest/RER/m^3” and based on the distribution in each region of coniferous and deciduous wood, an estimation was made for how much of the 10% fuel input was hardwood and softwood.

The industrial wood at the forest road is further fed into a mobile chopper immediately after being harvested (Werner et al., 2007). As the volume of the biomass has an impact related to the transportation, Norwegian spruce was chosen to represent coniferous forest and birch to represent deciduous forest, with 470 kg/m^3 and 630 kg/m^3 as the respective densities (Norwegian Institute of Wood Technology). If the wood is chopped a few days after

harvesting, another density would have been chosen, as the water content could be considerably lower (in dry weather) due to evaporation over the leaves (Werner et al., 2007).

Included in the aforementioned processes is the harvesting of the trees with chainsaws to suitable pieces, loading them onto a tractor-driven trailer and forwarding to the roadside (Werner et al., 2007). Depending on the end-use, chips can be produced onsite or the wood can be transported to a chipper (Fagernäs et al., 2006). In our case, we have chosen a wood chipper processing the timber logs into wood chips at the forest site, all original ecoinvent data, together with the harvesting and forwarding. The biomass is then transported directly to the respective power plant, which was calculated for each case. Wood chips are commonly used directly in coal-fired power plants or CHP production (IPCC, 2012), and the climate change impact of biomass combustion was calculated seperately, based on the GWPs developed, and were therefore not included in the model.

All the scenarios were modelled for the eight economic regions in European Russia (excluding Kaliningrad). For each region a centre point was chosen, an area that was approximately in the middle of the region, and it was assumed that there was a power plant at each of these centre points. The other assumption made was that every power plant produced the same amount of energy, so that the input was equally distributed. An overview of the points chosen can be found in the map in Figure 10.

The total final consumption (TFC) of coal and peat for electricity and heat production in Russia was 4 807 619 TJ in 2010 (IEA, 2012b). It is estimated that around 22,7% of the energy is produced in European Russia (Belobrov). Within European Russia it was assumed an equal distribution of the coal power, 2,8% per region (136 434 TJ), which was further used for the calculations connected to input of biomass and transportation.

Table 7 gives an overview of the input of biomass and coal for each region for the scenario of 10% co-firing.

Table 7: Input of coal [kg/MJ] and biomass [m^3/MJ] for each region in the scenario of 10% co-firing

Region	Hard coal [kg/MJ]	Hardwood biomass [m^3/MJ]	Softwood biomass [m^3/MJ]
North	0,0384	2,4E-06	8,0E-06
Northwest	0,0384	4,9E-06	4,7E-06
Central	0,0384	5,6E-06	3,7E-06
Volga-Vyatka	0,0384	5,1E-06	4,3E-06
Central Chernozem	0,0384	6,0E-06	3,2E-06
Volga	0,0384	6,7E-06	2,3E-06
North Caucasus	0,0384	7,0E-06	1,8E-06
Urals	0,0384	4,9E-06	4,6E-06

A lower heating value of 19 MJ/kg was used together with the chosen densities of the wood for the conversions to m^3/MJ, which was the ecoinvent unit for the chosen processes.

As each region varies in size, individual transportation routes with a specific radius were assigned for each region. An assumption was made that biomass and coal would be transported from all parts of the region to the centre point where the power plant is situated. The map with the regional transportation routes can be found below in Figure 10, in addition to a table with the values for each region.

Figure 10: Map of the modelled transportation routes for the eight regions in European Russia, as well as the centre point chosen for the coal power plant

The loading capacity of the truck is estimated to 21 tons and a fuel consumption of 3 litres per kilometre (Michelsen et al., 2008). The values for tonkm per cubic metre are the values that were used in Arda for each region, both for softwood and hardwood chips.

Table 8: Overview of the data connected to the transportation route for each region

Region	Distance to collection point [km]	Ton kilometre [tkm]	Ton kilometre per m3 [tkm/m^3]
North	564,3	11 850,5	286,2
Northwest	171,3	3 597,9	94,5
Central	353,0	7 412,2	199,7
Volga-Vyatka	327,6	6 880,2	182,5
Central Chernozem	197,2	4 142,0	113,3
Volga	340,9	7 158,1	200,9
North Caucasus	323,3	6 788,9	193,1
Urals	360,0	7 560,8	198,8

Further information regarding the calculations can be found in Appendix 8.2, Table 29 and Table 30.

3.5.3. Scenario 3: 20% co-firing with biomass

Technology today has the possibility of 20% co-firing in coal power plants and therefore this was chosen as a realistic scenario. For this scenario, the transportation routes are the same, but the fuel mix of coal and biomass varies. The amount of ton kilometre is the same as in scenario 2 (in Table 8). Below one can find the fuel input for each region for the scenario of 20% co-firing.

Table 9: Overview of the input of coal [kg/MJ] and biomass [m^3/MJ] for each region in the scenario of 20% co-firing

Region	Hard coal for heat [kg/MJ]	Hardwood biomass for heat [m^3/MJ]	Softwood biomass for heat [m^3/MJ]
North	0,0341	4,8E-06	1,6E-05
Northwest	0,0341	9,7E-06	9,3E-06
Central	0,0341	1,1E-05	7,5E-06
Volga-Vyatka	0,0341	1,0E-05	8,6E-06
Central Chernozem	0,0341	1,2E-05	6,4E-06
Volga	0,0341	1,3E-05	4,5E-06
North Caucasus	0,0341	1,4E-05	3,6E-06
Urals	0,0341	9,8E-06	9,3E-06

3.5.4. Scenario 4: 100% bioenergy as fuel

For 100% bioenergy a different technology would be used than a coal power plant, but as the functional unit is input of fuel mix only, the upstream processes and overall climate

change impact is of interest. With covering the coal demand in Russia, the input for European Russia for 1 MJ input is as follows:

Table 10: Overview of the input of coal [kg/MJ] and biomass [m^3/MJ] for each region in the scenario of 100% bioenergy

Region	Hardwood biomass for heat [m^3/MJ]	Softwood biomass for heat [m^3/MJ]
North	2,4E-05	8,0E-05
Northwest	4,9E-05	4,7E-05
Central	5,6E-05	3,7E-05
Volga-Vyatka	5,1E-05	4,3E-05
Central Chernozem	6,0E-05	3,2E-05
Volga	6,7E-05	2,3E-05
North Caucasus	7,0E-05	1,8E-05
Urals	4,9E-05	4,6E-05

The values for the other upstream processes remain the same. However, biogenic CO_2 and surface albedo are the factors where the amount of biomass for co-firing plays the most important role.

3.5.5. Biogenic CO_2 - Calculations and data

Concerning the calculations of biogenic CO_2, certain information was needed. A lower heating value of 19MJ/kg was chosen, and the conversion factor of 3,6 MJ/kWh was used. In addition, there is 50% carbon in dry mass, which equals 0,5 ton C/ton wood. This was further used to estimate there being 1,83 ton CO_2/ton wood, by multiplying carbon in wood with the molar weight of CO_2 divided by the molar weight of carbon. Despite a lot of research one specific rotation periods from the Russian boreal and temperate forest were not found and therefore values from the Intergovernmental Panel on Climate Change (IPCC) were used (IPCC, 2006). Below in Table 11 is an overview of the rotation periods, as well as the corresponding GWP_{bio} characterisation factor extracted from the paper by (Cherubini et al., 2011a), for the three most common time horizons of 20, 100 and 500 years.

Table 11: Overview of rotation periods [year] and the corresponding GWP_{bio} factor (Cherubini et al, 2011a)

Forest type	GWP_{bio}		
	TH = 20	TH = 100	TH = 500
CO_2	1,00	1,00	1,00
Boreal, coniferous (100 yrs)	0,96	0,43	0,08
Boreal, deciduous (85 yrs)	0,95	0,37	0,07
Temperate, coniferous (90 yrs)	0,95	0,39	0,07
Temperate, deciduous (75 yrs)	0,94	0,32	0,06

Furthermore, a final important factor needed for the calculations is the amount of biomass per hectare, which was taken from the IPCC guidelines on forest land (IPCC, 2006) and can be found below.

Table 12: Overview of the amount of biomass per hectare for each of the forest types [t dry mass/ha] (IPCC, 2006)

	Biomass per hectare [t dry mass/ha]	
	Boreal forest	Temperate forest
Coniferous	50	175
Deciduous/Broadleaved	57,1	200

Based on the estimated amount of hectares of exploitable forest in each of the regions in European Russia, it was first converted to tons of dry mass using the factors in Table 12 and then finding the amount of carbon in the exploitable forest for each region using the conversion factor of 0,5 t C/t wood. Next, the amount of CO_2 in the wood was calculated and by using the rotation periods, it was estimated how much carbon and CO_2 there was per year for the four combinations of forest. After this, the energy quantity in each of the forest combinations was calculated, using the lower heating value and rotation periods for results both in GJ and then further in TJ/year.

For each combination of forest type, the g CO_2-equivalent per MJ was found, using the GWP_{bio} and the CO_2 emissions from biomass combustion, being 96,5 g CO_2-eq/MJ. The values can be found in Table 23 in Appendix 8.1.3 for each of the time horizons.

Based on the percentage distribution of the m^3 biomass of the different forest types in each region, the final amount of g CO_2-equivalents per $MJ_{fuel\text{-}mix}$ was calculated, which can further be found in Chapter 4.2. The remaining data can be found in Appendix 8.3. For further results connected to the GWP_{bio} and the implications of these, see Chapter 4 and 5.

3.5.6. Surface albedo - Calculations and data

In connection with the albedo calculations, two sites were located for each of the eight regions, both close to the centre points that were chosen for the power plant. One of the sites had coordinates and elevation for an area of heavy forest, and the other site had a similar location in terms of elevation and forest biome, but was in an open landscape instead, for instance an open field or mountainous area. The sites should not be too far apart and all locations and elevations were found using Google Earth, which involves some inaccuracy, but was found as the most optimal of the tools available. The chosen locations can be found below in Table 13 and are representative for the whole region.

Table 13: Overview of the coordinates and elevation for each of the chosen sites for albedo calculations

Region	Forest area			Open landscape		
	Latitude	Longitude	Elevation [m.a.s.l.][4]	Latitude	Longitude	Elevation [m.a.s.l.]
North	64,4	40,4	29	64,3	40,4	29
Northwest	59,4	30,7	33	59,3	31,2	32
Central	56,2	36,5	247	56,2	36,5	247
Volga-Vyatka	56,6	47,7	76	56,6	47,8	86
Central Chernozem	51,9	39,6	116	52,0	39,3	119
Volga	51,6	45,9	287	51,5	45,9	268
North Caucasus	45,1	41,9	614	45,1	41,8	628
Urals	55,0	56,7	257	55,1	56,6	257

As a first part of the calculations, the two-way atmospheric transmittance parameter f_a was calculated using Equation (2.3.3) found in the methodology chapter. The values of K_T for each month averaged over 22 years were extracted from the Surface Meteorology and Solar Energy database of NASA (NASA, 2013). By entering the latitude and longitude for each site and selecting "insolation clearness index, k (Average, Min, Max), the values were extracted for each specific site and repeated for all the sites identified as forest areas (one per region). Finally, the parameter f_a was computed for each month, as a product between K_T and T_A. The results can be found in Appendix 8.1.1.

The next step was calculating the mean incoming solar radiation R_{TOA} per month. This was done through Equation (2.3.4) to (2.3.7) in a matlab script that can be found in Appendix 8.1.1, where the elevation was the only parameter needed to be changed for each region.

[4] Metres above sea level

When one had R_{TOA} calculated for each region, observational albedo data for the sites that were identified for each region could be extracted, both for forest area and open landscape using MODIS Land Subsetting tool (ORNL DAAC, 2010). For each of the sites, the geographical coordinates were entered and as product, "MCD43A MODIS/Terra+Aqua BRDF and Calculated Albedo" was selected as the product, which calculated the data by using a solar angle equal to 0,2. The spatial boundaries were set to "0 km" above/below and "0 km" left/right and the time series was selected as February 2000 to March 2013, so a time period of 13 years.

The extraction of data was conducted for all 16 sites (two for each region) but Northwestern and North Caucasus had to have some extra sites added for open landscape, as when analysing the results, it was shown that the original sites chosen were not ideal to represent "open landscape". When receiving the data, the Julian days were converted to averages for each month for each year (the albedo values are measured every 8 days), with focus on "black-sky shortwave" albedo. Furthermore, an average was made for each month based on all of the years. By calculating the monthly mean, the uncertainties were minimized for the variations that could occur that affect the albedo (Bright et al., 2011). Certain days had insufficient observational data to perform the BRDF/albedo inversion, giving an error value of 32 767. These were not taken into consideration and a general average was made based on the days with adequate data measured.

The next step was to find Δ Albedo (absolute value of the difference between forest and open landscape site) and the values can be found in Chapter 4.1.1.

By using Equation (2.3.11) with the area of the Earth being $5{,}10 \cdot 10^{14}\,m^2$ and the climate efficacy for albedo being 1,94, one was able to calculate the radiative forcing from change in albedo for each region, measured in W/m^2. As a final part, one used this value to find the annual mean radiative forcing from Land Use Change, measured in $(W/m^2)/m^2$.

For each forest type within each region (from two to four), one then uses the biomass yield for the forest type (amount of dry mass per hectare multiplied by 0,5 to get t C/ha) to find t CO_2/ha. This value multiplied with the annual mean radiative forcing for the respective region ((W/m^2)/kg CO_2) gives the instantaneous effective forcing ($W/(m^2$ kg $CO_2)$). The rotation period of the forest type together with the year (in time horizon) in an exponential

function, gives the albedo return function, which begins at 1 and then reduces itself towards zero with time (displayed in years). The integrated effective forcing (W yr/(m^2 kg CO_2)) is then found by the sum of the instantaneous effective forcing and the previous value of integrated effective forcing. The final step is then to find the GWP_{albedo} characterisation values, which are the integrated effective forcing value for a year, divided by the value for a fossil reference. See Equation (2.3.14). The values for the time horizons of 20, 100 and 500 years can be found in Chapter 4.1.2. The ERF-results for each forest type in each region can be found as graphs in Chapter 4.1.1, together with the biogenic CO_2-curves for integrated effective forcing.

For each combination of forest type, the g CO_2-equivalent per MJ was found, using the GWP_{albedo} and the CO_2 emissions from biomass combustion, being 96,5 g CO_2-eq/MJ. The values for each of the time horizons can be found in Appendix 8.1.3.

Based on the percentage distribution of the m^3 biomass of the different forest types in each region, the final amount of g CO_2-equivalents per MJ was calculated, which can further be found in Chapter 4.2. The remaining calculations are displayed in Appendix 8.1 and 8.3. For further results connected to the GWP_{albedo} and the implications of these, see Chapter 4 and 5.

4. Results and analysis

In this part, the work connected to biogenic CO_2 and the albedo effect is shown, based on the various formulas and data collected, which was explained in Chapter 2 and 3. In addition the results from the life cycle assessment for the eight regions in European Russia and the corresponding scenarios will be presented for the time horizons of 20, 100 and 500 years. All the results are shown graphically in order to more easily understand and compare the outcomes, in addition to looking more in depth at what processes contribute the most to climate change, how if differs in each region and where the climate forcings connected to biomass combustion and albedo have the largest impact. To conduct parts of the analyses, the software Arda was used, which has been developed at the Programme for Industrial Ecology at the Norwegian University of Science and Technology.

4.1. Characterisation of biogenic CO_2 and albedo

4.1.1. Absolute metrics

Based on the sites found for each region and the extraction of albedo-data from MODIS as explained in Chapter 3.5.6, Figure 11 below gives an overview of the monthly mean Δ albedo values. These are the net albedo values (absolute) between the sites chosen for forest and open landscape.

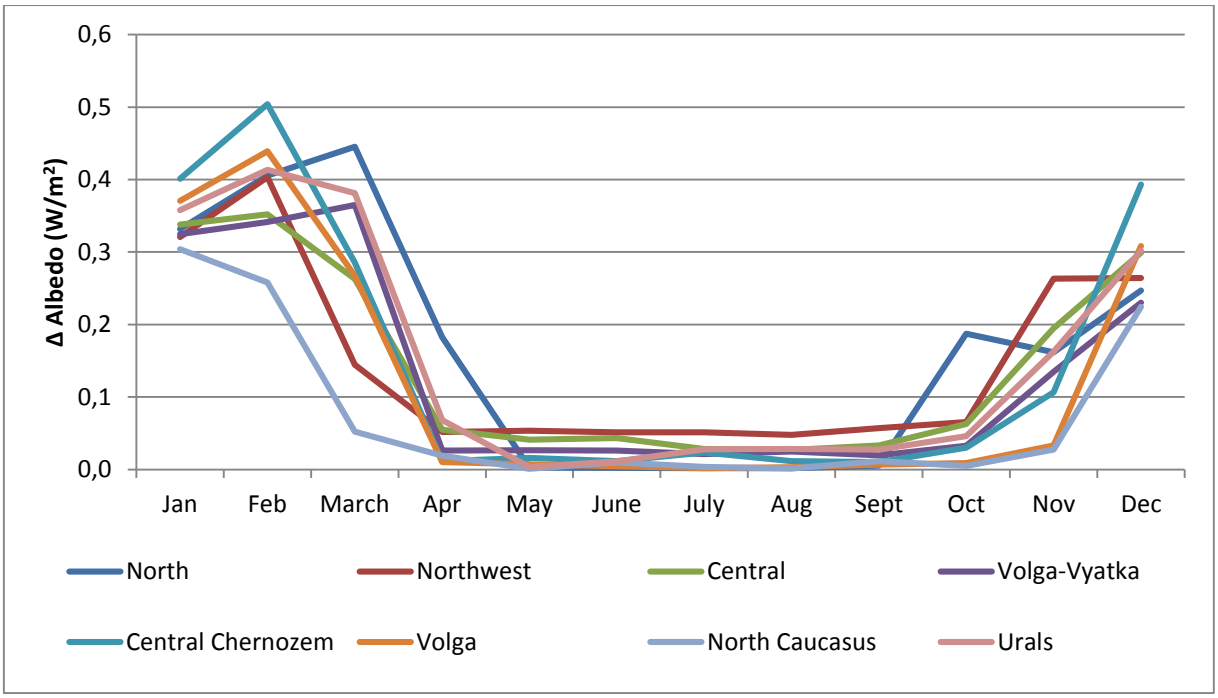

Figure 11: Overview of the monthly mean Δ albedo values for each region [W/m²]

The highest net values for albedo are during the winter months from mid-October to March. Central Chernozem has the overall highest differences, with its peak in February and a Δ albedo of 0,5 W/m^2. The Northern region also has high values in general, with a peak of 0,44 W/m^2 for the month of March. North Caucasus has on the other hand lower differences overall for each month, with its highest peak being in January with 0,37 W/m^2 as Δ albedo. As the snow season is longer in certain regions, the Δ albedo value remains higher, due to the solar radiation being reflected for a longer period of time in the open areas. For the exact numerical values, see Table 20 in Appendix 8.1.1.

Figure 12 below gives an overview of the effective radiative forcing (instantaneous) from biogenic CO_2 fluxes and changes in albedo associated with 1 kg of emission for the eight regions of European Russia which are analysed in this thesis. As there was up to four different forest types in each region, combinations of both boreal and temperate climate with either coniferous or deciduous forest, an average has been calculated for each region based on the forest distribution. The effective forcing of CO_2 pulse emissions from fossils or deforested biomass is shown for comparison. The exact values can be found in Table 21 and Table 22 in Appendix 8.1.2, in addition to the digital appendix.

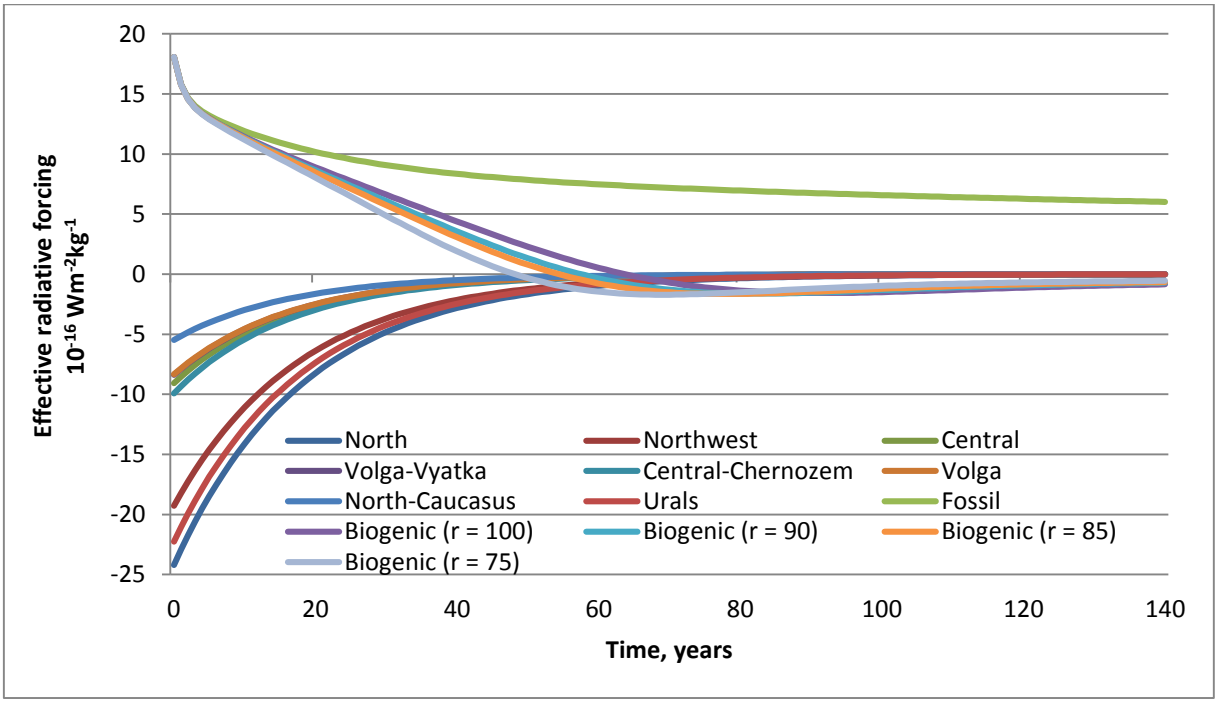

Figure 12: Effective radiative forcing from biogenic CO_2 fluxes and changes in albedo associated with 1 kg of emission for the eight regions. The effective forcing of CO_2 pulse emissions from fossils or deforested biomass is displayed for comparison. [10^{-16} Wm^{-2}kg^{-1}]

The graph continuously above the x-axis represents the fossil reference, which has a very slow atmospheric decay, and at year 500, still has an effective radiative forcing of around $4{,}18 \cdot 10^{-16}$ W/m^2kg CO_2. As a comparison, the biogenic references have an ERF of around $-0{,}07 \cdot 10^{-16}$ W/m^2kg CO_2, and represent the rotation period of the four different forest types in the various regions. Boreal forest with coniferous trees has a rotation period of 100 years, boreal with deciduous trees has a rotation period of 85 years, and temperate climate with coniferous or deciduous forest has a rotation period of 90 and 75 years respectively. For the cases of the surface albedo, one can see that it has the highest impact for the Northern, Northwestern and Urals region with values between $-24{,}2 \cdot 10^{-16}$ W/m^2kg CO_2 (Northern) and $-19{,}3 \cdot 10^{-16}$ W/m^2kg CO_2 (Northwestern) for year 1. The lowest impact is in the region of North-Caucasus, with an ERF of $-5{,}5 \cdot 10^{-16}$ W/m^2kg CO_2 in year 1. The values for all the regions go asymptotically towards zero between the time period of 75 to 100 years, which is also the rotation periods of the various forest types.

Based on the results displayed in Figure 12, one can draw certain conclusions. When biogenic CO_2 emissions come from combustion of forest biomass, their atmospheric decay is slower than that of fossil CO_2 for the first decades. The interaction which causes a postponement in the atmospheric CO_2 concentrations takes place in the upper layers of the oceans, which slowly outgas the CO_2 that is quickly absorbed soon after the pulse emission (Cherubini et al., 2012). This is only a “short-term” effect however, and CO_2 neutrality is still reached at the end of the rotation period.

If one were able to include NEP (Net Ecosystem Productivity) in the assessment, there would have been a clear inflection point in the biogenic CO_2 decay at the end of the rotation period. This is due to harvesting taking place and NEP stopping abruptly (Cherubini et al., 2012). Prior to this, the values would still be negative due to a negative NEP caused by the additional emissions from the site after harvest.

The graph also shows the importance of the cooling contribution from albedo in areas affected by a significant snow cover. This is especially visible for the cases of the North region, Northwestern region and the Urals, where the snow lays longer and the boreal

climate is represented. The effect is less for the remaining regions, especially North-Caucasus, which also is also reasonable due to the geographic placement.

Figure 13 below displays the average net effective radiative forcing for each region. This was reached by calculating the net ERF between each individual forest type in the region and the respective rotation period, and further finding the mean average for each of the regions.

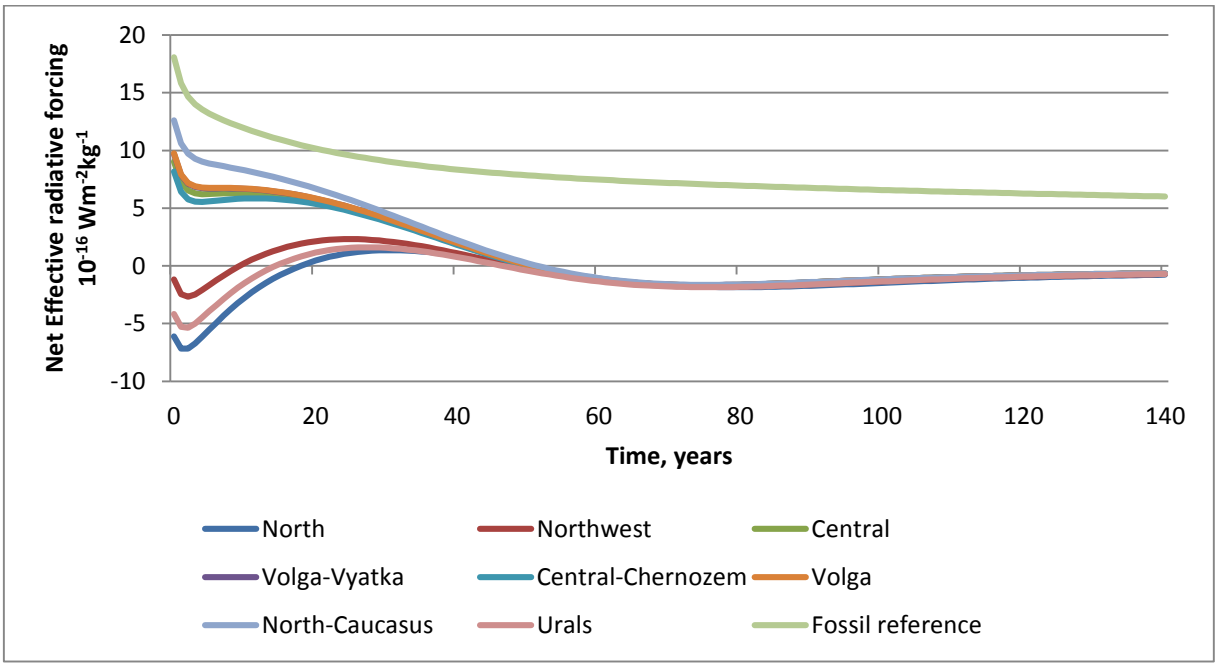

Figure 13: Net effective radiative forcing (instantaneous) for each region with fossil reference shown for comparison [10^{-16} $Wm^{-2}kg^{-1}$]

The graph presents the dynamics of the effective radiative forcing for each of regions, compared to a fossil-based reference system. The curves show the complexity of the systems and the large time dependency of the results. Central, Volga-Vyatka, Central Chernozem, Volga and Northern-Caucasus all have a net effective radiative forcing above the x-axis at year 1, with values from $8{,}2 \cdot 10^{-16}$ W/m^2kg CO_2 (Central Chernozem) to $12{,}6 \cdot 10^{-16}$ W/m^2kg CO_2 for the case of North-Caucasus. The fossil reference starts at $18{,}1 \cdot 10^{-16}$ W/m^2kg CO_2 and for all regions the net impact is lower than that of the fossil reference.

For the Northern, Northwestern and Urals region, there is a strong cooling contribution from albedo present due to the boreal climate, which manages to outweigh the warming from the biogenic CO_2. These regions are therefore influenced by a net negative impact in the short-run (first two decades), which results in a cooling effect, before decreasing to above the

x-axis until around year 50. For the remaining regions, the albedo contribution is not as strong in the beginning and the warming from the biogenic CO_2 fluxes clearly has the largest impact. From around year 50, the cooling effect is dominating for all regions, moving asymptotically towards zero, and having a value of around $-0{,}6 \cdot 10^{-16}$ W/m^{2}kg CO_2 by year 140. At this time interval, the fossil reference still has an estimated value of $6 \cdot 10^{-16}$ W/m^{2}kg CO_2.

The ERF's for albedo were used as a basis for finding the corresponding GWP equivalency factor, whilst for biogenic CO_2, they are based on the values developed by Cherubini et al (2012) and connected to the rotation period. A site can therefore have the same biogenic CO_2-value, but have different albedo values, as this is site-specific.

4.1.2. Normalised metrics

Below are two tables representing GWP equivalency factors for biogenic CO_2 and the albedo effect. The first one, Table 14, displays the GWP_{bio} factors which were developed by Cherubini et al and published in the article "CO_2 emissions from biomass combustion for bioenergy: atmospheric decay and contribution to global warming" in 2011 (Cherubini et al., 2011a). They were combusted with time-integrated effective radiative forcings and using CO_2 as a reference. The chosen factors are connected to the relevant rotation period of the forest type, and are displayed for the three most common time horizons of 20, 100 and 500 years.

Table 14: Biogenic CO_2 GWP equivalency factors for the selected regions and respective biomass for the three time horizons. Extracted from the paper by Cherubini et al, 2011a

Forest type	GWP_{bio}		
	TH = 20	TH = 100	TH = 500
CO_2	1,00	1,00	1,00
Boreal, coniferous (100 yrs)	0,96	0,43	0,08
Boreal, deciduous (85 yrs)	0,95	0,37	0,07
Temperate, coniferous (90 yrs)	0,95	0,39	0,07
Temperate, deciduous (75 yrs)	0,94	0,32	0,06

There is a significant difference in the three time horizons, with factors having increased with between 92% and 94% from the egalitarian perspective with a time frame of 500 years to the individualist perspective of 20 years. Moreover, the factor increases with the rotation

period, so the GWP_{bio} is higher for boreal forest with coniferous wood, which has a rotation period of 100 years, and for temperate forest with deciduous wood, with a rotation period of 75 years. This influences the contribution of direct biomass combustion to the impact on climate change significantly, which is elaborated more in the discussion part.

Table 15 below shows the GWP equivalency factors for the albedo effect for the time horizons of 20, 100 and 500 years. The factors were combusted with time-integrated effective radiative forcings and using CO_2 as a reference, by using the procedure explained in the methodology, Chapter 2.3.2.

Table 15: Albedo GWP equivalency factors for the selected regions and respective biomass for the three time horizons (con = coniferous, dec = deciduous)

Region	TH = 20				TH = 100				TH = 500			
	Boreal		Temperate		Boreal		Temperate		Boreal		Temperate	
	Con	Dec	Con	Dec	Con	Dec	Con	Dec	Con	Dec	Con	Dec
North	-1,32	-1,08			-0,6	-0,45			-0,19	-0,14		
Northwest	-1,64	-1,34	-0,45	-0,36	-0,74	-0,56	-0,19	-0,14	-0,23	-0,17	-0,06	-0,04
Central			-0,47	-0,38			-0,2	-0,15			-0,06	-0,05
Volga-Vyatka			-0,44	-0,35			-0,19	-0,14			-0,06	-0,04
Central Chernozem			-0,52	-0,42			-0,22	-0,16			-0,07	-0,05
Volga			-0,44	-0,35			-0,19	-0,14			-0,06	-0,04
North Caucasus			-0,44	-0,23			-0,12	-0,09			-0,04	-0,03
Urals	-1,89	-1,54	-0,52	-0,41	-0,86	-0,64	-0,22	-0,16	-0,27	-0,2	-0,07	-0,05

There is a significant difference in the GWP equivalency factors for the time horizon of 20 years and 500 years and there is also a distinct variance in the factors for boreal forest and temperate forest, which is connected to the climate being cooler and the length of seasonal snow cover.

The Northern, Northwestern and Urals region are the only regions with partly or fully boreal climate, therefore these are the only regions that have GWP equivalency factors corresponding to these forest scenarios. For the time horizon or 100 years, for boreal climate with coniferous wood, the factors vary from -0,60 (North) to -0,86 in the Urals, and for deciduous wood, -0,45 (North) and -0,64 in the case of Urals. For temperate forest with coniferous wood, the values vary from -0,12 in North Caucasus to -0,22 in Central Chernozem and the Urals. For the final combination, temperate climate with deciduous

wood, the GWP values vary from -0,09 in North Caucasus to -0,16 in both Central Chernozem and the Urals once again.

Table 16 below shows the net values of the GWP equivalency factors from biogenic CO_2 and albedo for the four types of forest for the time horizons of 20, 100 and 500 years.

Table 16: Net GWP equivalency factors between biogenic CO_2 and albedo for the selected regions and respective biomass for the three time horizons (con = coniferous, dec = deciduous)

Region	TH = 20				TH = 100				TH = 500			
	Boreal		Temperate		Boreal		Temperate		Boreal		Temperate	
	Con	Dec	Con	Dec	Con	Dec	Con	Dec	Con	Dec	Con	Dec
North	-0,36	-0,13			-0,17	-0,08			-0,11	-0,07		
Northwest	-0,68	-0,39	0,50	0,58	-0,31	-0,19	0,20	0,17	-0,15	-0,11	0,01	0,02
Central			0,48	0,56			0,19	0,17			0,01	0,01
Volga-Vyatka			0,51	0,58			0,20	0,18			0,01	0,02
Central Chernozem			0,43	0,52			0,17	0,15			0,00	0,01
Volga			0,51	0,59			0,20	0,18			0,01	0,02
North Caucasus			0,51	0,71			0,27	0,22			0,03	0,03
Urals	-0,93	-0,59	0,43	0,52	-0,43	-0,28	0,17	0,15	-0,19	-0,13	0,00	0,01

The albedo values are site specific and the biogenic CO_2 factors are connected to the rotation period. A site can therefore have the same biogenic CO_2 GWP characterisation factor, but different albedo values. The negative net GWP values for biogenic CO_2 and albedo for the Northern, Northwestern and Urals region indicate that in these areas the albedo effect is strong enough to contribute to a cooling effect. For the Northern region, it is definite as there is no temperate forest present, whilst for the Northwestern region there is temperate forest as well, which will close to outweigh the cooling effect from the boreal parts of the region. However, a small cooling effect overall is still present. For the Urals, the cooling effect from albedo is very strong and will contribute to cooling even if temperate forest is present. Due to their geographic location and presence of forest with long rotation periods, the results for these three regions are realistic. Northern Caucasus is the region with the highest positive net value, and there the albedo affect is not strong enough to have a proper impact and further outweighing the contribution from biogenic CO_2.

4.2. Scenario results

For the analysis conducted for each of the scenarios, the life cycle assessment in Arda was run solely for the upstream processes. Next the value for coal combustion was added, as well as the values calculated for direct biomass combustion and surface albedo. This was calculated for each of the eight regions for the scenarios, namely 10% co-firing with biomass, 20% co-firing with biomass, and the scenario of 100% bioenergy. Moreover the values were extracted for the three time horizons of 20, 100 and 500 years to be able to make the comparison.

The graph below, Figure 14, displays the total climate change impact in g CO_2-eq/$MJ_{fuel\ mix}$ for each of the three scenarios and the 100% coal-fired scenario is the line above the charts at 115 g CO_2-eq/$MJ_{fuel\ mix}$ as a reference. The time horizon is of 100 years. The value for total climate change impact for each case is found on top of each chart, and one can see the magnitude of the different parts of the analysis, namely the life cycle (upstream processes for coal and biomass), direct coal combustion, direct biogenic CO_2 combustion as well as the albedo effect, and how they contribute to the over all climate change impact. The black line in each of the charts indicates the net impact of biogenic CO_2 and the albedo effect, and is of interest to see where the albedo effect outweighs the impact from biogenic CO_2 and creates a cooling effect.

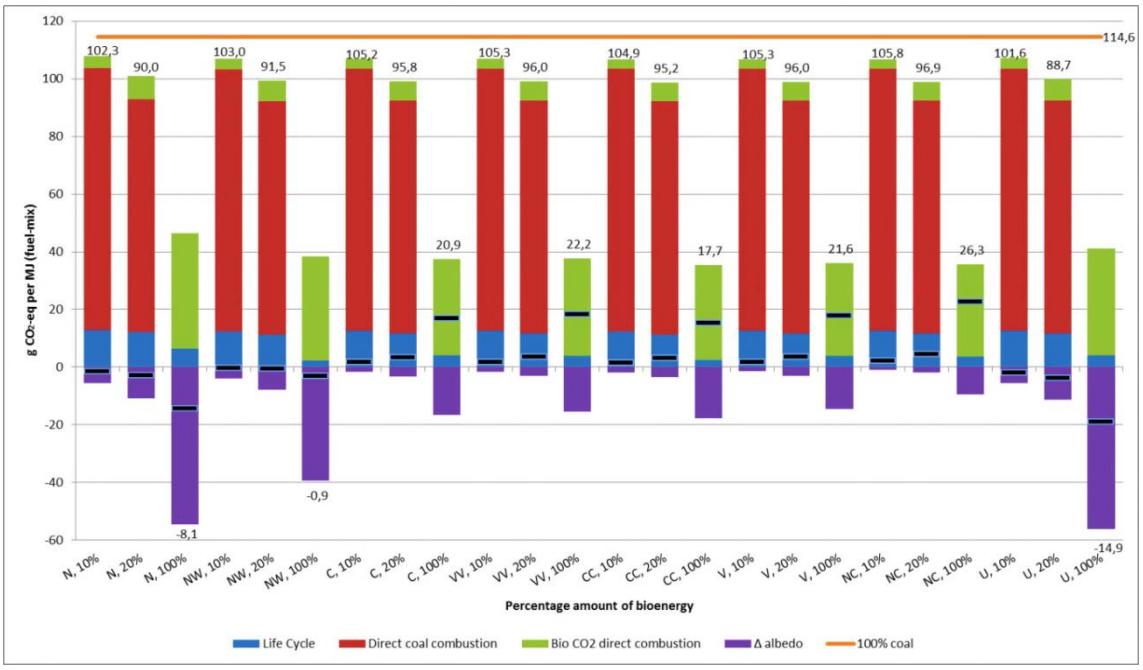

Figure 14: Total climate change impact of the three scenarios for each region at TH = 100 years (N=North, NW=Northwestern, C=Central, VV=Volga-Vyatka, CC=Central Chernozem, V=Volga, NC=North Caucasus, U=Urals) [g CO_2-eq/$MJ_{fuel-mix}$] The black line for each chart indicates the net impact of biogenic CO_2 and the albedo effect.

In the case of 10% co-firing, the overall reduction for each of the eight regions from 100% coal-firing is not extremely high, but there is in general a reduction in climate change impact for each region of between 9 and 13 g CO_2-eq/$MJ_{fuel\text{-}mix}$. The greatest difference is for the Urals and Northern region, both with an improvement of around 11% (reduction in emissions). These are also the regions with the largest contribution of the albedo effect. The smallest improvement is in North Caucasus with a reduction of 8%.

For the case of 20% co-firing, the improvement is more significant, and the total global warming potential is below 100 g CO_2-eq/$MJ_{fuel\text{-}mix}$ for all regions. The reductions vary between 18 and 26 g CO_2-eq/$MJ_{fuel\text{-}mix}$. Naturally, the greatest reductions here are also in the Urals and Northern region, with an improvement of 23% and 21% respectively. The lowest reduction was for North Caucasus with a reduction of around 15% in climate change impact.

The ideal scenario is if the coal demand would be completely covered by 100% bioenergy. There is a significant reduction for each region and this is where the direct biomass combustion and the albedo effect plays an important part in the total impact on climate change. The three most northern regions, North, Northwest and the Urals all have a final result below zero, of -8, -1 and -15 g CO_2-eq/$MJ_{fuel\text{-}mix}$ respectively. This implies that there is a cooling effect due to the large contribution from albedo, and thereby Δ albedo > biogenic CO_2. The black line representing the net value of these climate forcings also indicates this. The largest reduction is of 113% for the Urals region and the smallest reduction is 77% for North Caucasus with a final climate change impact of 26 g CO_2-eq/$MJ_{fuel\text{-}mix}$ respectively, which is still a substantial improvement.

Regarding the net value between biogenic CO_2 and albedo, at the time horizon of 100 years, the highest net differences between the climate change impact from biogenic CO_2 and albedo are for the Urals, with a difference of -19 g CO_2-eq/$MJ_{fuel\text{-}mix}$, and the Northern region with -15 g CO_2-eq/$MJ_{fuel\text{-}mix}$. The regions where the biogenic CO_2 is too high for the albedo to have a noteworthy impact is for the regions of North Caucasus with 23 g CO_2-eq/$MJ_{fuel\text{-}mix}$ and Volga-Vyatka with 18 g CO_2-eq/$MJ_{fuel\text{-}mix}$ respectively.

Figure 15 below represents the percentage contribution of each of the processes to the total climate change impact for the scenario of 10% co-firing with biomass for each region with a time horizon of 100 years.

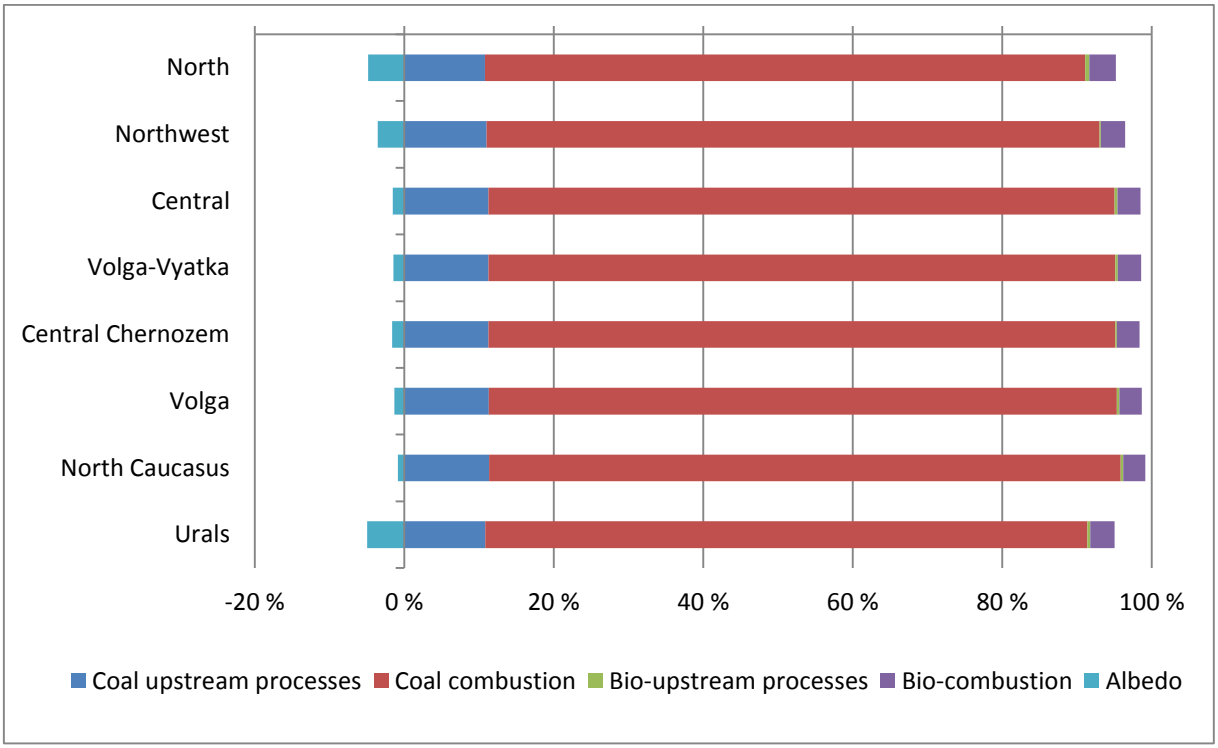

Figure 15: Percentage distribution of the climate change impact for each of the processes in the scenario of 10% co-firing with biomass for TH=100 years [%]

The largest contribution is from coal combustion, contributing with between 86% (North Caucasus) and 89% (Urals) of the total climate change impact for each region. The corresponding coal upstream processes contribute with around 12%. As it is only 10% co-firing and one is looking at 1 MJ fuel mix, the actual amount of biomass is not very substantial, and the bio-upstream processes therefore only contribute to between 0,2% (Central Chernozem) and 0,6% (North) of the overall emissions. The factors effecting it is mostly connected to the length of the transportation route designed for the region and the distribution between hardwood and softwood chips. The direct biomass combustion is responsible for between 3% (Urals) and 4% (North) of the total climate change impact, and the albedo effect has an impact of between 1% (North Caucasus) and 6% (Urals), but then in the terms of reducing the overall impact.

As the metric for climate change impact is based on GWP, it is heavily influenced by the selected time horizon, and the variations are especially noticeable for biogenic CO_2 and albedo. In the following three figures, Figure 16 to Figure 18, one can find an overview of the total climate change impact for each of the individual scenarios per region, with focus on the three time horizons 20, 100 and 500 years. The lines at the top of the chart visualise the emissions from the 100% coal-fired scenario for the three time horizons.

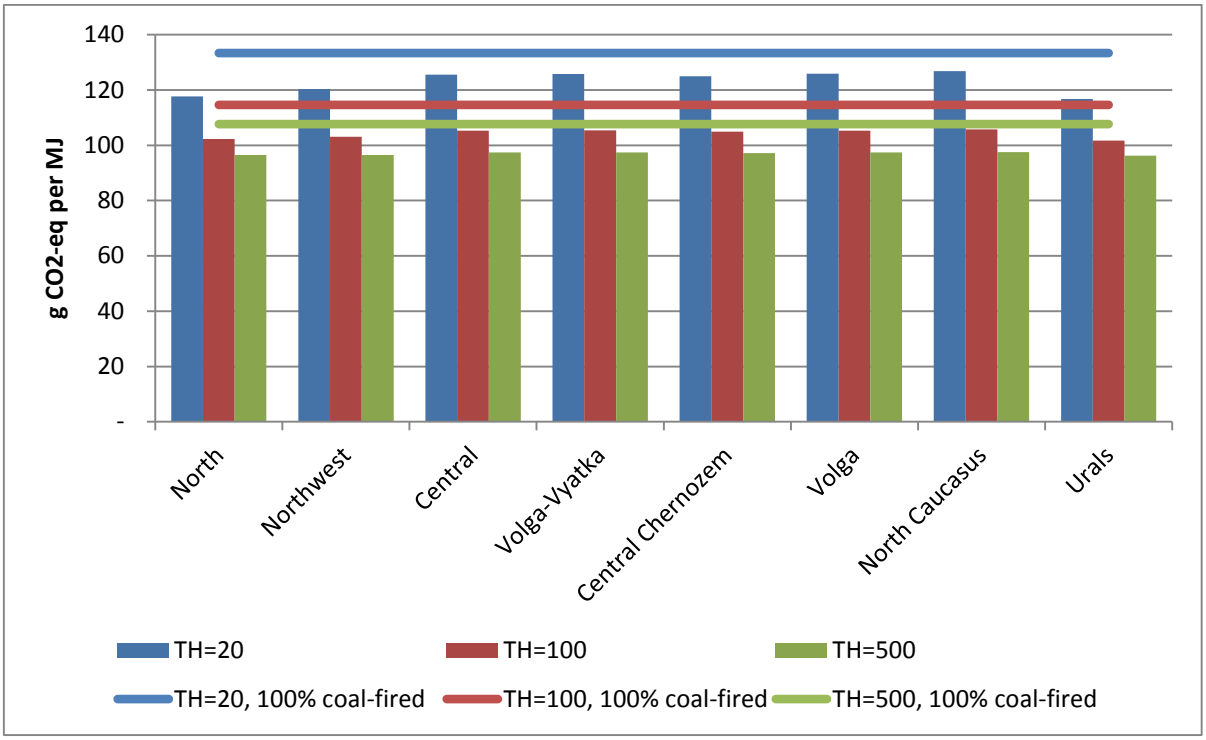

Figure 16: Total climate change impact for each region with co-firing of 10% biomass for TH=20, TH=100 and TH=500 [g CO_2-eq per $MJ_{fuel\text{-}mix}$]

The time horizon of 500 years is more precautionary than for the time horizons of 20 and 100 years, and therefore have lower results for all regions. For the time horizon of 20 years, the highest climate change impact is found in North Caucasus with 127 g CO_2-eq/$MJ_{fuel\text{-}mix}$ and the lowest in the Urals with 117 g CO_2-eq/ $MJ_{fuel\text{-}mix}$. As a reference, the total emissions for 100% coal-firing is for this time horizon 133 g CO_2-eq/$MJ_{fuel\text{-}mix}$. For the time horizon of 100 years, North Caucasus has a total climate change impact of 106 g CO_2-eq/$MJ_{fuel\text{-}mix}$ and the Urals have an impact of 102 g CO_2-eq/$MJ_{fuel\text{-}mix}$, with the 100% coal-firing having total emissions of 115 g CO_2-eq/$MJ_{fuel\text{-}mix}$. For the final time horizon of 500 years, the total GWP of the North Caucasus region is 98 g CO_2-eq/$MJ_{fuel\text{-}mix}$ and for the Urals it is 96 g CO_2-eq/$MJ_{fuel\text{-}mix}$ with the 100% coal-firing scenario having a climate change impact of 108 g CO_2-eq/$MJ_{fuel\text{-}mix}$.

The chart below describes the emissions for each time horizon for the various regions concerning the scenario of 20% co-firing with biomass.

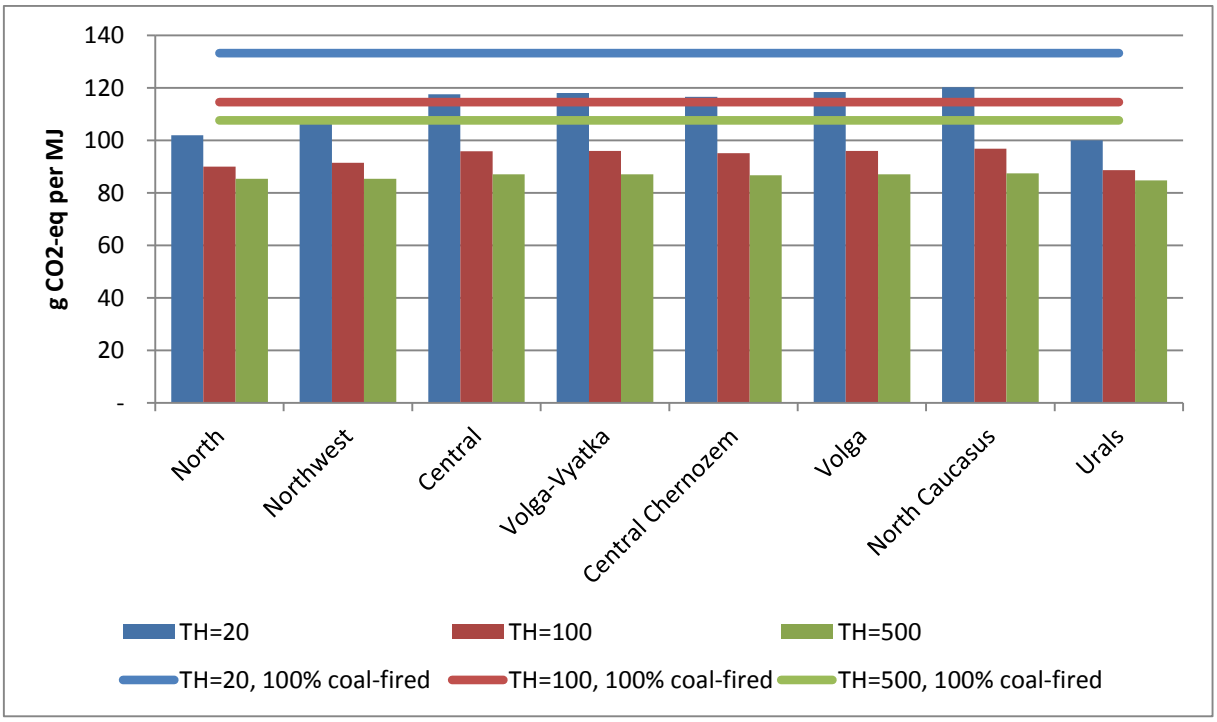

Figure 17: Total climate change impact for each region with co-firing of 20% biomass for TH=20, TH=100 and TH=500 [g CO_2-eq per $MJ_{fuel-mix}$]

In this scenario, the highest climate change impact for the time horizon of 20 years is found in North Caucasus with 120 g CO_2-eq/$MJ_{fuel-mix}$ and the lowest in the Urals with 100 g CO_2-eq/$MJ_{fuel-mix}$. The total emissions for 100% coal-firing is for this time horizon 133 g CO_2-eq/$MJ_{fuel-mix}$. For the time horizon of 100 years, North Caucasus has a total climate change impact of 97 g CO_2-eq/$MJ_{fuel-mix}$ and the Urals have an impact of 89 g CO_2-eq/$MJ_{fuel-mix}$, with the 100% coal-firing having total emissions of 115 g CO_2-eq/$MJ_{fuel-mix}$. Finally, for the time horizon of 500 years, the total GWP of the North Caucasus region is 87 g CO_2-eq/$MJ_{fuel-mix}$ and for the Urals it is 85 g CO_2-eq/$MJ_{fuel-mix}$ with the 100% coal-firing scenario having a climate change impact of 108 g CO_2-eq/$MJ_{fuel-mix}$.

As a final part, in Figure 18 below, the emissions for each time horizon for the various regions concerning the scenario of 100% co-firing with biomass are visualised.

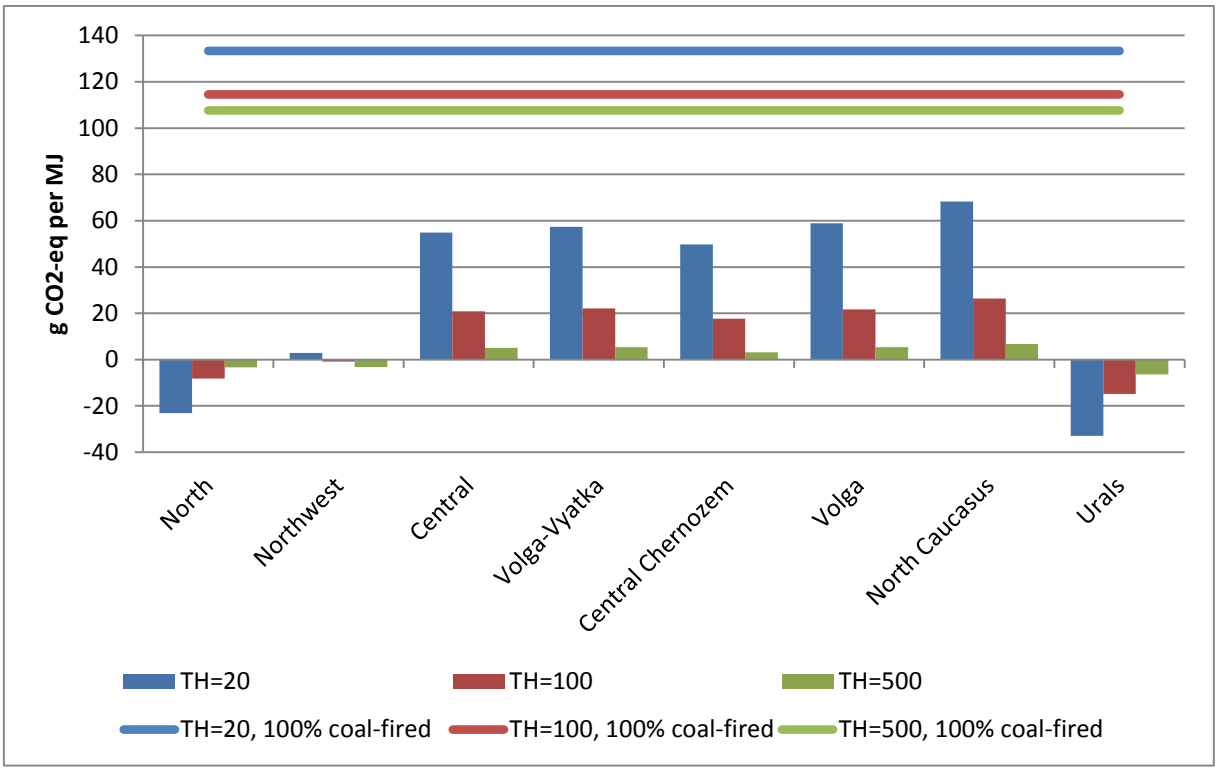

Figure 18: Total climate change impact for each region with 100% bioenergy for TH=20, TH=100 and TH=500 [g CO_2-eq per $MJ_{fuel\text{-}mix}$]

For the ideal case of 100% bioenergy, there are quite significant differences between for each region and time horizon. The highest climate change impact for the time horizon of 20 years is found in North Caucasus with 68 g CO_2-eq/$MJ_{fuel\text{-}mix}$ and the lowest in the Urals with -33 g CO_2-eq/$MJ_{fuel\text{-}mix}$. As a reference, the total emissions for 100% coal-firing is 133 g CO_2-eq/$MJ_{fuel\text{-}mix}$ for this time horizon. With the time horizon being 100 years, North Caucasus has a total climate change impact of 26 g CO_2-eq/$MJ_{fuel\text{-}mix}$ and the Urals have an impact of -15 g CO_2-eq/$MJ_{fuel\text{-}mix}$, with the 100% coal-firing having total emissions of 115 g CO_2-eq/$MJ_{fuel\text{-}mix}$. In the end, for the time horizon of 500 years, the total climate change impact of the North Caucasus region is 7 g CO_2-eq/$MJ_{fuel\text{-}mix}$ and for the Urals it is -6 g CO_2-eq/$MJ_{fuel\text{-}mix}$ with the 100% coal-firing scenario having a climate change impact of 108 g CO_2-eq/$MJ_{fuel\text{-}mix}$. The numerical values connected to Figure 16 to Figure 18 can be found in Table 34 in Appendix 8.3.

The results for the time horizon of 20 years are clearly higher than for the time horizon of 500 years. To emphasise the impacts of biogenic CO_2 and albedo, for the Urals, for

TH=20 years, the climate change impact from albedo is -129 g CO_2-eq/$MJ_{fuel\text{-}mix}$, whilst it is -17 g CO_2-eq/$MJ_{fuel\text{-}mix}$ for the time horizon of 500 years. However, due to the high impact from direct biomass combustion, the net value evens it more out so there are no "extreme" values. Despite this, in the Urals, as well as for the Northern and Northwestern region, the albedo effect is high enough to give an overall cooling effect in the scenario of 100% bioenergy. The region of North Caucasus has the lowest values overall, and the remaining four regions have very similar values from -14 to -18 g CO_2-eq/$MJ_{fuel\text{-}mix}$ in the time horizon of 100 years.

To further illustrate the impact of the time horizons, for the case of the Northern region, the impact on climate change at TH=500 from biogenic CO_2 and albedo is 8% and 13,7% of the impact when TH=20. The albedo effect is also stronger at TH=20, causing a much larger cooling effect and having a net negative impact at TH=20 with -8,8 g CO_2-eq/$MJ_{fuel\text{-}mix}$ compared to 11,6 g CO_2-eq/$MJ_{fuel\text{-}mix}$ at TH=500.

4.3. Potential future co-firing scenarios

To summarise the scenarios and future possibilities, the current harvest in Russia is 173,6 mill m^3 and approximately 1 649 200 TJ/yr in terms of energy potential. The current coal demand (fuel input) is around 2 471 719 TJ/yr (260,2 mill m^3). If one assumes that all of the current harvest is used for wood production, to cover various percentages of coal demand, the current harvest needs to increase with the following:

a) 10% coal demand scenario

Will result in a 15% increase in harvesting, a total of 3% of the Net Annual Increment (NAI) and 5% of the Annual Increment Available for Exploitation (AIAE). The increase in harvest together with the current harvest, would result in a total of 23% of NAI, 36% of AIAE and 32% of Annual Allowable Cut (AAC).

b) 20% coal demand scenario

The harvest would have to increase with 30%, which is a total of 6% of NAI and 10% of the AIAE. In total, the increase in harvest together with the current harvest would result in a total of 27% of NAI, 41% of AIAE and 36% of AAC.

c) 50% coal demand scenario

Will result in a 75% increase in harvesting, a total of 15% of NAI and 24% of the AIAE. The increase in harvest, together with the current harvest would result in a total of 37% of NAI, 55% of AIAE and 48% of AAC.

d) 100% coal demand scenario

As a final scenario, if the coal demand in Russia would be covered 100% by bioenergy, this would require an increase in harvest by 150%, which is a total of 31% of the NAI and 47% of the AIAE. In total, the increase in harvest together with the current harvest equals 51% of NAI , 79% of AIAE and 69% of AAC.

To reach a coal-free Russia in terms of power generation, harvest needs to be increased significantly, but even for the 100% coal demand coverage, only close to 50% of the annual increment available for exploitation is being used. The numerical values can be found in Appendix 8.4, Table 35 and Table 36.

5. Discussion

In this part, first the key assumptions and limitations will be presented. Furthermore, the results of the various analyses will be looked at more closely, both by comparing the outcomes relative to each other, as well as connecting them to already existing results. As a final part, the implications of the results will be discussed, focusing on future scenarios, policy recommendations and research.

5.1. Key assumptions and limitations

As a first point, properties for coal such as the lower heating value (LHV), varies for each mine and even within the mine itself. The lower the heating value implies that more coal is necessary for 1 MJ of fuel input. Coal types such as lignite, which has a lower quality than for instance anthracite, has therefore a much larger negative impact on the environment during combustion. The average LHV for the Russian Federation from ecoinvent (ecoinvent, 2010) has been used for this assessment. Even if the value could have been more accurate by being connected to specific mines, this is still a representative value, as the main focus of this thesis is the impact on climate change from biomass.

The developed scenarios include all the relevant processes needed to assess the emissions connected to 1 MJ fuel input. The input needed of coal and biomass has been calculated and made specific for each of the regions in European Russia, together with the transportation routes. The remaining background processes of the wood chip production are however based on standard inventory from ecoinvent. As the forestry activities can differ substantially from region to region, and even within regions (Michelsen et al., 2012) and the electricity mix for the processes being a “European average”, some inaccuracy is expected. Due to a limited amount of relevant studies done on Russia and very few decent sources being in English, gathering data for this part of the inventory has been challenging. However, as the results show, upstream emissions for biomass only contribute a minor part of the total climate change impact, with the direct biomass combustion and albedo effect being of far more importance. Therefore priority was given to gathering data and developing this part of the assessment, rather than for the upstream processes.

Estimations were made for the distribution of boreal and temperate forest, as well as the amount of coniferous and deciduous wood in each region. These estimations were based on

the most accurate and up-to-date data found, but as Russia is such a vast country, with over 20% of the world's forest resources, there are uncertainties in the assessments. In addition, as the fuel input was in m^3 per MJ, one had to convert from values in hectare forest to m^3, and used the density of Norwegian spruce to characterise coniferous wood (softwood) and birch for deciduous wood (hardwood). However, the estimations used in this thesis are more representative than i.e. using an average for the whole of the European Russia, as the percentage distribution is specified for each of the nine regions.

Concerning the rotation periods and yields for the forest types in the Russian Federation, the average estimations from IPCC were used (IPCC, 2006). The values from IPCC are still representative for the four forest types present in European Russia and the main impact on the results will be connected to how fast the carbon is removed from the atmosphere (Michelsen et al., 2012). Overall, the difference is not as substantial compared to i.e. assigning GWP_{bio} representing short rotation periods to the forest areas in this assessment, which evidently have long rotation periods.

Choosing appropriate site locations for gathering albedo data is of importance. By using Google Earth, two sites were chosen for each region, one forest site and one with open landscape. For the Northwestern and Northern Caucasus region, extra sites were added for open landscape, as when analysing the results, it showed that the original sites chosen were not ideal to represent "open landscape". To better the accuracy for each region and make the average more representative, one could have increased the number of sites for each region. Due to time constraints, this was not prioritised. The results have however been quality checked and as there were two to four values calculated for each region, based on the forest types, the calculations connected to the climate change impact from albedo are thorough for each site in question.

For estimating RF_a, one has to rely on simplified numerical models such as the ones presented in this thesis, by making use of the single two-way transmittance parameter f_a. Ideally one would rather make use of more sophisticated radiative transfer (Fu and Liou, 1993; Hatzianastassiou et al., 2005), especially those coupled with a chemical transport model or that give the possibility for user-defined input data regarding the cloud cover and aerosol optical properties. Obtaining f_a requires information on the atmospheric absorption

or the scattering of incoming and outgoing shortwave radiation, and in this thesis, f_a is based on K_T, which is further based on satellite measurements of surface irradiance collected for a 22-year period from the dataset provided by NASA's Surface meteorology and Solar Energy (SSE). Reviews done by (Schmetz, 1989) and (Pinker et al., 1995) claim that the daily insolation estimates from geostationary satellite data are generally within 10-15% of the ground-based measurements (Bright et al., 2012). Therefore it was concluded that the radiative transfer data was still was reliable for the final assessment.

Furthermore, since the chosen sites are user-defined, there are uncertainties in the calculation of $\Delta RF_{\alpha}(t)$ based on the data concerning albedo, α_{new}, α_{old} and f_a, as well as the albedo decay function, $y_{\alpha}(t)$. The functional form of $y_{\alpha}(t)$ is case-dependent and more research is needed to increase the empirical understanding of the physical factors that drive vegetation albedo change in time on managed land. For now, the parameter therefore poses an uncertainty in the derivation in this area. When possible, the results should be presented together with results that describe the sensitivity to changes in τ and the functional formulation of $y_{\alpha}(t)$ (Bright et al., 2012). Regarding the data collected from MODIS representing the cloud-cleared surface albedo data, this has shown to have minimal uncertainty connected to it if pixels for high quality is used, which is the case in this thesis (Jin et al., 2003a; Jin et al., 2003b; Liang et al., 2002; Stroeve et al., 2005; Wang et al., 2004). As one also gathers data for multiple years (Feb 2000 to March 2013) and develop monthly averages, the uncertainties of α_{new} and α_{old} are reduced. Overall the data collected is as optimal as it can get with regards to the scope of the thesis and time frame for the work and analyses conducted.

Regarding the functional unit, by looking at 1 MJ input fuel mix, rather than 1 MJ electricity or heat, one does not let efficiency degrees and the infrastructure connected to the power plant be a part of the analysis. This makes it easier to compare the various alternatives, especially with the scenario of 100% bioenergy, which would use a different power plant infrastructure than in the 100% coal-fired scenario for instance.

As a final part, calculating the temporary change in atmospheric CO_2 concentrations caused by biogenic CO_2 emissions and cooling effects from changes in surface albedo following the harvest is not incorporated as a common practice yet for LCA practitioners. Any attempt of

highlighting these issues and trying to quantify the impact is therefore of importance. With a limited amount of studies done on Russia, this study has given a good starting point for exploring the potential further in this country. Since the study is divided into eight regions in European Russia and particularly with the albedo effect being site-specific, the results are more accurate and representative than for instance having a general average of European Russia.

5.2. Further discussion of results

The magnitude of the albedo contribution can vary a lot depending on several factors. Aside from the local climate variables, elevation and vegetation dynamics affecting the atmospheric transmittance of solar radiation, an important aspect is the yield of biomass per unit area affected. The amount of emissions here is inversely proportional to the effect of the increased yields (Cherubini et al., 2012).

With a lower amount of dead organic material left on the site to decompose due to cleaning the site, the contribution to global warming from biogenic CO_2 fluxes decreases. At the same time, the albedo effect is highly influenced in two contrasting ways. By increasing the cleaning of the site after harvest, it becomes a smoother surface and thereby less snow is needed to cover the area to provide a homogeneous solar radiation reflectivity. However, due to collecting the forest residues, one also increases the biomass yield of the site, which results in reducing the area harvested per unit. The effects of the increased biomass yield outweighs the effects caused by the smoother surfaces and in total the albedo cooling effect is actually reduced (Cherubini et al., 2012).

Regarding the equivalency factors, Table 14 and Table 15 give an overview of the GWPs for the three most common time horizons of 20, 100 and 500 years for biogenic CO_2 and albedo respectively. These equivalency factors make is possible for LCA practitioners to quantify the temporary change in atmospheric CO_2 concentration the same way as for other common greenhouse gases, for which the emissions are included in the IRF that is the basis for the respective factor (Cherubini et al., 2012).

The carbon cycle and albedo change dynamics are affected by the biomass species and location amongst others, and therefore the characterisation of biogenic CO_2 and albedo are case-specific. This is one of the main differences from the calculations of the GWP for the

other greenhouse gases and enables a more accurate attribution of climate change impact from biogenic CO_2 emissions and albedo to a life cycle inventory for a bioenergy system. Therefore no other modelling tools or frameworks are needed for this part (see e.g. (Bright et al., 2011; McKechnie et al., 2010)).

The equivalency factors were used to calculate the climate change impact of biogenic CO_2 and albedo. However, one also needs to assess the emissions concerning the upstream processes and the climate change impact of co-firing and bioenergy therefore increases. This is not only due to the coal combustion in the co-firing scenarios, but also the upstream processes connected to transport and conversion processes which often are depended on fossil fuels such as diesel. The total climate effects also depend on the type of fuel mix used, the system boundaries and the reference energy system which the bioenergy chain is compared to (Cherubini et al., 2009). As the scope has been 1 MJ of fuel mix input, the upstream processes are the main focus in this thesis.

The upstream processes vary for each scenario and region. Looking at the coal upstream processes and combustion as an isolated case, the result is 115 g CO_2-eq/MJ_{fuel}. In an article by Cherubini et al (2012) which used standardised ecoinvent data, the results was 105 g CO_2-eq/MJ_{fuel} (Cherubini et al., 2012). The main reason for the difference is that this was a general case for reference, whilst in our case, the data is specific for the Russian Federation, which amongst others has higher emissions connected to the hard coal production.

For the upstream emissions for biomass, the easiest to compare is for the scenario of 100% bioenergy, with the time horizon of 100 years. Due to different lengths of the transportation routes and the amount of coniferous and deciduous biomass used as fuel input for each region, there are some variations. The highest emissions are in the Northern region with 6,3 g CO_2-eq/$MJ_{fuel\text{-}mix}$ and the lowest in Northwest with 2,3 g CO_2-eq/$MJ_{fuel\text{-}mix}$ followed by Central Chernozem with emissions of 2,5 g CO_2-eq/$MJ_{fuel\text{-}mix}$. The remaining regions have values ranging from 3,8 g CO_2-eq/$MJ_{fuel\text{-}mix}$ for Volga to the Urals with 4,2 g CO_2-eq/$MJ_{fuel\text{-}mix}$, and the complete overview can be found in Appendix 8.3.

To compare to similar studies, an article by Cherubini et al (2012) looks into four cases with different types of biomass (Cherubini et al., 2012). For heat production using domestic

wood, Canadian wood had upstream processes of 10 g CO_2-eq/$MJ_{fuel-mix}$, wood from the Pacific Northwest in the United States had biomass upstream emissions of 17 g CO_2-eq/$MJ_{fuel-mix}$, whilst for Wisconsin (USA), the total emissions were 18 g CO_2-eq/$MJ_{fuel-mix}$. For the case of Norway, the emissions were significantly lower with 4 g CO_2-eq/$MJ_{fuel-mix}$. A study by Kabir et al found that upstream processes for wood chips from whole tree had an impact of 5,6 g CO_2-eq/$MJ_{fuel-mix}$ (Kabir and Kumar, 2012). It is apparent that the biomass upstream emissions vary substantially. The upstream emissions connected to the regions in European Russia are somewhat lower than expected, but still feasible. This is due to using generic ecoinvent data for the harvesting, forwarding and wood chipping, rather than more country specific. However, the upstream emissions are not the processes with the most crucial contribution to the overall climate change impact, compared to combustion of both coal and biomass, in addition to the albedo effect.

The overall results for each region clearly illustrate that biogenic CO_2 and albedo cannot be overlooked, as they substantially influence the climate change impact for bioenergy systems. This especially applies to the regions with boreal climate and thereby have longer snow seasons and stronger cooling effect. With the time horizon of 100 years, the total climate change impact for the North and Urals region were decreased with over 100% due to albedo effect being of higher value than direct biomass combustion. As emphasised in an article by Bright et al (2012), it is therefore important to maximize the benefits from the albedo change in the short term, while at the same time preserving the integrity of the forest as a strong carbon sink. However, there is still a lot unknown concerning the albedo dynamics in an actively managed boreal forest and the time profile of the albedo change. Therefore it is recommended to continue research on this area before any implementation of climate-effective biomass management strategies (Bright et al., 2012).

5.2.1. GWP of biogenic CO_2; 0, 1 or site-specific?

Previous studies such as Bright et al. and Cherubini et al. from 2012 both show that substantially misleading conclusions can be achieved if biogenic CO_2 emissions are improperly characterised, regardless of the type of biomass and the contributions from the albedo effect (Bright et al., 2012; Cherubini et al., 2012), and this study is no exception. If one was to assume carbon neutrality and use an equivalency factor of zero, the direct impact to climate change from bioenergy would be highly underestimated. If one used a

factor of one, which is the equivalent of the fossil reference, it would be over-estimated (Bright et al., 2012).

As an example, if one were to conduct the LCA without taking biogenic CO_2 and albedo into consideration, one would for the Northern region with TH=100 have a final result of 6,3 g CO_2-eq/$MJ_{fuel\text{-}mix}$. Due to direct biomass combustion of 40 g CO_2-eq/$MJ_{fuel\text{-}mix}$ and the cooling effect of albedo with -55 g CO_2-eq/$MJ_{fuel\text{-}mix}$, the final result actually becomes -8 g CO_2-eq/$MJ_{fuel\text{-}mix}$. It is therefore apparent that improper accounting can result in highly ineffective and counter-productive climate mitigation efforts. One further needs to realise that the situation for biogenic CO_2 is complex and that it is not appropriate to account with a value of either 0 or 1 (Bright et al., 2012).

5.3. Future scenarios and implications

The future potential co-firing scenarios in Russia, presented in Chapter 4.3, are feasible in the long-term. However, the development of infrastructure and policies need to be a priority for the scenarios to become realistic.

5.3.1. Implications of increased harvest and export

"Opportunities for expanding bioenergy for heat production in non-OECD countries are larger than in the OECD because of their rapid energy demand growth" (IEA, 2012e). An increase in bioenergy implies an increase in harvesting, which can create certain implications apart from the ones already mentioned. If harvesting is to be developed, equipment that is more productive is needed, and these systems would require less labour. There may therefore be effects on the labour market in the more rural areas (Goltsev et al., 2010). In spite of this, increased harvest will also create prosperity in various regions by expanding the industry and investment in rural areas and thereby having a positive impact (Junginger et al., 2006). Moreover, there are great opportunities for Russia to export biomass to European countries especially, in addition to the current export of oil, gas and coal. Overall the harvesting needs to be a compromise between investment costs, production and the effects on society (Goltsev et al., 2010).

IPCC also focuses on the possibilities of increasing the regional economic development, in addition to replacing the fossil fuel based systems for heat and power generation (IPCC, 2012). The availability of biomass in a territory will vary though and for certain areas it

will be hard to supply a biomass-fired power plant that produces the same amount of electricity as a large scale coal power plant without having significant impacts on the environment (Sebastián et al., 2011). The effects on biodiversity is an important aspect. Moreover, depending on the geographic location (if the albedo effect plays a part or not) and the carbon density of the converted forest, the biomass plantations may lead to significant CO_2 emissions. These emissions would then reduce the annual accumulated climate benefit drastically for substituting fossil fuels with the bioenergy derived from such a forest area (IPCC, 2012).

Looking into the future trends in bioenergy, one of the main issues will also be if the biomass should be used as biofuel in stationary energy systems for heat and electricity, or if it should rather be used as feedstock for liquid biofuel production for transportation (Cherubini et al., 2009). However, the efficiency for converting biomass to fuel is a lot lower than for biomass to bioenergy. For production of transportation fuels, more emissions would therefore occur, resulting in a higher impact on climate change.

Regarding the exporting potential, logistics and infrastructure are quite essential for the set-up of large scale biomass systems and the related necessary facilities such as ports and ships (IEA, 2012e). Studies such as (Sikkema et al., 2010; Sikkema et al., 2011) have shown that long-distance transport by ship is feasible concerning transportation costs and energy usage. However for i.e. Scandinavia and Russia, the meteorological conditions need to be taken into consideration in terms of having available vessels that are suitable for these type of missions (IPCC, 2012). Moreover, even if technologies are currently being developed, there is also a lack of technically mature technologies to densify biomass at a low cost to further keep the costs for handling and transportation down (IPCC, 2012; Kabir and Kumar, 2012).

There is a possibility that these barriers could prevent imports and exports from increasing fast enough to meet the demand (IEA, 2012e). According to the Forest Sector Outlook Study by the Food and Agriculture Organization of the United Nations, export in the future is only envisioned for biomass pellets originating from regions where the necessary economic and transport conditions are available (FAO, 2012). This would currently exclude Siberia and the Far East, but if prioritised and investments were made, it could be feasible in the long term due to the extensive unexploited forest potential there.

The aforementioned study also highlights the potential impacts of the climate change on the forest in Russia. The climate change is likely to contribute to an increased average forest productivity nationwide and the growth conditions are especially favourable for the deciduous species (FAO, 2012), so there would potentially be an increase of hardwood. Moreover, it is predicted that forest areas with high latitudes will have an increased industrial development (FAO, 2012). This is quite interesting, as the development of new regions here will have a negative impact on the forest areas, but as it is in the boreal climate with seasonal snow cover, the albedo effect will have a significant impact in connection with climate change and forest management.

5.3.2. Policy recommendations

The increased demand for bioenergy for heat and electricity production worldwide is largely driven by government policies. Some bioenergy power technologies manage to become competitive with fossil fuel based power plants during the projection period in regions that have established a carbon price. CHP and co-firing in coal power plants have especially given promising results (IEA, 2012e). Carbon pricing in Russia remains a prospective plan to be implemented. According to Russia's strategy 2020, a broad policy document concerning the national development until 2020, provisions are made of carbon taxation in mid-term, around year 2016 (Chernenko, 2012). Standards for renewable energy sources as well as subsidies are other examples of policies that contribute to the growth in the demand for bioenergy for heat and electricity (IEA, 2012e).

Not only in Russia, but more general, for most power plant companies the decision to co-fire with biomass, even if it only requires minor retro-fitting, will be driven by economic interests rather than environmental concerns (Mann and Spath, 2001). This is the case for most other sectors as well. There may be an increased interest if incentives are introduced, such as subsidies from the government with regulatory policies, or there is an electricity deregulation or issues with fuel supply, so that one needs to change strategy and become more energy efficient.

In addition, without it being the main priority for Russian companies, there is an increasing focus globally of becoming more "green" as companies and thinking about their environmental footprints. Companies may therefore wish to receive their power supply from

renewable resources or partially renewable resources in the future as a part of their environmental strategy, which could become an incentive for the power plant companies (Mann and Spath, 2001).

The International Energy Agency (IEA) have certain policy recommendations in connection with bioenergy on a global scale, which are highlighted in their publication Energy Technology Perspective 2012. Firstly an increased amount of research is needed in mapping land suitability and bioenergy feedstock, so one can see what are the most promising locations for increasing the bioenergy harvest, as well as what type of feedstock is the most appropriate. In addition, internationally agreed sustainability criteria, indicators and assessment methods for bioenergy should be implemented, which also provides the basis for developing a scheme for resource efficiency and sustainable production (IEA, 2012c).

Furthermore, recently the United Nations launched its Sustainable Energy for All initiative, which amongst others has a target of doubling the share of renewable energy globally by 2030. There are also the ongoing targets of the European Union since 2009 through the Renewable Energy Directive, which has set legally binding targets that the share of renewable energy (covering electricity, heat and biofuels) in gross final energy consumption has to equal 20% by 2020 (IEA, 2012e). Even if Russia is not a part of the European Union, there will be an increased pressure in the future for the country to further develop its environmental focus (IEA, 2012b), and it would be beneficial for the country to start their climate mitigation strategies sooner rather than later. This is also highlighted through the recently published roadmap "EU-Russia Energy Cooperation until 2050", which "aims at improving the investment opportunities in the energy sector to ensure continued energy production, to secure and expand transportation infrastructure as well as to reduce the environmental impact" (EC for Energy, 2013).

Globally, further investigation of the climate change impact of CO_2 emissions from temporary carbon loss is needed, and it should be looked into the possibilities of including biogenic CO_2 in the national GHG reporting for bioenergy production, and stepping away from the current carbon neutral accounting recommended by the OECD. Furthermore, LCA studies and climate accounting schemes such as the second phase of the Kyoto Protocol that started 1st January 2013 (Russia decided not to renew their commitment) should

transparently acknowledge these issues and incorporate the climate forcings in the reporting (Bright et al., 2012).

5.3.3. Recommendations for future research

On a large scale, increased research efforts should be made on feedstock and the land availability to identify what are the most promising feedstock types and locations for developing harvest to large-scale bioenergy production and meet the future demands. In addition there should be more funding and support mechanisms for emerging technologies within the bioenergy field, with special focus on BIGCC (biomass integrated gasification combined cycle), torrefaction and pyrolysis. With this the IEA hope that the technologies can reach commercial production within the next 10 years (IEA, 2012c).

With a more narrow scope, further investigation is needed to see how albedo estimation procedures can be incorporated into life cycle GHG accounting standards and regulations, alongside biogenic CO_2 (Bright et al., 2012). With more studies conducted on what is looked upon as the two most important contributions to global climate change, an increased awareness is hopefully achieved, significant enough for the governmental and international policies to take these climate forcings into account. More research should also be focused on stepping away from stand-alone LCA or carbon footprint type assessments, and rather going towards more integrated frameworks which have a higher temporal and spatial resolution, and are not restricted to emission-based metrics (Bright et al., 2011).

As a final part, due to the limited amount of existing research on the bioenergy possibilities in Russia, it is highly recommended that this will become a priority in the future. Moreover, there should be an increase in the amount of literature in English, making it more accessible for the global research community.

6. Conclusion

The main objective of this thesis has been to look at the climate change impacts of co-firing biomass from Russian forest areas with coal.

There is a significant amount of exploitable forest resources in the Russian Federation and the harvesting needs to increase by 30% to cover 20% of the current coal demand in Russia with bioenergy. If the coal demand is to be covered completely (100% bioenergy), the harvesting needs to increase by 150%. This is a substantial growth, but still only 50% of the annual increment available for exploitation would be utilised, and the new total harvest would be 69% of the annual allowable cut. For this to be feasible in the long term, policies would need to be introduced to promote renewable energy sources in Russia, in addition to focusing on developing the infrastructure in richly wooded areas. Russia also has great potential of becoming a large exporter of bioenergy to the European power sector.

Through the life cycle assessment, effective radiative forcing has been used as a basis for the climate metrics for the temporary effects of biogenic CO_2 and albedo, and the final results have been expressed both with absolute and normalised metrics (i.e. in terms of g CO_2-eq per $MJ_{fuel\text{-}mix}$). The inclusion of these factors have had a significant impact and has reinforced conclusions drawn in previous literature, especially concerning the cooling effects in high latitude boreal areas and forest with long rotation periods. The chosen time horizon is also of importance and the impacts of bioenergy and co-firing are generally higher for shorter time horizons, but considerably decrease over time. Certain areas, such as the Northern and Urals region of European Russia, both have a net negative global warming contribution (net global cooling effect) from the beginning of the assessment period in the case of 100% bioenergy production.

Further research is needed to understand the relationships between physical properties of managed forest and albedo, and how this can be used in forest management strategies for mitigating climate change in the future. Moreover it should be investigated how biogenic CO_2 and albedo can be included in climate accounting mechanisms both on a national and global scale, and thereby acknowledging the importance of these climate forcings, especially when designing bioenergy policies for boreal forest areas.

7. References

Backman, C. A. 1997. The forest sector of European Russia. *Polar Geography,* 21**,** 272-296.

Bala, G.,Caldeira, K.,Wickett, M.,Phillips, T. J.,Lobell, D. B.,Delire, C. & Mirin, A. 2007. Combined climate and carbon-cycle effects of large-scale deforestation. *Proceedings of the National Academy of Sciences of the United States of America,* 104**,** 6550-6555.

Bare, J. C.,Hofstetter, P.,Pennington, D. W. & Haes, H. A. U. 2000. Midpoints versus endpoints: The sacrifices and benefits. *The International Journal of Life Cycle Assessment,* 5**,** 319-326.

Belobrov, V. *Electricity markets in Russia* [Online]. Available: http://www.academia.edu/2204254/Electricity_Markets_in_Russia_english_updated_ [Accessed 15.03 2013].

Brattebø, H.,Røine, K.,Opoku, H. & Ehrenfeld, J. R. 2007. *Introduction to Industrial Ecology - Theory, Methods and Applications,* Trondheim, Norwegian University of Science and Technology.

Bright, R. M.,Cherubini, F. & Strømman, A. H. 2012. Climate impacts of bioenergy: Inclusion of carbon cycle and albedo dynamics in life cycle impact assessment. *Environmental Impact Assessment Review,* 37**,** 2-11.

Bright, R. M.,Strømman, A. H. & Peters, G. P. 2011. Radiative Forcing Impacts of Boreal Forest Biofuels: A Scenario Study for Norway in Light of Albedo. *Environmental Science & Technology,* 45**,** 7570-7580.

Chernenko, N. 2012. Carbon pricing on the Russian electricity market. Cambridge: Faculty of Economics, University of Cambridge.

Cherubini, F.,Bird, N. D.,Cowie, A.,Jungmeier, G.,Schlamadinger, B. & Woess-Gallasch, S. 2009. Energy- and greenhouse gas-based LCA of biofuel and bioenergy systems: Key issues, ranges and recommendations. *Resources, Conservation and Recycling,* 53**,** 434-447.

Cherubini, F.,Bright, R. M. & Strømman, A. H. 2012. Site-specific global warming potentials of biogenic CO_2 for bioenergy: contributions from carbon fluxes and albedo dynamics. *Environmental Research Letters,* 7**,** 045902.

Cherubini, F.,Peters, G. P.,Berntsen, T.,Strømman, A. H. & Hertwich, E. 2011a. CO_2 emissions from biomass combustion for bioenergy: atmospheric decay and contribution to global warming. *GCB Bioenergy,* 3**,** 413-426.

Cherubini, F. & Strømman, A. H. 2011b. Life cycle assessment of bioenergy systems: State of the art and future challenges. *Bioresource Technology,* 102**,** 437-451.

European Commission for Energy. 2013. *Roadmap - EU-Russia Energy Cooperation until 2050*. Brussels: European Commission for Energy.

ecoinvent 2010. ecoinvent v2.2. The Swiss Centre for Life Cycle Inventories.

Fagernäs, L.,Johansson, A.,Wilén, C.,Sipilä, K.,Mäkinen, T.,Helynen, S.,Daugherty, E.,Den Uil, H.,Vehlow, J.,Kåberger, T. & Rogulska, M. 2006. Bioenergy in Europe opportunities and barriers.

Food and Agriculture Organization of the United Nations (FAO) 2012. *The Russian Federation Forest Sector - Outlook Study to 2030,* Rome, FAO/UNECE.

Fu, Q. & Liou, K. N. 1993. Parameterization of the radiative properties of cirrus clouds. *Journal of the Atmospheric Sciences,* 50**,** 2008-2025.

GBEP 2008. *A review of the Current State of Bioenergy Development in G8+5 Countries,* Rome, Italy, Global Bioenergy Partnership (GBEP), Food and Agriculture Organization of the United Nations.

Goedkoop, M., Heijungs, R., Huijbregts, M., Schryver, A. D.,Struijs, J. & Zelm, R. v. 2009. ReCiPe 2008, A life cycle impact assessment method which comprises harmonised category indicators at the midpoint and endpoint level.

Goltsev, V.,Ilavský, J.,Karjalainen, T. & Gerasimov, Y. 2010. Potential of energy wood resources and technologies for their supply in Tihvin and Boksitogorsk Districts of the Leningrad Region. *Biomass and Bioenergy,* 34**,** 1440-1448.

Hansen, J.,Sato, M.,Ruedy, R.,Nazarenko, L.,Lacis, A.,Schmidt, G. A.,Russell, G.,Aleinov, I.,Bauer, M.,Bauer, S.,Bell, N.,Cairns, B.,Canuto, V.,Chandler, M.,Cheng, Y.,Del Genio, A.,Faluvegi, G.,Fleming, E.,Friend, A.,Hall, T.,Jackman, C.,Kelley, M.,Kiang, N.,Koch, D.,Lean, J.,Lerner, J.,Lo, K.,Menon, S.,Miller, R.,Minnis, P.,Novakov, T.,Oinas, V.,Perlwitz, J.,Perlwitz, J.,Rind, D.,Romanou, A.,Shindell, D.,Stone, P.,Sun, S.,Tausnev, N.,Thresher, D.,Wielicki, B.,Wong, T.,Yao, M. & Zhang, S. 2005. Efficacy of climate forcings. *Journal of Geophysical Research: Atmospheres,* 110**,** D18104.

Hatzianastassiou, N.,Matsoukas, C.,Fotiadi, A.,Pavlakis, K. G.,Drakakis, E.,Hatzidimitriou, D. & Vardavas, I. 2005. Global distribution of Earth's surface shortwave radiation budget. *Atmospheric Chemistry and Physics,* 5**,** 2847-2867.

Hertwich, E. G. & Hammitt, J. K. 2001. A decision-analytic framework for impact assessment: Part 2: Midpoints, endpoints, and criteria for method development. *International Journal of Life Cycle Assessment,* 6**,** 265-272.

International Energy Agency (IEA) 2011. *World Energy Outlook 2011,* Paris Cedex, OECD Publishing.

International Energy Agency (IEA) 2012a. *Coal Information 2012,* Paris Cedex, OECD Publishing.

International Energy Agency (IEA) 2012b. *Energy Balances of non-OECD Countries 2012,* Paris, OECD Publishing.

International Energy Agency (IEA) 2012c. *Energy Technology Perspectives 2012,* Paris Cedex, OECD Publishing.

International Energy Agency (IEA) 2012d. *Electricity Information 2012,* Paris Cedex, OECD Publishing.

International Energy Agency (IEA) 2012e. *World Energy Outlook 2012,* Paris Cedex, OECD Publishing.

Intergovernmental Panel on Climate Change (IPCC) 2007. 2007. *What Factors Determine Earth's Climate?* [Online]. Available: http://www.ipcc.ch/publications_and_data/ar4/wg1/en/faq-1-1.html [Accessed 27.05 2013].

Intergovernmental Panel on Climate Change (IPCC) 2006. 2006 IPCC Guidelines for National Greenhouse Gas Inventories. Japan: IGES.

Intergovernmental Panel on Climate Change (IPCC) 2012. Renewable Energy Sources and Climate Change Mitigation - Special Report of the Intergovernmental Panel on Climate Change, Chapter 2: Bioenergy. Cambridge, United Kingdom and New York, NY, USA: IPCC 2012.

Jin, Y.,Schaaf, C. B.,Gao, F.,Li, X.,Strahler, A. H.,Lucht, W. & Liang, S. 2003a. Consistency of MODIS surface bidirectional reflectance distribution function and albedo retrievals: 1.

Algorithm performance. *Journal of Geophysical Research D: Atmospheres,* 108**,** ACL 2-1 ACL 2-13.

Jin, Y.,Schaaf, C. B.,Woodcock, C. E.,Gao, F.,Li, X.,Strahler, A. H.,Lucht, W. & Liang, S. 2003b. Consistency of MODIS surface bidirectional reflectance distribution function and albedo retrievals: 2. Validation. *Journal of Geophysical Research D: Atmospheres,* 108**,** ACL 3-1 ACL 3-15.

Junginger, M.,Faaij, A.,Rosillo-Calle, F. & Wood, J. 2006. The growing role of biofuels - Opportunities, challenges and pitfalls. *International Sugar Journal,* 108**,** 618-629.

Kabir, M. R. & Kumar, A. 2012. Comparison of the energy and environmental performances of nine biomass/coal co-firing pathways. *Bioresource Technology,* 124**,** 394-405.

Kraxner, F.,Leduc, S.,Aoki, K.,Fuss, S.,Obersteiner, M.,Schepaschenko, D. & Shvidenko, A. 2011. Forest-based bioenergy in the Eurasian context. Laxenburg, Austria: International Institute for Applied Systems Analysis (IIASA).

Kviljo, M. 2012. Life Cycle Assessment of coal based electricity generation with focus on coal bed methane. Trondheim: NTNU.

Lenton, T. M. & Vaughan, N. E. 2009. The radiative forcing potential of different climate geoengineering options. *Atmospheric Chemistry and Physics,* 9**,** 5539-5561.

Liang, S.,Fang, H.,Chen, M.,Shuey, C. J.,Walthall, C.,Daughtry, C.,Morisette, J.,Schaaf, C. & Strahler, A. 2002. Validating MODIS land surface reflectance and albedo products: Methods and preliminary results. *Remote Sensing of Environment,* 83**,** 149-162.

Mann, M. K. & Spath, P. L. 2001. A life cycle assessment of biomass cofiring in a coal-fired power plant. *Clean Prod Processes,* 3**,** 81-91.

McKechnie, J., Colombo, S.,Chen, J.,Mabee, W. & MacLean, H. L. 2010. Forest Bioenergy or Forest Carbon? Assessing Trade-Offs in Greenhouse Gas Mitigation with Wood-Based Fuels. *Environmental Science & Technology,* 45**,** 789-795.

McShaffrey, D. *Map of biomes* [Online]. Department of Biology and Environmental Science, Marietta College. Available: http://www.marietta.edu/~biol/biomes/biomes.htm.

Michelsen, O., Cherubini, F. & Strømman, A. H. 2012. Impact Assessment of Biodiversity and Carbon Pools from Land Use and Land Use Changes in Life Cycle Assessment, Exemplified with Forestry Operations in Norway. *Journal of Industrial Ecology,* 16**,** 231-242.

Michelsen, O.,Solli, C. & Strømman, A. H. 2008. Environmental Impact and Added Value in Forestry Operations in Norway. *Journal of Industrial Ecology,* 12**,** 69-81.

NASA 2013. Surface Meteorology and Solar Energy (SSE) Release v.6.0. NASA Langly Atmospheric Science Data Center.

Norwegian Institute of Wood Technology. *Tree species, Handbook on Wood Technology* [Online]. Norwegian Institute of Wood Technology. Available: www.treteknisk.no/Aktuelle_treslag_YsJhL.pdf.file [Accessed 15.03 2013].

Organisation for Economic Co-operation and Development (OECD) 1991. *Estimations of greenhouse gas emissions and sinks,* Paris Cedex, OECD Publishing.

Offermann, R., Seidenberger, T., Thrän, D., Kaltschmitt, M., Zinoviev, S. & Miertus, S. 2011. Assessment of global bioenergy potentials. *Mitigation and Adaptation Strategies for Global Change,* 16**,** 103-115.

ORNL DAAC 2010. MODIS subsetted land products, Collection 5. ORNL DAACOak Ridge, Tennessee, USA: Oak Ridge National Laboratory Distributed Active Archive Center.

Pantskhava, E. S. & Pozharnov, V. A. 2006. Biofuel and power engineering. Russia's capabilities. *Thermal Engineering (English translation of Teploenergetika),* 53**,** 231-239.

Park, C. 2008. *Oxford Dictionary of Environment and Concervation,* New York, USA, Oxford University Press Inc.

Peterson, M. *Russian Vegetation and the Extent of the Boreal Forest* [Online]. The Department of Geography/Geology, University of Nebraska at Omaha. Available: http://maps.unomaha.edu/peterson/funda/MapLinks/Russia_files/image014.jpg [Accessed 04.03 2013].

Pinker, R. T.,Frouin, R. & Li, Z. 1995. A review of satellite methods to derive surface shortwave irradiance. *Remote Sensing of Environment,* 51**,** 108-124.

Randerson, J. T.,Liu, H.,Flanner, M. G.,Chambers, S. D.,Jin, Y.,Hess, P. G.,Pfister, G.,Mack, M. C.,Treseder, K. K.,Welp, L. R.,Chapin, F. S.,Harden, J. W.,Goulden, M. L.,Lyons, E.,Neff, J. C.,Schuur, E. A. G. & Zender, C. S. 2006. The impact of boreal forest fire on climate warming. *Science,* 314**,** 1130-1132.

Schmetz, J. 1989. Towards a surface radiation climatology: Retrieval of downward irradiances from satellites. *Atmospheric Research,* 23**,** 287-321.

Sebastián, F.,Royo, J. & Gómez, M. 2011. Cofiring versus biomass-fired power plants: GHG (Greenhouse Gases) emissions savings comparison by means of LCA (Life Cycle Assessment) methodology. *Energy,* 36**,** 2029-2037.

Sikkema, R.,Junginger, M.,Pichler, W.,Hayes, S. & Faaij, A. P. C. 2010. The international logistics of wood pellets for heating and power production in Europe: Costs, energy-input and greenhouse gas balances of pellet consumption in Italy, Sweden and the Netherlands. *Biofuels, Bioproducts and Biorefining,* 4**,** 132-153.

Sikkema, R.,Steiner, M.,Junginger, M.,Hiegl, W.,Hansen, M. T. & Faaij, A. 2011. The European wood pellet markets: Current status and prospects for 2020. *Biofuels, Bioproducts and Biorefining,* 5**,** 250-278.

Smeets, E. M. W.,Faaij, A. P. C.,Lewandowski, I. M. & Turkenburg, W. C. 2007. A bottom-up assessment and review of global bio-energy potentials to 2050. *Progress in Energy and Combustion Science,* 33**,** 56-106.

Stroeve, J.,Box, J. E.,Gao, F.,Liang, S.,Nolin, A. & Schaaf, C. 2005. Accuracy assessment of the MODIS 16-day albedo product for snow: Comparisons with Greenland in situ measurements. *Remote Sensing of Environment,* 94**,** 46-60.

Strømman, A. 2009. Methodological Essentials of Life Cycle Assessment. Trondheim: Norwegian University of Science and Technology.

Trenberth, K. E., Fasullo, J. T. & Kiehl, J. 2008. Earth's Global Energy Budget. *American Meteorological Society*.

UC Berkeley. 2004. *The Forest Biome* [Online]. Available: http://www.ucmp.berkeley.edu/glossary/gloss5/biome/forests.html [Accessed 14.04 2013].

Wang, K., Liu, J., Zhou, X., Sparrow, M., Ma, M., Sun, Z. & Jiang, W. 2004. Validation of MODIS global land surface albedo product using ground measurements in a semidesert region on the Tibetan Plateau. *Journal of Geophysical Research D: Atmospheres,* 109**,** D05107 1-9.

Werner, F., Altaus, H.-J., Künniger, T. & Richter, K. 2007. Life Cycle Inventories of Wood as Fuel and Construction Material No. 9. *Final report ecoinvent 2000.* Dübendorf, Switzerland: Swiss Centre for Life Cycle Inventories.

8. Appendix

8.1. Characterisation of biogenic CO_2 and albedo

8.1.1. Calculations for albedo effect

Below in Figure 17, is the 22-year average K_T (radiation reaching the Earth's surface) for the forest sites for each region. The data was extracted from the Surface Meteorology and Solar Energy database of NASA (NASA, 2013).

Table 17: Overview of the 22-year average K_T extracted for each of the forest sites for each region

Region	Latitude	Longitude	Jan	Feb	Mar	Apr	May	Jun	Jul	Aug	Sep	Oct	Nov	Dec
North	64,39	40,39	0,34	0,43	0,48	0,51	0,47	0,49	0,49	0,44	0,42	0,38	0,39	0,26
Northwest	59,38	30,72	0,40	0,47	0,49	0,50	0,50	0,49	0,49	0,48	0,44	0,39	0,40	0,36
Central	56,19	36,54	0,42	0,48	0,50	0,48	0,48	0,45	0,47	0,46	0,40	0,38	0,39	0,37
Volga-Vyatka	56,55	47,71	0,42	0,48	0,50	0,51	0,51	0,50	0,51	0,48	0,42	0,38	0,40	0,39
Central Chernozem	51,93	39,61	0,44	0,50	0,50	0,45	0,48	0,46	0,47	0,49	0,43	0,39	0,38	0,41
Volga	51,57	45,93	0,44	0,52	0,54	0,46	0,50	0,48	0,50	0,51	0,46	0,40	0,39	0,41
North Caucasus	45,08	41,89	0,41	0,45	0,44	0,46	0,50	0,50	0,54	0,54	0,51	0,47	0,40	0,37
Urals	55,02	56,66	0,41	0,47	0,50	0,52	0,50	0,50	0,51	0,46	0,42	0,35	0,41	0,43

Table 18 gives an overview of the values of f_a, which is the product of K_T found in Table 17 and the solar constant T = 0,854.

Table 18: Displays the values of f_a for each of the forest sites, based on $K_T \cdot T_A$

Region	Jan	Feb	Mar	Apr	May	Jun	Jul	Aug	Sep	Oct	Nov	Dec
North	0,290	0,367	0,410	0,436	0,401	0,418	0,418	0,376	0,359	0,325	0,333	0,222
Northwest	0,342	0,401	0,418	0,427	0,427	0,418	0,418	0,410	0,376	0,333	0,342	0,307
Central	0,359	0,410	0,427	0,410	0,410	0,384	0,401	0,393	0,342	0,325	0,333	0,316
Volga-Vyatka	0,359	0,410	0,427	0,436	0,436	0,427	0,436	0,410	0,359	0,325	0,342	0,333
Central Chernozem	0,376	0,427	0,427	0,384	0,410	0,393	0,401	0,418	0,367	0,333	0,325	0,350
Volga	0,376	0,444	0,461	0,393	0,427	0,410	0,427	0,436	0,393	0,342	0,333	0,350
North Caucasus	0,350	0,384	0,376	0,393	0,427	0,427	0,461	0,461	0,436	0,401	0,342	0,316
Urals	0,350	0,401	0,427	0,444	0,427	0,427	0,436	0,393	0,359	0,299	0,350	0,367

The matlab script used to further find R_{TOA} can be found below.

```
% Solar insolation calculation parameter inputs
Rsc = 1367; % W/m2, Solar constant
%
L = x; % Latitude (degrees); Here you enter the latitude of the site for
each region
%
```

```
pie = 3.141592654; % pie

% Downward daily solar radiation at TOA ("Extraterrestrial solar radiation
on horizontal surface") -- Duffie & Beckman, (1991); Kalogirou, (2009)
R_TOA = zeros(365,1);
for i = 1:365; % i = Julian Day
dec = 23.45*sind(360*(284+i)/365); % Angle of declination in degrees
sshr = acosd(-tand(L)*tand(dec)); % Sunset hr. angle in degrees
R_TOA(i,:) =
((Rsc/pie)*(1+0.033*cosd((360*i)/365)))*(((cosd(L)*cosd(dec)*sind(sshr))+((
(pie*sshr)/180)*sind(L)*sind(dec)))); % TOA irradiance on day "i"
end

R_TOA_ann = sum(R_TOA)/365; % Mean annual instantaneous R_TOA (local
W/m2/year, south Norway)
% Monthly mean incoming radiation at top of atmosphere ("TOA")
R_TOA_month = zeros(1,12);
R_TOA_month(:,1) = (sum(R_TOA(1:31,1)))/31; %  January mean
R_TOA_month(:,2) = (sum(R_TOA(32:59,1)))/28; % February mean...
R_TOA_month(:,3) = (sum(R_TOA(60:90,1)))/31;
R_TOA_month(:,4) = (sum(R_TOA(91:120,1)))/30;
R_TOA_month(:,5) = (sum(R_TOA(121:151,1)))/31;
R_TOA_month(:,6) = (sum(R_TOA(152:181,1)))/30;
R_TOA_month(:,7) = (sum(R_TOA(182:212,1)))/31;
R_TOA_month(:,8) = (sum(R_TOA(213:243,1)))/31;
R_TOA_month(:,9) = (sum(R_TOA(244:273,1)))/30;
R_TOA_month(:,10) = (sum(R_TOA(274:304,1)))/31;
R_TOA_month(:,11) = (sum(R_TOA(305:334,1)))/30;
R_TOA_month(:,12) = (sum(R_TOA(335:365,1)))/31;
```

Based on the matlab script, the R_{TOA} values were found, which can be seen in Table 19 below for each region.

Table 19: Monthly R_{TOA} values for each of the forest sites [W/m²]

Region	Jan	Feb	Mar	Apr	May	Jun	Jul	Aug	Sep	Oct	Nov	Dec
North	16,7	66,3	165,5	296,9	414,8	473,9	444,1	340,2	209,0	94,1	26,5	6,2
Northwest	44,1	100,5	200,0	322,2	425,6	474,7	449,8	360,3	240,8	129,1	56,0	29,8
Central	64,1	122,9	221,2	337,5	432,7	476,7	454,3	372,5	260,2	151,3	76,8	48,4
Volga-Vyatka	61,7	120,3	218,8	335,8	431,9	476,5	453,8	371,1	258,0	148,8	74,4	46,2
Central Chernozem	92,5	152,8	248,4	356,6	441,6	479,7	460,1	387,7	284,8	180,7	105,7	75,6
Volga	95,0	155,4	250,7	358,2	442,3	480,0	460,6	388,9	286,9	183,2	108,2	78,1
North Caucasus	140,5	200,5	289,6	383,9	453,4	482,9	467,4	408,9	321,2	226,5	153,6	122,8
Urals	71,7	131,1	228,8	342,9	435,2	477,6	455,9	376,8	267,1	159,4	84,6	55,6

Below in Table 20 the numerical values of the monthly mean Δ albedo for each region in W/m^2 are displayed.

Table 20: Overview of the monthly mean Δ albedo values for each region [W/m^2]

Region	Jan	Feb	March	Apr	May	June	July	Aug	Sept	Oct	Nov	Dec
North	0,332	0,405	0,445	0,183	0,003	0,002	0,002	0,002	0,005	0,187	0,162	0,247
Northwest	0,321	0,403	0,145	0,052	0,054	0,052	0,051	0,048	0,057	0,066	0,264	0,264
Central	0,338	0,352	0,263	0,055	0,041	0,043	0,028	0,027	0,033	0,063	0,195	0,299
Volga-Vyatka	0,325	0,342	0,365	0,026	0,026	0,026	0,021	0,025	0,020	0,033	0,135	0,230
Central Chernozem	0,401	0,504	0,285	0,012	0,016	0,012	0,024	0,012	0,010	0,030	0,106	0,393
Volga	0,371	0,439	0,267	0,010	0,007	0,004	0,002	0,003	0,007	0,009	0,033	0,308
North Caucasus	0,304	0,258	0,052	0,019	0,001	0,010	0,004	0,001	0,012	0,005	0,028	0,224
Urals	0,358	0,413	0,381	0,068	0,004	0,011	0,028	0,028	0,027	0,046	0,162	0,302

8.1.2. Absolute metrics

Below in Table 21, the values for effective radiative forcing (ERF) for the four forest types, as well as the fossil reference can be found.

- Boreal forest, coniferous wood (r=100)
- Boreal forest, deciduous wood (r=85)
- Temperate forest, coniferous wood (r=90)
- Temperate forest, deciduous wood (r=75)

The values are displayed for 0-140 years and the unit is 10E-16 W m^{-2} kg^{-1}, which is also what is found in Figure 12. The complete values can be found in the digital appendix.

Table 21: Effective radiative forcing values for the four forest types and fossil reference for the time period of 0-140 years [10E^{-16} W m^{-2} kg^{-1}]

	Instantaneous Effective forcing [10E-16 W m^{-2} kg^{-1}]				
Time [year]	Fossil	Biogenic (r = 100)	Biogenic (r = 90)	Biogenic (r = 85)	Biogenic (r = 75)
0	18,09	18,09	18,09	18,09	18,09
1	15,82	15,78	15,77	15,77	15,76
2	14,66	14,58	14,57	14,56	14,55
3	13,99	13,87	13,85	13,84	13,82
4	13,54	13,37	13,35	13,34	13,30
5	13,19	12,98	12,95	12,93	12,88
6	12,89	12,63	12,59	12,57	12,51
7	12,62	12,31	12,26	12,23	12,15
8	12,37	12,00	11,94	11,91	11,82
9	12,13	11,71	11,64	11,60	11,49
10	11,91	11,42	11,34	11,29	11,16
11	11,69	11,15	11,05	11,00	10,85
12	11,49	10,88	10,77	10,70	10,53
13	11,30	10,62	10,49	10,42	10,21
14	11,11	10,36	10,22	10,13	9,90
15	10,94	10,10	9,95	9,85	9,59
16	10,77	9,86	9,68	9,57	9,28
17	10,61	9,61	9,42	9,29	8,97
18	10,46	9,37	9,15	9,02	8,66
19	10,31	9,13	8,89	8,74	8,35
20	10,17	8,90	8,64	8,47	8,03
21	10,04	8,66	8,38	8,20	7,72
22	9,91	8,43	8,12	7,92	7,40
23	9,79	8,20	7,86	7,65	7,09
24	9,67	7,97	7,61	7,38	6,77
25	9,56	7,74	7,35	7,10	6,46
26	9,46	7,52	7,10	6,83	6,14

Instantaneous Effective forcing [10E-16 W m^{-2} kg^{-1}]					
Time [year]	Fossil	Biogenic (r = 100)	Biogenic (r = 90)	Biogenic (r = 85)	Biogenic (r = 75)
27	9,35	7,29	6,84	6,56	5,82
28	9,26	7,06	6,59	6,28	5,50
29	9,16	6,84	6,33	6,01	5,18
30	9,07	6,61	6,08	5,74	4,87
31	8,99	6,39	5,82	5,46	4,55
32	8,90	6,16	5,57	5,19	4,24
33	8,82	5,94	5,31	4,92	3,93
34	8,75	5,72	5,06	4,65	3,62
35	8,67	5,49	4,81	4,38	3,32
36	8,60	5,27	4,55	4,11	3,02
37	8,53	5,05	4,30	3,85	2,73
38	8,47	4,83	4,06	3,58	2,44
39	8,41	4,61	3,81	3,33	2,16
40	8,35	4,39	3,56	3,07	1,89
41	8,29	4,17	3,32	2,82	1,63
42	8,23	3,95	3,08	2,57	1,37
43	8,18	3,74	2,85	2,32	1,12
44	8,12	3,52	2,61	2,09	0,89
45	8,07	3,31	2,39	1,85	0,66
46	8,02	3,10	2,16	1,63	0,44
47	7,98	2,89	1,94	1,40	0,23
48	7,93	2,69	1,73	1,19	0,04
49	7,89	2,49	1,52	0,98	-0,15
50	7,84	2,29	1,32	0,78	-0,32
51	7,80	2,09	1,12	0,59	-0,49
52	7,76	1,90	0,93	0,41	-0,64
53	7,72	1,71	0,74	0,23	-0,78
54	7,68	1,53	0,57	0,06	-0,91
55	7,65	1,35	0,39	-0,10	-1,03
56	7,61	1,18	0,23	-0,25	-1,13
57	7,57	1,01	0,07	-0,39	-1,23
58	7,54	0,84	-0,08	-0,53	-1,32
59	7,51	0,68	-0,22	-0,66	-1,39
60	7,47	0,53	-0,35	-0,77	-1,46
61	7,44	0,38	-0,48	-0,88	-1,52
62	7,41	0,24	-0,60	-0,98	-1,57
63	7,38	0,10	-0,71	-1,08	-1,61
64	7,35	-0,03	-0,82	-1,16	-1,64
65	7,32	-0,16	-0,92	-1,24	-1,67
66	7,30	-0,28	-1,01	-1,31	-1,69
67	7,27	-0,40	-1,09	-1,37	-1,70
68	7,24	-0,50	-1,16	-1,42	-1,71
69	7,21	-0,61	-1,23	-1,47	-1,71

Instantaneous Effective forcing [10E-16 W m^{-2} kg^{-1}]					
Time [year]	Fossil	Biogenic (r = 100)	Biogenic (r = 90)	Biogenic (r = 85)	Biogenic (r = 75)
70	7,19	-0,70	-1,30	-1,51	-1,71
71	7,16	-0,79	-1,35	-1,55	-1,70
72	7,14	-0,88	-1,40	-1,58	-1,69
73	7,11	-0,96	-1,45	-1,60	-1,67
74	7,09	-1,03	-1,49	-1,62	-1,66
75	7,07	-1,10	-1,52	-1,63	-1,64
76	7,04	-1,17	-1,55	-1,64	-1,61
77	7,02	-1,22	-1,57	-1,65	-1,59
78	7,00	-1,28	-1,59	-1,65	-1,56
79	6,98	-1,32	-1,60	-1,65	-1,54
80	6,95	-1,37	-1,61	-1,64	-1,51
81	6,93	-1,40	-1,62	-1,63	-1,48
82	6,91	-1,44	-1,62	-1,62	-1,45
83	6,89	-1,47	-1,62	-1,61	-1,42
84	6,87	-1,49	-1,62	-1,59	-1,39
85	6,85	-1,51	-1,61	-1,57	-1,36
86	6,83	-1,53	-1,60	-1,55	-1,33
87	6,81	-1,55	-1,59	-1,53	-1,30
88	6,79	-1,56	-1,58	-1,51	-1,27
89	6,77	-1,56	-1,56	-1,49	-1,24
90	6,76	-1,57	-1,54	-1,46	-1,22
91	6,74	-1,57	-1,53	-1,44	-1,19
92	6,72	-1,57	-1,51	-1,42	-1,16
93	6,70	-1,57	-1,49	-1,39	-1,14
94	6,68	-1,56	-1,47	-1,36	-1,11
95	6,66	-1,56	-1,44	-1,34	-1,09
96	6,65	-1,55	-1,42	-1,31	-1,06
97	6,63	-1,54	-1,40	-1,29	-1,04
98	6,61	-1,52	-1,38	-1,26	-1,02
99	6,60	-1,51	-1,35	-1,24	-1,00
100	6,58	-1,50	-1,33	-1,22	-0,98
101	6,56	-1,48	-1,31	-1,19	-0,96
102	6,55	-1,47	-1,28	-1,17	-0,94
103	6,53	-1,45	-1,26	-1,15	-0,92
104	6,51	-1,43	-1,24	-1,12	-0,90
105	6,50	-1,41	-1,22	-1,10	-0,88
106	6,48	-1,39	-1,19	-1,08	-0,87
107	6,47	-1,37	-1,17	-1,06	-0,85
108	6,45	-1,35	-1,15	-1,04	-0,83
109	6,44	-1,33	-1,13	-1,02	-0,82
110	6,42	-1,32	-1,11	-1,00	-0,81
111	6,40	-1,30	-1,09	-0,99	-0,79
112	6,39	-1,28	-1,07	-0,97	-0,78

Instantaneous Effective forcing [10E-16 W m^{-2} kg^{-1}]					
Time [year]	Fossil	Biogenic (r = 100)	Biogenic (r = 90)	Biogenic (r = 85)	Biogenic (r = 75)
113	6,37	-1,26	-1,05	-0,95	-0,77
114	6,36	-1,24	-1,03	-0,93	-0,76
115	6,35	-1,22	-1,02	-0,92	-0,74
116	6,33	-1,20	-1,00	-0,90	-0,73
117	6,32	-1,18	-0,98	-0,89	-0,72
118	6,30	-1,16	-0,97	-0,87	-0,71
119	6,29	-1,14	-0,95	-0,86	-0,70
120	6,27	-1,12	-0,94	-0,85	-0,69
121	6,26	-1,11	-0,92	-0,83	-0,68
122	6,25	-1,09	-0,91	-0,82	-0,67
123	6,23	-1,07	-0,89	-0,81	-0,66
124	6,22	-1,06	-0,88	-0,80	-0,66
125	6,21	-1,04	-0,87	-0,79	-0,65
126	6,19	-1,03	-0,85	-0,78	-0,64
127	6,18	-1,01	-0,84	-0,77	-0,63
128	6,16	-1,00	-0,83	-0,76	-0,63
129	6,15	-0,98	-0,82	-0,75	-0,62
130	6,14	-0,97	-0,81	-0,74	-0,61
131	6,13	-0,95	-0,80	-0,73	-0,61
132	6,11	-0,94	-0,79	-0,72	-0,60
133	6,10	-0,93	-0,78	-0,71	-0,59
134	6,09	-0,92	-0,77	-0,70	-0,59
135	6,07	-0,90	-0,76	-0,70	-0,58
136	6,06	-0,89	-0,75	-0,69	-0,57
137	6,05	-0,88	-0,74	-0,68	-0,57
138	6,04	-0,87	-0,73	-0,67	-0,56
139	6,02	-0,86	-0,73	-0,67	-0,56
140	6,01	-0,85	-0,72	-0,66	-0,55

Below in Table 22 the values for effective radiative forcing (ERF) for each of the eight regions can be found, displayed in 10E-16 W m^{-2} kg^{-1}. These are the average values based on the ERF for the two to four forest types in each region. The values are displayed for 0-140 years, which can also be seen in Figure 12. The complete values can be found in the digital appendix.

Table 22: Effective radiative forcing values for the surface albedo for each region for the time period of 0-140 years [10E-16 W m^{-2} kg^{-1}]

Instantaneous Effective forcing [10E-16 W m^{-2} kg^{-1}]								
t [yr]	North	North-west	Central	Volga-Vyatka	Central-Chernozem	Volga	North-Caucasus	Urals
0	-24,21	-19,27	-9,06	-8,39	-9,92	-8,32	-5,46	-22,26
1	-22,93	-18,23	-8,53	-7,90	-9,33	-7,83	-5,14	-21,05
2	-21,72	-17,25	-8,03	-7,43	-8,78	-7,37	-4,84	-19,92
3	-20,58	-16,31	-7,55	-6,99	-8,27	-6,94	-4,55	-18,84
4	-19,50	-15,43	-7,11	-6,58	-7,78	-6,53	-4,29	-17,82
5	-18,47	-14,60	-6,69	-6,20	-7,32	-6,15	-4,03	-16,86
6	-17,50	-13,81	-6,30	-5,83	-6,89	-5,79	-3,80	-15,95
7	-16,58	-13,07	-5,93	-5,49	-6,49	-5,45	-3,57	-15,09
8	-15,71	-12,37	-5,58	-5,17	-6,11	-5,13	-3,36	-14,28
9	-14,88	-11,70	-5,25	-4,86	-5,75	-4,83	-3,17	-13,51
10	-14,10	-11,07	-4,94	-4,58	-5,41	-4,54	-2,98	-12,78
11	-13,36	-10,47	-4,65	-4,31	-5,09	-4,28	-2,81	-12,10
12	-12,66	-9,91	-4,38	-4,06	-4,80	-4,03	-2,64	-11,45
13	-12,00	-9,38	-4,13	-3,82	-4,51	-3,79	-2,49	-10,83
14	-11,37	-8,88	-3,88	-3,60	-4,25	-3,57	-2,34	-10,25
15	-10,77	-8,40	-3,66	-3,39	-4,00	-3,36	-2,20	-9,70
16	-10,21	-7,95	-3,44	-3,19	-3,77	-3,16	-2,08	-9,18
17	-9,67	-7,52	-3,24	-3,00	-3,55	-2,98	-1,95	-8,69
18	-9,17	-7,12	-3,05	-2,83	-3,34	-2,80	-1,84	-8,22
19	-8,69	-6,74	-2,87	-2,66	-3,14	-2,64	-1,73	-7,78
20	-8,23	-6,38	-2,71	-2,51	-2,96	-2,49	-1,63	-7,36
21	-7,80	-6,04	-2,55	-2,36	-2,79	-2,34	-1,54	-6,97
22	-7,39	-5,71	-2,40	-2,22	-2,63	-2,20	-1,45	-6,60
23	-7,01	-5,41	-2,26	-2,09	-2,47	-2,08	-1,36	-6,24
24	-6,64	-5,12	-2,13	-1,97	-2,33	-1,95	-1,28	-5,91
25	-6,29	-4,85	-2,00	-1,86	-2,19	-1,84	-1,21	-5,60
26	-5,97	-4,59	-1,89	-1,75	-2,07	-1,73	-1,14	-5,30
27	-5,65	-4,34	-1,78	-1,65	-1,95	-1,63	-1,07	-5,01
28	-5,36	-4,11	-1,67	-1,55	-1,83	-1,54	-1,01	-4,75
29	-5,08	-3,89	-1,58	-1,46	-1,73	-1,45	-0,95	-4,49
30	-4,81	-3,68	-1,49	-1,38	-1,63	-1,36	-0,90	-4,25
31	-4,56	-3,49	-1,40	-1,30	-1,53	-1,29	-0,84	-4,03
32	-4,33	-3,30	-1,32	-1,22	-1,44	-1,21	-0,79	-3,81
33	-4,10	-3,13	-1,24	-1,15	-1,36	-1,14	-0,75	-3,61
34	-3,89	-2,96	-1,17	-1,08	-1,28	-1,07	-0,71	-3,42
35	-3,68	-2,80	-1,10	-1,02	-1,21	-1,01	-0,66	-3,24
36	-3,49	-2,65	-1,04	-0,96	-1,14	-0,95	-0,63	-3,06
37	-3,31	-2,51	-0,98	-0,91	-1,07	-0,90	-0,59	-2,90
38	-3,14	-2,38	-0,92	-0,85	-1,01	-0,85	-0,56	-2,75
39	-2,98	-2,25	-0,87	-0,80	-0,95	-0,80	-0,52	-2,60

Instantaneous Effective forcing [10E-16 W m^{-2} kg^{-1}]								
t [yr]	North	North-west	Central	Volga-Vyatka	Central-Chernozem	Volga	North-Caucasus	Urals
40	-2,82	-2,13	-0,82	-0,76	-0,89	-0,75	-0,49	-2,46
41	-2,67	-2,02	-0,77	-0,71	-0,84	-0,71	-0,46	-2,33
42	-2,54	-1,91	-0,73	-0,67	-0,79	-0,67	-0,44	-2,21
43	-2,40	-1,81	-0,68	-0,63	-0,75	-0,63	-0,41	-2,09
44	-2,28	-1,72	-0,64	-0,60	-0,71	-0,59	-0,39	-1,98
45	-2,16	-1,63	-0,61	-0,56	-0,66	-0,56	-0,37	-1,88
46	-2,05	-1,54	-0,57	-0,53	-0,63	-0,53	-0,35	-1,78
47	-1,94	-1,46	-0,54	-0,50	-0,59	-0,50	-0,33	-1,68
48	-1,84	-1,38	-0,51	-0,47	-0,56	-0,47	-0,31	-1,59
49	-1,75	-1,31	-0,48	-0,44	-0,52	-0,44	-0,29	-1,51
50	-1,66	-1,24	-0,45	-0,42	-0,49	-0,41	-0,27	-1,43
51	-1,57	-1,17	-0,43	-0,39	-0,47	-0,39	-0,26	-1,36
52	-1,49	-1,11	-0,40	-0,37	-0,44	-0,37	-0,24	-1,28
53	-1,41	-1,05	-0,38	-0,35	-0,41	-0,35	-0,23	-1,22
54	-1,34	-1,00	-0,36	-0,33	-0,39	-0,33	-0,21	-1,15
55	-1,27	-0,95	-0,34	-0,31	-0,37	-0,31	-0,20	-1,09
56	-1,20	-0,90	-0,32	-0,29	-0,35	-0,29	-0,19	-1,03
57	-1,14	-0,85	-0,30	-0,28	-0,33	-0,27	-0,18	-0,98
58	-1,08	-0,80	-0,28	-0,26	-0,31	-0,26	-0,17	-0,93
59	-1,03	-0,76	-0,27	-0,25	-0,29	-0,24	-0,16	-0,88
60	-0,97	-0,72	-0,25	-0,23	-0,27	-0,23	-0,15	-0,83
61	-0,92	-0,68	-0,24	-0,22	-0,26	-0,22	-0,14	-0,79
62	-0,88	-0,65	-0,22	-0,21	-0,24	-0,20	-0,13	-0,75
63	-0,83	-0,61	-0,21	-0,19	-0,23	-0,19	-0,13	-0,71
64	-0,79	-0,58	-0,20	-0,18	-0,22	-0,18	-0,12	-0,67
65	-0,75	-0,55	-0,19	-0,17	-0,20	-0,17	-0,11	-0,64
66	-0,71	-0,52	-0,18	-0,16	-0,19	-0,16	-0,11	-0,60
67	-0,67	-0,49	-0,17	-0,15	-0,18	-0,15	-0,10	-0,57
68	-0,64	-0,47	-0,16	-0,14	-0,17	-0,14	-0,09	-0,54
69	-0,60	-0,44	-0,15	-0,14	-0,16	-0,14	-0,09	-0,51
70	-0,57	-0,42	-0,14	-0,13	-0,15	-0,13	-0,08	-0,49
71	-0,54	-0,40	-0,13	-0,12	-0,14	-0,12	-0,08	-0,46
72	-0,52	-0,38	-0,12	-0,11	-0,13	-0,11	-0,07	-0,44
73	-0,49	-0,36	-0,12	-0,11	-0,13	-0,11	-0,07	-0,41
74	-0,46	-0,34	-0,11	-0,10	-0,12	-0,10	-0,07	-0,39
75	-0,44	-0,32	-0,10	-0,10	-0,11	-0,10	-0,06	-0,37
76	-0,42	-0,30	-0,10	-0,09	-0,11	-0,09	-0,06	-0,35
77	-0,40	-0,29	-0,09	-0,09	-0,10	-0,08	-0,06	-0,33
78	-0,38	-0,27	-0,09	-0,08	-0,09	-0,08	-0,05	-0,32
79	-0,36	-0,26	-0,08	-0,08	-0,09	-0,08	-0,05	-0,30
80	-0,34	-0,25	-0,08	-0,07	-0,08	-0,07	-0,05	-0,28
81	-0,32	-0,23	-0,07	-0,07	-0,08	-0,07	-0,04	-0,27
82	-0,30	-0,22	-0,07	-0,06	-0,08	-0,06	-0,04	-0,26

Instantaneous Effective forcing [10E-16 W m^{-2} kg^{-1}]								
t [yr]	North	North-west	Central	Volga-Vyatka	Central-Chernozem	Volga	North-Caucasus	Urals
83	-0,29	-0,21	-0,06	-0,06	-0,07	-0,06	-0,04	-0,24
84	-0,27	-0,20	-0,06	-0,06	-0,07	-0,06	-0,04	-0,23
85	-0,26	-0,19	-0,06	-0,05	-0,06	-0,05	-0,03	-0,22
86	-0,25	-0,18	-0,05	-0,05	-0,06	-0,05	-0,03	-0,21
87	-0,23	-0,17	-0,05	-0,05	-0,06	-0,05	-0,03	-0,20
88	-0,22	-0,16	-0,05	-0,04	-0,05	-0,04	-0,03	-0,19
89	-0,21	-0,15	-0,05	-0,04	-0,05	-0,04	-0,03	-0,18
90	-0,20	-0,14	-0,04	-0,04	-0,05	-0,04	-0,03	-0,17
91	-0,19	-0,14	-0,04	-0,04	-0,04	-0,04	-0,02	-0,16
92	-0,18	-0,13	-0,04	-0,04	-0,04	-0,04	-0,02	-0,15
93	-0,17	-0,12	-0,04	-0,03	-0,04	-0,03	-0,02	-0,14
94	-0,16	-0,12	-0,03	-0,03	-0,04	-0,03	-0,02	-0,13
95	-0,15	-0,11	-0,03	-0,03	-0,04	-0,03	-0,02	-0,13
96	-0,15	-0,10	-0,03	-0,03	-0,03	-0,03	-0,02	-0,12
97	-0,14	-0,10	-0,03	-0,03	-0,03	-0,03	-0,02	-0,11
98	-0,13	-0,09	-0,03	-0,03	-0,03	-0,02	-0,02	-0,11
99	-0,12	-0,09	-0,03	-0,02	-0,03	-0,02	-0,02	-0,10
100	-0,12	-0,08	-0,02	-0,02	-0,03	-0,02	-0,01	-0,10
101	-0,11	-0,08	-0,02	-0,02	-0,02	-0,02	-0,01	-0,09
102	-0,11	-0,08	-0,02	-0,02	-0,02	-0,02	-0,01	-0,09
103	-0,10	-0,07	-0,02	-0,02	-0,02	-0,02	-0,01	-0,08
104	-0,10	-0,07	-0,02	-0,02	-0,02	-0,02	-0,01	-0,08
105	-0,09	-0,06	-0,02	-0,02	-0,02	-0,02	-0,01	-0,08
106	-0,09	-0,06	-0,02	-0,02	-0,02	-0,02	-0,01	-0,07
107	-0,08	-0,06	-0,02	-0,01	-0,02	-0,01	-0,01	-0,07
108	-0,08	-0,06	-0,02	-0,01	-0,02	-0,01	-0,01	-0,06
109	-0,07	-0,05	-0,01	-0,01	-0,02	-0,01	-0,01	-0,06
110	-0,07	-0,05	-0,01	-0,01	-0,01	-0,01	-0,01	-0,06
111	-0,07	-0,05	-0,01	-0,01	-0,01	-0,01	-0,01	-0,05
112	-0,06	-0,04	-0,01	-0,01	-0,01	-0,01	-0,01	-0,05
113	-0,06	-0,04	-0,01	-0,01	-0,01	-0,01	-0,01	-0,05
114	-0,06	-0,04	-0,01	-0,01	-0,01	-0,01	-0,01	-0,05
115	-0,05	-0,04	-0,01	-0,01	-0,01	-0,01	-0,01	-0,04
116	-0,05	-0,04	-0,01	-0,01	-0,01	-0,01	-0,01	-0,04
117	-0,05	-0,03	-0,01	-0,01	-0,01	-0,01	-0,01	-0,04
118	-0,05	-0,03	-0,01	-0,01	-0,01	-0,01	-0,01	-0,04
119	-0,04	-0,03	-0,01	-0,01	-0,01	-0,01	0,00	-0,04
120	-0,04	-0,03	-0,01	-0,01	-0,01	-0,01	0,00	-0,03
121	-0,04	-0,03	-0,01	-0,01	-0,01	-0,01	0,00	-0,03
122	-0,04	-0,03	-0,01	-0,01	-0,01	-0,01	0,00	-0,03
123	-0,04	-0,03	-0,01	-0,01	-0,01	-0,01	0,00	-0,03
124	-0,03	-0,02	-0,01	-0,01	-0,01	-0,01	0,00	-0,03
125	-0,03	-0,02	-0,01	-0,01	-0,01	-0,01	0,00	-0,03

Instantaneous Effective forcing [10E-16 W m^{-2} kg^{-1}]								
t [yr]	North	North-west	Central	Volga-Vyatka	Central-Chernozem	Volga	North-Caucasus	Urals
126	-0,03	-0,02	-0,01	0,00	-0,01	0,00	0,00	-0,02
127	-0,03	-0,02	-0,01	0,00	-0,01	0,00	0,00	-0,02
128	-0,03	-0,02	0,00	0,00	-0,01	0,00	0,00	-0,02
129	-0,03	-0,02	0,00	0,00	0,00	0,00	0,00	-0,02
130	-0,02	-0,02	0,00	0,00	0,00	0,00	0,00	-0,02
131	-0,02	-0,02	0,00	0,00	0,00	0,00	0,00	-0,02
132	-0,02	-0,02	0,00	0,00	0,00	0,00	0,00	-0,02
133	-0,02	-0,01	0,00	0,00	0,00	0,00	0,00	-0,02
134	-0,02	-0,01	0,00	0,00	0,00	0,00	0,00	-0,02
135	-0,02	-0,01	0,00	0,00	0,00	0,00	0,00	-0,02
136	-0,02	-0,01	0,00	0,00	0,00	0,00	0,00	-0,01
137	-0,02	-0,01	0,00	0,00	0,00	0,00	0,00	-0,01
138	-0,02	-0,01	0,00	0,00	0,00	0,00	0,00	-0,01
139	-0,02	-0,01	0,00	0,00	0,00	0,00	0,00	-0,01
140	-0,01	-0,01	0,00	0,00	0,00	0,00	0,00	-0,01

8.1.3. Normalised metrics

Table 23 gives an overview of the total g CO_2-eq/MJ for each of the forest types in each region in connection with the direct biomass combustion for all three time horizons. This was calculated by using the relevant GWP_{bio} and a factor of 96,49 g CO_2-eq/MJ. The values below were further used together with the percentage distribution in Table 6 to calculate the final contribution to climate change from biogenic CO_2 in each of the scenarios.

Table 23: Overview of total g CO_2-eq per MJ in each of the forest types for each region concerning biogenic CO_2 [g CO_2-eq/MJ]. Displayed for all three time horizons.

All regions	Boreal forest		Temperate forest	
	Coniferous	Deciduous	Coniferous	Deciduous
TH = 20	92,63	91,67	91,67	90,22
TH = 100	41,49	35,22	37,63	30,39
TH = 500	7,72	6,27	6,75	5,79

The total g CO_2-eq/MJ for each of the forest types in each region in connection with the surface albedo for all three time horizons can be found in Table 24. This was calculated by using the relevant GWP_{albedo} and a factor of 96,49 g CO_2-eq/MJ. Together with the percentage distribution in Table 6, the values below were further used to calculate the final climate change impact from albedo in each of the scenarios.

Table 24: Overview of total g CO_2-eq per MJ in each of the forest types for each region concerning albedo for all three time horizons [g CO_2-eq/MJ]. (Con=coniferous, dec=deciduous)

Regions	TH = 20				TH = 100				TH = 500			
	Boreal forest		Temperate forest		Boreal forest		Temperate forest		Boreal forest		Temperate forest	
	Con	Dec	Con	Dec	Con	Dec	Con	Dec	Con	Dec	Con	Dec
North	-57,9	-43,4	-	-	-127,7	-104,1	-	-	-17,9	-13,4	-	-
Northwest	-71,7	-53,7	-18,5	-13,6	-158,1	-128,9	-43,2	-34,7	-22,2	-16,6	-5,7	-4,2
Central	-	-	-19,6	-14,4	-	-	-45,7	-36,7	-	-	-6,0	-4,4
Volga-Vyatka	-	-	-18,2	-13,3	-	-	-42,3	-33,9	-	-	-5,6	-4,1
Central Chernozem	-	-	-21,5	-15,8	-	-	-50,0	-40,1	-	-	-6,6	-4,9
Volga	-	-	-18,0	-13,2	-	-	-42,0	-33,7	-	-	-5,6	-4,1
North Caucasus	-	-	-11,8	-8,7	-	-	-42,3	-22,1	-	-	-3,6	-2,7
Urals	-82,8	-62,1	-21,4	-15,7	-182,6	-148,9	-49,9	-40,0	-25,6	-19,1	-6,6	-4,8

8.2. Foreground matrix and inventory for scenario

Below the foreground matrix for the case of 10% co-firing with biomass in the Northern region and the corresponding inventory can be found.

Table 25: Foreground matrix A_{ff} for the scenario of 10% co-firing in the Northern region

					A_ff			
Name	Full Name	Location	Unit	y_f	Combustion	Fuel, coal	Fuel, wood chips, hardwood	Fuel, wood chips, softwood
Combustion	Coal and biomass combustion	RU	MJ	1				
Fuel, coal	Hard coal, at mine/RU/kg	RU	kg	0	0,0384			
Fuel, wood chips, hardwood	Wood chips, hardwood, u=80%, at forest/RER/m^3	RU	m^3	0	2,40E-06			
Fuel, wood chips, softwood	Wood chips, softwood, u=140%, at forest/RER/m^3	RU	m^3	0	8,00E-06			

The inventory is shown in Table 26 to Table 28.

Table 26: Inventory for Fuel input, coal, for the Northern region in European Russia

Fuel, coal	1	kg
Input:		
Blasting/RER/kg	0,000767	kg
Diesel, burned in building machine/GLO/MJ	0,0418	MJ
Electricity, high voltage, production UCTE, at grid/ UCTE/ kWh	0,093	kWh
Heat, at hard coal industrial furnace 1-10MW/ RER/ MJ	0,0737	MJ
Disposal, spoil from coal mining, in surface landfill/ GLO/ kg	7,4009	kg
Disposal, tailings from hard coal milling, in impoundment/ GLO/ kg	0,271	kg
Tap water, at user/ RER/ kg	0,503	kg
Open cast mine, hard coal/GLO/unit	1,10E-11	Unit
Underground mine, hard coal/GLO/unit	2,23E-11	Unit
Transport, freight, rail/ RER/ tkm	0,501	tkm
Stressors:		
Heat, waste/ air/ low population density	3,35E-01	MJ
Methane, fossil/ air/ low population density	1,96E-02	kg
Particulates, > 10 um/ air/ low population density	1,99E-04	kg
Radon-222/ air/ low population density	1,20E-02	kBq
Coal, hard, unspecified, in ground/ resource/ in ground	1,23E+00	kg
Gas, mine, off-gas, process, coal mining/ resource/ in ground	1,49E-02	Nm^3
Occupation, dump site/ resource/ land	6,90E-03	m^2a
Occupation, mineral extraction site/ resource/ land	2,70E-03	m^2a
Transformation, from unknown/ resource/ land	8,00E-05	m^2
Transformation, to dump site/ resource/ land	5,70E-05	m^2
Transformation, to mineral extraction site/ resource/land	2,30E-05	m^2
Water, well, in ground/ resource/ in water	1,24E-03	m^3
Aluminium/ water/ ground-	1,00E-06	kg
Ammonium, ion/ water/ ground-	1,00E-06	kg
Chloride/ water/ ground-	1,12E-02	kg
Dissolved solids/ water/ ground-	1,50E-06	kg
Fluoride/ water/ ground-	3,00E-06	kg
Iron, ion/ water/ ground-	2,00E-06	kg
Manganese/ water/ ground-	1,00E-06	kg
Nickel, ion/ water/ ground-	1,00E-07	kg
Solids, inorganic/ water/ ground-	3,30E-05	kg
Strontium/ water/ ground-	5,00E-06	kg
Sulfate/ water/ ground-	5,00E-04	kg
Zinc, ion/ water/ ground-	1,00E-07	kg

Table 27: Inventory for Fuel input, wood chips from hardwood, for the Northen region in European Russia

Fuel, wood chips, hardwood	1	m^3
Input:		
Industrial wood, hardwood, under bark, u=80%, at forest road/RER/m^3	0,329	m^3
Wood chopping, mobile chopper, in forest/RER/kg	239	kg
Transport to power plant, hardwood, truck/tkm (own calculation)	286,18	tkm

Table 28: Inventory for Fuel input, wood chips from hardwood, for the Northen region in European Russia

Fuel, wood chips, softwood	1	m^3
Input:		
Industrial wood, softwood, under bark, u=140%, at forest road/RER/m^3	0,341	m^3
Wood chopping, mobile chopper, in forest/RER/kg	169	kg
Transport to power plant, softwood, truck/tkm (own calculation)	286,18	tkm

For the reference case of 100% coal-firing, the processes for bioenergy were not included and for the scenario of 100% bioenergy, the processes for coal were excluded. For each of the regions, the input of wood chips from hardwood and softwood varied, and the distribution for each scenario can be found in Table 7 (10% co-fire), Table 9 (20% co-fire) and Table 10 (100% bioenergy), in addition to the coal input in the fuel mix. Furthermore, the transportation in ton kilometre varied for each region, and the overview can be found in Table 8. The emissions from direct biomass combustion and albedo effect were calculated seperately and for coal combustion 101 g CO_2-eq/MJ was used (IPCC, 2006).

For more information concerning the calculations for the transportation routes, see Table 30 and Table 31 below for the scenario of 10% co-firing (total tkm/m^3 is the same for each scenario). Loading capacity is 21 tons and fuel consumption is 3 litres per km.

Table 29: Overview of the amount of wood needed per truck-trip for the scenario of 10% co-firing (and covering 10% of the coal demand in the region).

Region	Amount of wood, 10% co-firing [m^3]	Amount of softwood, 10% co-firing [m^3]	Amount of hardwood, 10% co-firing [m^3]	Amount of wood per truck-trip [m^3]
North	1 415 971	1 087 416	328 555	41,4
Northwest	1 301 476	636 591	664 884	38,1
Central	1 269 141	509 273	759 868	37,1
Volga-Vyatka	1 289 147	588 045	701 101	37,7
Central Chernozem	1 250 664	436 520	814 144	36,6
Volga	1 218 189	308 650	909 539	35,6
North Caucasus	1 202 385	246 422	955 963	35,2
Urals	1 300 190	631 531	668 659	38,0
Total	10 247 161	4 444 449	5 802 712	37,5

To find the final tonkm per m^3, the total amount of tonkm for each region was divided by the amount of wood per truck trip in m^3, found in Table 29 above.

Table 30: Calculations connected to the transportation routes for each region for the scenario of 10% co-firing

Region	Km to power plant [km]	Total times distance is needed	Total amount of km [km]	Total fuel consumption [L]	Lt of diesel per MJ [L/MJ]	Ton kilmetre [tkm]	Tonkm per ton [tkm/t]	Tonkm per m^3 [tkm/m^3]
North	564,3	34 194	19 296 042	6 432 014	4,7E-04	11850,5	564,3	286,2
Northwest	171,3	34 194	5 858 466	1 952 822	1,4E-04	3597,9	171,3	94,5
Central	353,0	34 194	12 069 130	4 023 043	2,9E-04	7412,2	353,0	199,7
Volga-Vyatka	327,6	34 194	11 202 995	3 734 332	2,7E-04	6880,2	327,6	182,5
Central Chernozem	197,2	34 194	6 744 433	2 248 144	1,6E-04	4142,0	197,2	113,2
Volga	340,9	34 194	11 655 382	3 885 127	2,8E-04	7158,1	340,9	200,9
North Caucasus	323,3	34 194	11 054 251	3 684 750	2,7E-04	6788,9	323,3	193,1
Urals	360,0	34 194	12 311 224	4 103 741	3,0E-04	7560,8	360,0	198,8

8.3. Numerical values for climate change impact

Below in Table 31 to Table 33 the climate change impact for upstream processes for biomass, direct biomass combustion and albedo in g CO_2-eq/$MJ_{fuel\text{-}mix}$ can be found. The values correspond to the forest types present in each region, for the three time horizons. The values are for the scenario of 100% bioenergy, which can be used to further find the biomass upstream values for 10% co-firing and 20% co-firing.

Table 31: Climate change impact of biomass upstream processes for the case of 100% bioenergy in each region [g CO_2-eq/$MJ_{fuel\text{-}mix}$]. Displayed for all three time horizon.

Region	TH=20	TH=100	TH=500
100% coal-fired	32,3	13,6	6,61
North	6,73	6,33	6,17
Northwest	2,42	2,28	2,22
Central	4,36	4,1	4,0
Volga-Vyatka	4,25	4,0	3,9
Central Chernozem	2,68	2,52	2,46
Volga	4,08	3,83	3,74
North Caucasus	4,01	3,77	3,68
Urals	4,44	4,18	4,07

Table 32: Climate change impact of direct biomass combustion for the scenario of 100% bioenergy for each forest type in each region [g CO_2-eq/$MJ_{fuel\text{-}mix}$]. Displayed for all three time horizons. (Con=coniferous, dec=deciduous)

Region	TH = 20					TH = 100					TH = 500				
	Boreal		Temperate		Total	Boreal		Temperate		Total	Boreal		Temperat		Total
	Con	Dec	Con	Dec		Con	Dec	Con	Dec		Con	Dec	Con	Dec	
North	71,1	21,3	-	-	92,4	31,9	8,2	-	-	40,0	5,9	1,5	-	-	7,4
Northwest	22,7	23,4	22,4	23	91,5	10,1	9,0	9,2	7,8	36,1	1,9	1,6	1,7	1,5	6,6
Central	-	-	36,8	54	90,8	-	-	15,1	18,2	33,3	-	-	2,7	3,5	6,2
Volga-Vyatka	-	-	41,8	49,1	90,9	-	-	17,2	16,5	33,7	-	-	3,1	3,1	6,2
Central Chernozem	-	-	32,0	58,7	90,7	-	-	13,1	19,8	32,9	-	-	2,4	3,8	6,1
Volga	-	-	23,2	67,4	90,6	-	-	9,5	22,7	32,2	-	-	1,7	4,3	6,0
North Caucasus	-	-	18,8	71,7	90,5	-	-	7,7	24,2	31,9	-	-	1,4	4,6	6,0
Urals	31,5	33,0	13,4	13,9	91,8	14,1	12,7	5,5	4,7	37,0	2,6	2,3	1,0	0,9	6,8

Table 33: Climate change impact of surface albedo for the scenario of 100% bioenergy for each forest type in each region [g CO_2-eq/$MJ_{fuel-mix}$]. Displayed for all three time horizons. (Con=coniferous, dec=deciduous)

Region	TH = 20					TH = 100					TH = 500				
	Boreal		Temperate		Total	Boreal		Temperate		Total	Boreal		Temperat		Total
	Con	Dec	Con	Dec		Con	Dec	Con	Dec		Con	Dec	Con	Dec	
North	-98,1	-24,1	-	-	-122,2	-44,4	-10,1	-	-	-54,5	-13,7	-3,1	-	-	-16,8
Northwest	-38,7	-32,9	-10,6	-8,9	-91,0	-17,5	-13,7	-4,5	-3,5	-39,3	-5,4	-4,2	-1,4	-1,1	-12,1
Central	-	-	-18,3	-21,9	-40,3	-	-	-7,9	-8,6	-16,5	-	-	-2,4	-2,7	-5,1
Volga-Vyatka	-	-	-19,3	-18,5	-37,8	-	-	-8,3	-7,3	-15,5	-	-	-2,6	-2,2	-4,8
Central Chernozem	-	-	-17,5	-26,1	-43,6	-	-	-7,5	-10,3	-17,8	-	-	-2,3	-3,2	-5,5
Volga	-	-	-10,6	-25,1	-35,8	-	-	-4,6	-9,9	-14,4	-	-	-1,4	-3	-4,4
North Caucasus	-	-	-8,7	-17,6	-26,2	-	-	-2,4	-6,9	-9,3	-	-	-0,7	-2,1	-2,9
Urals	-62,1	-53,6	-7,3	-6,2	-129,1	-28,1	-22,3	-3,1	-2,4	-56	-8,7	-6,9	-1,0	-0,7	-17,3

Below in Table 34 one can find the numerical values which Figure 16 to Figure 18 are based on. The values represent total climate change impact in g CO_2-eq/$MJ_{fuel-mix}$ for each of the scenarios and corresponding time horizon.

Table 34: Total climate change impact for each scenario for each region [g CO_2-eq/$MJ_{fuel-mix}$]. Displayed for all three time horizons.

	10% co-firing			20% co-firing			100% bioenergy		
Region	TH=20	TH=100	TH=500	TH=20	TH=100	TH=500	TH=20	TH=100	TH=500
100% coal-fire	133,3	114,6	107,61	133,3	114,6	107,6	133,3	114,6	107,6
North	117,7	102,3	96,52	102,0	90,0	85,4	-23,1	-8,1	-3,29
Northwest	120,3	103,0	96,52	107,2	91,5	85,4	2,94	-0,9	-3,27
Central	125,5	105,2	97,35	117,6	95,8	87,1	54,9	20,9	5,1
Volga-Vyatka	125,7	105,3	97,38	118,1	96,0	87,1	57,4	22,2	5,34
Central Chernozem	125,0	104,9	97,16	116,6	95,2	86,7	49,8	17,7	3,12
Volga	125,9	105,3	97,38	118,4	96,0	87,2	58,9	21,6	5,33
North Caucasus	126,8	105,8	97,52	120,3	96,9	87,4	68,3	26,3	6,8
Urals	116,7	101,6	96,2	100,1	88,7	84,8	-32,9	-14,9	-6,46

8.4. Potential future co-firing scenarios

Calculations in connection with the potential future co-firing scenarios and the percentage amount it will cover of the current Net Annual Increment (NAI), Annual increment available for exploitation (AIAE) and Annual Allowable Cut (AAC) is shown in Table 35 and Table 36. Covering the complete coal demand is the equivalent of 2 471 719 TJ or 260,18 mill m^3 of dry mass.

Table 35: Values in m^3 and % connected to the needed increase of current harvest for the scenarios 10% and 20% co-firing, as well as 100% bioenergy.

	Russia (NAI)	Russia (AIAE)	Russia (AAC)	Increase of current harvest
Total estimated potential [mill m^3]	853	552	633	173,6
10% of coal demand [mill m^3]	26,0	26,0	26,0	26,0
% of each scenario	3,1 %	4,7 %	4,1 %	15,0 %
20% of coal demand [mill m^3]	52,0	52,0	52,0	52,0
% of each scenario	6,1 %	9,4 %	8,2 %	30,0 %
50% of coal demand [mill m^3]	130,1	130,1	130,1	130,1
% of each scenario	15,3 %	23,6 %	20,6 %	74,9 %
100% of coal demand [mill m^3]	260,2	260,2	260,2	260,2
% of each scenario	30,5 %	47,1 %	41,1 %	149,9 %

Table 36: Percentage amount the current harvest together with the increased harvest will account for of NAI, AEIE and AAC.

	10% co-firing	20% co-firing	50% co-firing	100% bioenergy
Current harvest + new harvest [mill m^3]	199,6	225,6	303,7	433,8
% of NAI	23,4 %	26,5 %	35,6 %	50,9 %
% of AEIE	36,1 %	40,9 %	55,0 %	78,5 %
% of AAC	31,5 %	35,6 %	48,0 %	68,5 %